Available online at www.sciencedirect.com

ScienceDirect

Nuclear Physics B 904 (2016) 39–85

NUCLEAR PHYSICS B

www.elsevier.com/locate/nuclphysb

Pseudofermion dynamical theory for the spin dynamical correlation functions of the half-filled 1D Hubbard model

J.M.P. Carmelo [a,b,c], T. Čadež [c,a,b,d]

[a] *Department of Physics, University of Minho, Campus Gualtar, P-4710-057 Braga, Portugal*
[b] *Center of Physics of University of Minho and University of Porto, P-4169-007 Oporto, Portugal*
[c] *Beijing Computational Science Research Center, Beijing 100193, China*
[d] *Jožef Stefan Institute, 1000 Ljubljana, Slovenia*

Received 24 September 2015; received in revised form 16 December 2015; accepted 5 January 2016

Available online 7 January 2016

Editor: Hubert Saleur

Abstract

A modified version of the metallic-phase pseudofermion dynamical theory (PDT) of the 1D Hubbard model is introduced for the spin dynamical correlation functions of the half-filled 1D Hubbard model Mott–Hubbard phase. The Mott–Hubbard insulator phase PDT is applied to the study of the model longitudinal and transverse spin dynamical structure factors at finite magnetic field h, focusing in particular on the singularities at excitation energies in the vicinity of the lower thresholds. The relation of our theoretical results to both condensed-matter and ultra-cold atom systems is discussed.

1. Introduction

The Hubbard model with nearest-neighbor hopping integral t and on-site repulsion U is possibly the most studied lattice system of correlated electrons. It features electrons that can hop between nearest-neighboring lattice sites due to the finite hopping integral t. When two electrons are on the same site, they have to pay the energy U due to their mutual repulsion. This introduces

E-mail address: carmelo@fisica.uminho.pt (J.M.P. Carmelo).

http://dx.doi.org/10.1016/j.nuclphysb.2016.01.009

additional electronic correlations beyond those due to the Pauli principle. The model properties depend on the ratio $u \equiv U/4t$.

The calculation of dynamical correlation functions is one of the main challenges in low-dimensional theories. Some systems with spectral gap can be dealt with by the form-factor approach to quantum correlation functions [1–7]. The advantage of this method is that it is in principle not constrained to very low energies. The form-factor approach can also be implemented for spin lattice systems such as the Heisenberg *XXX* and *XXZ* chains [8–13].

The 1D Hubbard model is solvable by the Bethe ansatz (BA) [14–17]. This technique provides the exact spectrum of the energy eigenstates, yet it has been difficult to apply to the derivation of high-energy dynamical spectral and correlation functions. (In this paper we use the designation *high energy* for all energy scales larger than the model low-energy limit associated with the Tomonaga–Luttinger-liquid regime [18–21].) For instance, form factors of the 1D Hubbard model electronic creation and annihilation operators is an open problem that has not been solved. Even the eventually easier problem of determining form factors of the spin operators in the Hubbard model at finite magnetic field remains as well unsolved. For the model metallic phase, the method used in Refs. [22,23] has been the first breakthrough to address the problem of the high-energy dynamical correlation functions in the $u \rightarrow \infty$ limit. Specifically, in these references the one-electron spectral functions of the model metallic phase have been derived for the whole (k, ω) plane. That method relies on the spinless-fermion phase shifts imposed by Heisenberg spins $1/2$. Such elementary objects naturally arise from the $u \rightarrow \infty$ electron wave-function factorization [24–26].

A related pseudofermion dynamical theory (PDT) relying on a representation of the model BA solution in terms of the pseudofermions generated by a unitary transformation from the corresponding pseudoparticles considered in Ref. [27] was introduced in Refs. [28,29]. It is an extension of the $u \rightarrow \infty$ method of Refs. [22,23] to the whole finite $u > 0$ range of the metallic phase of the 1D Hubbard model. A key property is that the pseudofermions are inherently constructed to their energy spectrum having no interaction terms. This allows the expression of the dynamical correlation functions in terms of pseudofermion spectral functions. However, creation or annihilation of pseudofermions under transitions to excited states imposes phase shifts to the remaining pseudofermions. Within the PDT such phase shifts fully control the one- and two-electron spectral-weight distributions over the (k, ω) plane.

The PDT of Refs. [28,29] has been the first breakthrough for the derivation of analytical expressions of the metallic phase of the 1D Hubbard model high-energy dynamical correlation functions for the whole finite $u > 0$ range. Applications of the 1D Hubbard model metallic-phase PDT to the study of spectral features of actual condensed-matter systems are presented in Refs. [30–33].

After the PDT for the metallic phase of the 1D Hubbard model was introduced, a set of novel methods have been developed to also tackle the high-energy physics of 1D correlated quantum problems, beyond the low-energy Tomonaga–Luttinger-liquid limit [34]. In the case of the 1D Hubbard model such methods reach the same results as the PDT. For instance, the momentum, electronic density $n_e < 1$, and on-site repulsion $u = U/4t > 0$ dependence of the exponents that control the line shape of the one-electron spectral function of the model metallic phase calculated in Refs. [35,36] in the framework of a mobile impurity model using input from the BA solution is exactly the same as that obtained previously by use of the metallic-phase PDT [30–33].

However, the latter PDT as reported in Refs. [28,29] does not apply to the study of the spin dynamical correlation functions of the 1D Hubbard model Mott–Hubbard insulator phase, which for the whole $u > 0$ range corresponds to electronic density $n_e = 1$. (For that density it is usually

called half-filled 1D Hubbard model.) Important examples of such spin dynamical correlation functions are the spin dynamical structure factors,

$$S^{aa}(k,\omega) = \sum_{j=1}^{L} e^{-ikj} \int_{-\infty}^{\infty} dt\, e^{-i\omega t} \langle GS|\hat{S}^a_j(t)\hat{S}^a_j(0)|GS\rangle\,,$$

$$= \sum_{f} |\langle f|\hat{S}^a_k|GS\rangle|^2 \delta(\omega - \omega^\tau(k))\,. \quad (1)$$

Here $a = x, y, z$, the spectra read $\omega^\tau(k) = E^\tau_f - E_{GS}$, E^τ_f refers to the energies of the excited energy eigenstates that contribute to the $\tau = l$ longitudinal and $\tau = t$ transverse dynamical structure factors, E_{GS} is the initial ground state energy, and $\hat{S}^a_k$ are for $a = x, y, z$ the Fourier transforms of the usual local spin operators $\hat{S}^a_j$, respectively.

The studies of this paper do not address dynamical correlation functions associated with energy gapped excitations of the half-filled 1D Hubbard model such as the one-electron spectral functions and the charge dynamical structure factor [37]. Here we rather consider spin dynamical correlation functions associated with spin gapless excitations of the Mott–Hubbard insulator, such as the spin dynamical structure factors, Eq. (1). Previous studies of these factors focused mainly onto the model at magnetic fields $h = 0$ when $S^{zz}(k,\omega) = S^{xx}(k,\omega) = S^{yy}(k,\omega)$ [38, 39]. The studies of Ref. [38] have proposed an expression for the BA spin-band two-hole form factor and explicitly calculated the corresponding contribution to the spin dynamical structure factor at $h = 0$. Its evolution as a function of u was studied in Ref. [39]. On the other hand, Ref. [40] presents results on one of the few studies about dynamical correlation functions of the 1D Hubbard model Mott–Hubbard insulator phase at finite magnetic field. However it addresses a problem different from that studied here: The low-energy limit of the dynamical density-density response function, which has no threshold singularities.

Our present study and results refer to the Mott–Hubbard insulator phase of the 1D Hubbard model at a finite magnetic field h in the *thermodynamic limit* (TL) for $u = U/4t > 0$ values. For $h > 0$ one has that $S^{zz}(k,\omega) \neq S^{xx}(k,\omega)$. Here we modify the PDT introduced in Refs. [28,29] for the model metallic phase to study the spin dynamical properties of the half-filled 1D Hubbard model at finite magnetic field h. The Mott–Hubbard insulator phase PDT introduced in this paper is then used to clarify one of the unresolved questions concerning the physics of that model by deriving the exact momentum, repulsive interaction $u = U/4t$, and spin-density m dependences of the exponents that control the singularities at the spectra lower thresholds in $S^{zz}(k,\omega)$ and $S^{xx}(k,\omega)$.

The remainder of the paper is organized as follows. In Section 2 the results on the model exact BA solution pseudoparticle and pseudofermion representations needed for our study are presented. The PDT introduced in Refs. [28,29] for the metallic phase of the 1D Hubbard model is suitably modified in Section 3 for the present case of the spin dynamical correlation functions of the half-filled 1D Hubbard model. Such a modified form of the PDT is used in Sec. 4 to derive the longitudinal and transverse dynamical structure factors in the vicinity of their spectra lower thresholds. Finally, Sec. 5 presents the concluding remarks including a brief discussion of the relation of our theoretical results to both condensed-matter [41] and ultra-cold atom [42] systems.

2. The pseudoparticle and pseudofermion representations of the 1D Hubbard model exact BA solution

In this section we provide useful information on the pseudoparticle representation of the 1D Hubbard model BA solution needed for its representation in terms of the related pseudofermions, which is also briefly outlined. The Mott–Hubbard insulator PDT introduced in Section 3 relies on the latter representation.

The Hubbard model under periodic boundary conditions on a 1D lattice with an even number $L \rightarrow \infty$ of sites and in a chemical potential μ and magnetic field h is given by,

$$\hat{H} = t\,\hat{T} + U\,\hat{V}_D + 2\mu\,\hat{S}^z_\eta + 2\mu_B h\,\hat{S}^z_s\,, \tag{2}$$

where μ_B is the Bohr magneton,

$$\hat{T} = -\sum_{\sigma=\uparrow,\downarrow}\sum_{j=1}^{L}\left(c^\dagger_{j,\sigma}\,c_{j+1,\sigma} + c^\dagger_{j+1,\sigma}\,c_{j,\sigma}\right); \qquad \hat{V}_D = \sum_{j=1}^{L}\hat{\rho}_{j,\uparrow}\hat{\rho}_{j,\downarrow};$$
$$\hat{\rho}_{j,\sigma} = c^\dagger_{j,\sigma}\,c_{j,\sigma} - 1/2\,, \tag{3}$$

are the kinetic-energy operator in units of t, and the electron on-site repulsion operator in units of U, respectively, and

$$\hat{S}^z_\eta = -\frac{1}{2}(L - \hat{N})\,; \qquad \hat{S}^z_s = -\frac{1}{2}(\hat{N}_\uparrow - \hat{N}_\downarrow)\,, \tag{4}$$

are the diagonal generators of the global η-spin and spin $SU(2)$ symmetry algebras, respectively. Here we use in general units of lattice constant one, so that the number of lattice sites N_a equals the lattice length L. Moreover, in Eqs. (2) and (3) the operator $c^\dagger_{j,\sigma}$ (and $c_{j,\sigma}$) creates (and annihilates) a spin-projection σ electron at lattice site $j = 1,\ldots,L$. The electron number operators read $\hat{N} = \sum_{\sigma=\uparrow,\downarrow}\hat{N}_\sigma$ and $\hat{N}_\sigma = \sum_{j=1}^{L}\hat{n}_{j,\sigma} = \sum_{j=1}^{L}c^\dagger_{j,\sigma}\,c_{j,\sigma}$.

2.1. The model exact BA solution pseudoparticle representation for general densities

Although the studies of this paper refer to the 1D Hubbard model, Eq. (2), at electronic density $n_e = N/L = 1$, we start by considering the general case of arbitrary electronic density and spin density $m = n_\uparrow - n_\downarrow$ where $n_\sigma = N_\sigma/L$. The lowest weight states (LWSs) and highest weight states (HWSs) of the η-spin and spin $SU(2)$ symmetry algebras have numbers $S_\alpha = -S^z_\alpha$ and $S_\alpha = S^z_\alpha$, respectively, for $\alpha = \eta, s$. Here S_η and S^z_η are the states η-spin and η-spin projection and S_s and S^z_s their spin and spin projection, respectively. In this paper the LWS formulation of 1D Hubbard model BA solution is used. The model in its full Hilbert space can be described either directly within the BA solution [24,43] or by application onto the LWSs of the η-spin and spin $SU(2)$ symmetry algebras off-diagonal generators [44].

The 1D Hubbard model BA equations introduced in Ref. [16] for the TL read in our pseudoparticle momentum distribution functional notation [27],

$$q_j = k^c(q_j) + \frac{2}{L}\sum_{n=1}^{\infty}\sum_{j'=1}^{L_{sn}} N_{sn}(q_{j'})\arctan\left(\frac{\sin k^c(q_j) - \Lambda^{sn}(q_{j'})}{nu}\right)$$
$$+\frac{2}{L}\sum_{n=1}^{\infty}\sum_{j'=1}^{L_{\eta n}} N_{\eta n}(q_{j'})\arctan\left(\frac{\sin k^c(q_j) - \Lambda^{\eta n}(q_{j'})}{nu}\right), \qquad j = 1,\ldots,L\,, \tag{5}$$

and

$$q_j = \delta_{\alpha,\eta}\sum_{\iota=\pm 1}\arcsin(\Lambda^{\alpha n}(q_j) - i\,\iota\,u) + \frac{2\,(-1)^{\delta_{\alpha,\eta}}}{L}\sum_{j'=1}^{L} N_c(q_{j'})\arctan\left(\frac{\Lambda^{\alpha n}(q_j) - \sin k^c(q_{j'})}{nu}\right) - \frac{1}{L}\sum_{n'=1}^{\infty}\sum_{j'=1}^{L_{\alpha n'}} N_{\alpha n'}(q_{j'})\Theta_{n\,n'}\left(\frac{\Lambda^{\alpha n}(q_j) - \Lambda^{\alpha n'}(q_{j'})}{u}\right),$$
$$j = 1,\ldots,L_{\alpha n}\,,\quad \alpha = \eta, s\,,\quad n = 1,\ldots,\infty\,. \tag{6}$$

The sets of $j = 1,\ldots,L$ and $j = 1,\ldots,L_{\alpha n}$ quantum numbers q_j in Eqs. (5) and (6), respectively, which are defined below, play the role of microscopic momentum values of different BA excitation branches. In these equations and throughout this paper $\delta_{\alpha,\eta}$ is the usual Kronecker symbol and the rapidity function $\Lambda^{\alpha n}(q_j)$ is the real part of the following complex rapidity [16],

$$\Lambda^{\alpha n,l}(q_j) = \Lambda^{\alpha n}(q_j) + i\,(n+1-2l)\,u\,,\qquad l = 1,\ldots,n\,, \tag{7}$$

where the rapidity function $\Lambda^{\alpha n}(q_j)$ is real, $j = 1,\ldots,L_{\alpha n}$, $\alpha = \eta, s$, and $n = 1,\ldots,\infty$.

Furthermore, in Eqs. (5) and (6) $\Theta_{n\,n'}(x)$ is the function,

$$\Theta_{n\,n'}(x) = \delta_{n,n'}\left\{2\arctan\left(\frac{x}{2n}\right) + \sum_{l=1}^{n-1} 4\arctan\left(\frac{x}{2l}\right)\right\} + (1-\delta_{n,n'})\left\{2\arctan\left(\frac{x}{|n-n'|}\right) + 2\arctan\left(\frac{x}{n+n'}\right) + \sum_{l=1}^{\frac{n+n'-|n-n'|}{2}-1} 4\arctan\left(\frac{x}{|n-n'|+2l}\right)\right\}, \tag{8}$$

where $n, n' = 1,\ldots,\infty$ and,

$$q_j = \frac{2\pi}{L}\,I_j^{\beta}\,,\qquad j = 1,\ldots,L_\beta\,,\qquad \beta = c, \eta n, sn\,,\qquad n = 1,\ldots,\infty\,, \tag{9}$$

are the $\beta = c, \alpha n$ band momentum values. The indices $\alpha = \eta, s$ and numbers $n = 1,\ldots,\infty$ refer to different BA excitation branches that both in Ref. [27] and within the PDT of Refs. [28,29] are associated with β pseudoparticles as defined in the following. The c pseudoparticles and $s1$ pseudoparticles (often called s pseudoparticles) play a major role in the one-electron and two-electron physics of the metallic phase of the 1D Hubbard model [45,46]. The PDT relies on a representation of the BA solution in terms of β pseudofermions, which are related to the β pseudoparticles by a unitary transformation uniquely defined below in Section 3.

For a given energy and momentum eigenstate, the $j = 1,\ldots,L_\beta$ quantum numbers I_j^{β} on the right-hand side of Eq. (9) are either integers or half-odd integers according to the following boundary conditions [16],

$$I_j^{\beta} = 0, \pm 1, \pm 2, \ldots \quad \text{for } I_\beta \text{ even}\,,$$
$$= \pm 1/2, \pm 3/2, \pm 5/2, \ldots \quad \text{for } I_\beta \text{ odd}\,. \tag{10}$$

Here,

$$I_\beta = \delta_{\beta,c}\, N_{\rm ps}^{SU(2)} + \delta_{\beta,\alpha n}\,(L_\beta - 1)\,, \qquad \alpha = \eta, s\,, \qquad n = 1, \ldots, \infty\,. \tag{11}$$

The $\beta = c, \alpha n$ band successive set of momentum values q_j, Eq. (9), have only occupancies zero and one and the usual separation, $q_{j+1} - q_j = 2\pi/L$. The number L_β in Eq. (11) is that of the β-band discrete momentum values given by,

$$L_\beta = N_\beta + N_\beta^h\,, \qquad \beta = c, \alpha n\,, \qquad \alpha = \eta, s\,, \qquad n = 1, \ldots, \infty\,. \tag{12}$$

A number $N_\beta \leq L_\beta$ of these momentum values are occupied. The β-band momentum distribution functions $N_\beta(q_j)$ in Eqs. (5) and (6) thus read $N_\beta(q_j) = 1$ and $N_\beta(q_j) = 0$ for occupied and unoccupied discrete momentum values, respectively,

Specifically, we call a β *pseudoparticle* each of the N_β β-band occupied momentum values. The remaining N_β^h momentum values are unoccupied, their number reading [16],

$$N_c^h = L - N_c; \qquad N_{\alpha n}^h = 2S_\alpha + \sum_{n'=n+1}^{\infty} 2(n'-n)N_{\alpha n'}\,, \quad \alpha = \eta, s,\ n = 1, \ldots, \infty. \tag{13}$$

We call β*-band holes* such unoccupied momentum values.

The total number of pseudoparticles $N_{\rm ps}$, the pseudoparticle number $N_{\rm ps}^{SU(2)}$ appearing in Eq. (11), and the related pseudoparticle number $N_{\alpha\,{\rm ps}}$ are given by,

$$N_{\rm ps} = N_c + N_{\rm ps}^{SU(2)}\,; \qquad N_{\rm ps}^{SU(2)} = \sum_{\alpha=\eta,s} N_{\alpha\,{\rm ps}}\,; \qquad N_{\alpha\,{\rm ps}} = \sum_{n=1}^{\infty} N_{\alpha n} \qquad \alpha = \eta, s\,. \tag{14}$$

The numbers $N_{\rm ps}^{SU(2)}$ and $N_{\alpha\,{\rm ps}}$ obey the following exact sum rules,

$$N_{\rm ps}^{SU(2)} = \sum_{\alpha=\eta,s}\sum_{n=1}^{\infty} N_{\alpha n} = \frac{1}{2}(L - N_{s1}^h - N_{\eta 1}^h)\,;$$
$$N_{\alpha\,{\rm ps}} = \sum_{n=1}^{\infty} N_{\alpha n} = \frac{1}{2}(L_\alpha - N_{\alpha 1}^h)\,, \quad \alpha = \eta, s\,, \tag{15}$$

where $N_{\alpha 1}^h$ is the number of αn-band holes for $\alpha = \eta, s$ and $n = 1$ and,

$$L_\eta = N_c^h = L - N_c\,; \qquad L_s = N_c\,. \tag{16}$$

Other exact sum rules obeyed by the set of numbers $\{N_{\alpha n}\}$ are,

$$M_{\rm sp}^{SU(2)} = \sum_{\alpha=\eta,s}\sum_{n=1}^{\infty} n\, N_{\alpha n} = \frac{1}{2}(L - 2S_s - 2S_\eta)\,;$$
$$M_{\alpha\,{\rm sp}} = \sum_{n=1}^{\infty} n\, N_{\alpha n} = \frac{1}{2}(L_\alpha - 2S_\alpha)\,, \quad \alpha = s, \eta\,, \tag{17}$$

where $M_{s\,{\rm sp}} = \sum_{n=1}^{\infty} n\, N_{sn}$ is the number of spin-singlet pairs considered below in Sec. 2.2 and $M_{\eta\,{\rm sp}} = \sum_{n=1}^{\infty} n\, N_{\eta n}$ that of η*-spin-singlet pairs*, which do not exist for the quantum problem studied in this paper. (The corresponding rotated η-spins 1/2 operators is an issue briefly reported in Appendix A.)

The β band discrete momentum values q_j, Eq. (9), belong to well-defined domains, $q_j \in [q_\beta^-, q_\beta^+]$, where,

$$
\begin{aligned}
q_c^{\pm} &= \pm\frac{\pi}{L}(L-1) \approx \pm\pi \text{ for } N_{\rm ps}^{SU(2)} \text{ odd}\,; \\
q_c^{\pm} &= \pm\frac{\pi}{L}(L-1\pm 1) \approx \pm\pi \text{ for } N_{\rm ps}^{SU(2)} \text{ even}\,, \\
q_{\alpha n}^{\pm} &= \pm\frac{\pi}{L}(L_{\alpha n}-1)\,.
\end{aligned}
\tag{18}
$$

The momentum and energy eigenvalues have the following general form for all 4^L energy eigenstates,

$$
P = \sum_{j=1}^{L} q_j\, N_c(q_j) + \sum_{n=1}^{\infty}\sum_{j=1}^{L_{sn}} q_j\, N_{sn}(q_j) + \sum_{n=1}^{\infty}\sum_{j=1}^{L_{\eta n}} (\pi - q_j)\, N_{\eta n}(q_j) + \frac{\pi}{2}\,(2S_\eta^z + L_\eta)\,, \tag{19}
$$

and

$$
\begin{aligned}
E = &\sum_{j=1}^{L}\left(N_c(q_j)\, E_c(q_j) + U/4 - \mu_\eta\right) + \sum_{\alpha=\eta,s}\sum_{n=1}^{\infty}\sum_{j=1}^{L_{\alpha n}} N_{\alpha n}(q_j)\, E_{\alpha n}(q_j) \\
&+ \sum_{\alpha=\eta,s} 2\mu_\alpha\,(S_\alpha + S_\alpha^z)\,,
\end{aligned}
\tag{20}
$$

respectively. Here,

$$
2\mu_s = 2\mu_B\,|h|\,; \qquad 2\mu_\eta = 2|\mu|\,, \qquad n_e \neq 1\,; \qquad 2\mu_\eta = 2\mu_0\,, \qquad n_e = 1\,, \tag{21}
$$

and

$$
\begin{aligned}
&E_c(q_j) = -2t\cos k^c(q_j) - U/2 + \mu_\eta - \mu_s\,, \\
&E_{\alpha n}(q_j) = 2n\mu_\alpha + \delta_{\alpha,\eta}\left(4t\,{\rm Re}\left\{\sqrt{1-(\Lambda^{\eta n}(q_j) - inu)^2}\right\} - nU\right), \\
&\quad \alpha = \eta, s,\ n = 1,\ldots,\infty.
\end{aligned}
\tag{22}
$$

The energy scale $2\mu^0$ in Eq. (21) is the $n_e = 1$ Mott–Hubbard gap [14,15,47]. It is behind the spectra of the one-electron and charge excitations of the half-filled 1D Hubbard model considered in the studies of this paper being gapped. For $u > 0$ it is an even function of m that remains finite for all spin densities, $m \in [-1, 1]$. For instance, in the limits $m \to 0$ [14,15] and $m \to \pm 1$ it reads,

$$
\begin{aligned}
2\mu^0 &= U - 4t + 8t\int_0^\infty d\omega \frac{J_1(\omega)}{\omega\,(1+e^{2\omega u})} = \frac{16\,t^2}{U}\int_1^\infty d\omega \frac{\sqrt{\omega^2-1}}{\sinh\left(\frac{2\pi t\omega}{U}\right)}\,, \qquad m \to 0\,, \\
&= \sqrt{(4t)^2 + U^2} - 4t\,, \qquad m \to \pm 1\,,
\end{aligned}
\tag{23}
$$

respectively. Its $u \ll 1$ limiting behaviors [47] are $2\mu^0 \approx (8/\pi)\sqrt{t\,U}\,e^{-2\pi\left(\frac{t}{U}\right)}$ at $m = 0$ and $2\mu^0 \approx U^2/8t$ for $m = \pm 1$ and the $u \gg 1$ behavior is $2\mu^0 \approx (U - 4t)$ for the whole $m \in [-1, 1]$ range.

2.2. The Mott–Hubbard insulator phase spin sn pseudoparticle quantum liquid

Here we report the information on the spin sector of the half-filled 1D Hubbard model BA solution *sn* pseudoparticle representation needed for our study. The $\mu = 0$; $S_\eta = 0$; $n_e = 1$, and $S_s = 0$; $m = 0$ absolute ground state is both a LWS and HWS of the η-spin and spin $SU(2)$ symmetry algebras. Thus as in the case of other lattices [48], it is both a η-spin and spin singlet. Its c band is full so that it is populated by $N_c = L$ c pseudoparticles. For $u > 0$ both its one-electron and charge excitations are gapped. Their generation from the absolute ground state involves annihilation of c pseudoparticles that render N_c smaller than L, which for a $N_c = L$ ground state are high-energy processes.

In this paper we consider the half-filled 1D Hubbard model in the subspace spanned by the set of energy eigenstates whose c band is full and thus is populated by $N_c = L$ c pseudoparticles, as in the case of the $\mu = 0$; $S_\eta = 0$; $n_e = 1$, and $S_s = 0$; $m = 0$ absolute ground state. We call it $N_c = L$ *subspace*. Since all states belonging to it have $S_\eta = 0$ and $S^z_\eta = 0$, for simplicity in the remaining of this paper we call S and S^z their spin S_s and spin projection S^z_s, respectively.

Moreover, we denote the energy eigenstates that span the $N_c = L$ subspace by $|u, l_{\rm r}, S, S^z\rangle$ where, besides the u value, spin S, and spin projection S^z, $l_{\rm r}$ represents the set of $N_{sn} > 0$ occupied quantum numbers I^{sn}_j, Eq. (10) for $\beta = sn$, of all $n = 1, \ldots, \infty$ branches with finite occupancy that uniquely specify each state. Concerning our BA representation in terms of energy eigenstates $|u, l_{\rm r}, S, -S\rangle$ that are LWSs, which we call *Bethe states*, the non-LWSs are generated from them as,

$$|u, l_{\rm r}, S, S^z\rangle = \frac{1}{\sqrt{\mathcal{C}}}(\hat{S}^+)^{n_s}|u, l_{\rm r}, S, -S\rangle\,;$$
$$\mathcal{C} = (n_s!)\prod_{j=1}^{n_s}(2S+1-j)\,, \qquad n_s = 1, \ldots, 2S\,, \tag{24}$$

where $\hat{S}^+$ is the usual off-diagonal generator of the global spin $SU(2)$ symmetry algebra.

A *particle subspace* (PS) of the $N_c = L$ subspace is spanned by a $n_e = 1$ ground state with a value of spin density in the range $m \in [-1, 1]$ and the set of excited energy eigenstates generated from it by a finite number of *sn* pseudoparticle processes that conserve the number $N_c = L$ of c pseudoparticles. For such excited energy eigenstates the corresponding deviation densities $\delta N_{sn}/L$ and $\delta S/L$ vanish as $L \to \infty$. For a PS there are though no restrictions on the value of the excitation energy and excitation momentum.

For simplicity, we consider a PS spanned by a $n_e = 1$ ground state that is a spin LWS whose spin density value is thus in the range $m \in]0, 1]$ and its excited energy eigenstates. (This is without loss in generality, concerning PSs associated with $n_e = 1$ ground states that are spin HWSs with spin densities $m \in [-1, 0[$.) Since the PSs considered in our study are part of the larger $N_c = L$ subspace, they do not contain the gapped excited energy eigenstates associated with the charge and one-electron excitations whose energy spectrum involves the Mott–Hubbard gap $2\mu^0$, Eq. (23).

For the spin LWS ground states considered here the $\beta = c, sn$ band limiting momentum values $q^{\pm}_\beta$, Eq. (18), are given by $q^{\pm}_\beta \approx \pm q_\beta$ where q_β reads [45],

$$q_c = \pi\,; \qquad q_{s1} = k_{F\uparrow}\,; \qquad q_{sn} = (k_{F\uparrow} - k_{F\downarrow}) = \pi\, m\,; \qquad q_{\eta n} = 0\,. \tag{25}$$

Indeed the c momentum band is full, the ηn momentum bands do not exist and thus $q_{\eta n} = 0$ for $n = 1, \ldots, \infty$, the $s1$ momentum band is partially filled for $0 < m < 1$, and for sn branches such that $n > 1$ the sn momentum band is empty.

Hence for the spin LWS ground states under consideration the sn-band pseudoparticle momentum distribution functions read,

$$N^0_{s1}(q_j) = \theta(q_{Fs1} - |q_j|)\,; \qquad N^0_{sn}(q_j) = 0\,, \qquad n > 1\,, \tag{26}$$

where $\theta(x)$ is given by $\theta(x) = 1$ for $x > 0$ and $\theta(x) = 0$ for $x \leq 0$. Within the TL considered here one has that,

$$q^{\pm}_{Fs1} \approx \pm q_{Fs1}\,, \qquad q_{Fs1} = k_{F\downarrow} = \pi\, m_{\downarrow}\,. \tag{27}$$

The $s1$-band Fermi momentum values $q^{\pm}_{Fs1}$ including $\mathcal{O}(1/L)$ corrections are given in Eqs. (C.9)–(C.11) of Ref. [27]. Such corrections preserve the relation $q^{\pm}_{Fs1} = -q^{\mp}_{Fs1}$.

Under transitions from a ground state to a PS excited energy eigenstate there may occur shake-up effects. They are generated by transitions to PS excited energy eigenstates under which the boundary conditions of Eq. (10) are changed. This is behind overall $\beta = c$-band and $\beta = sn$-bands discrete momentum shifts, $q_j \rightarrow q_j + (2\pi/L)\,\Phi^0_\beta$, where Φ^0_β is given by,

$$\begin{aligned}
&\Phi^0_c = 0\,; \qquad \delta N_{s\,\mathrm{ps}} \quad \text{even}\,; \qquad \Phi^0_c = \pm\frac{1}{2}\,; \qquad \delta N_{s\,\mathrm{ps}} \quad \text{odd}\,; \\
&\Phi^0_{sn} = 0; \qquad \delta N_{sn} \quad \text{even}; \qquad \Phi^0_{sn} = \pm\frac{1}{2}\,; \qquad \delta N_{sn} \quad \text{odd}, \quad n = 1, \ldots, \infty\,,
\end{aligned} \tag{28}$$

where $\delta N_{s\,\mathrm{ps}}$ is the deviation in the number $N_{s\,\mathrm{ps}}$ in Eq. (15), which in the present case reads $N_{s\,\mathrm{ps}} = \sum_{n=1}^{\infty} N_{sn} = (N_c + N^h_{s1})/2$. Note that although in the present case the above transitions preserve the number of c pseudoparticles $N_c = L$, they may produce c-band overall momentum shifts, $q_j \rightarrow q_j + (2\pi/L)\,\Phi^0_c$.

For the half-filled 1D Hubbard model in the PSs considered here the sn quantum liquid associated with that quantum problem involves the following subset of $n = 1, \ldots, \infty$ BA equations,

$$\begin{aligned}
q_j = {} & \frac{2}{L}\sum_{j'=1}^{L} \arctan\left(\frac{\Lambda^{sn}(q_j) - \sin k^c(q_{j'})}{nu}\right) \\
& - \frac{1}{L}\sum_{n'=1}^{\infty}\sum_{j'=1}^{L_{sn'}} N_{sn'}(q_{j'})\Theta_{n\,n'}\left(\frac{\Lambda^{sn}(q_j) - \Lambda^{sn'}(q_{j'})}{u}\right), \\
& j = 1, \ldots, L_{sn}\,,\ n = 1, \ldots, \infty\,, \\
k^c(q_j) = {} & q_j - \frac{2}{L}\sum_{n=1}^{\infty}\sum_{j'=1}^{L_{sn}} N_{sn}(q_{j'}) \arctan\left(\frac{\sin k^c(q_j) - \Lambda^{sn}(q_{j'})}{nu}\right), \qquad j = 1, \ldots, L\,.
\end{aligned} \tag{29}$$

Here L_{sn} is the number L_β in Eq. (12) for $\beta = sn$,

$$L_{sn} = N_{sn} + N^h_{sn}\,; \qquad N^h_{sn} = (2S + \sum_{n'=n+1}^{\infty} 2(n'-n)N_{sn'})\,, \qquad n = 1, \ldots, \infty\,, \tag{30}$$

and $\Lambda^{sn}(q_j)$ is the real part of the sn complex rapidity [16],

$$\Lambda^{sn,l}(q_j) = \Lambda^{sn}(q_j) + i\,(n + 1 - 2l)\,u\,, \qquad l = 1, \ldots, n\,, \tag{31}$$

where $j = 1, \ldots, L_{sn}$ and $n = 1, \ldots, \infty$.

Since for the present quantum problem the c-band is full, the momentum rapidity function $k^c(q_j)$ is fully determined only by the occupancies of the sn pseudoparticles, which are described in Eq. (29) by the corresponding sn-band momentum distribution functions $N_{sn'}(q_{j'})$. It turns out that the $N_c = L$ c pseudoparticles explicit role in the quantum problem physics is through a mere contribution $\pm\pi$ to the excitation momentum when $\Phi_c^0 = \pm 1/2$ in Eq. (28).

The PS energy functionals are derived from the use in the BA equations, Eq. (29), and general energy spectra, Eq. (20), of distribution functions of form $N_{sn}(q_j) = N_{sn}^0(q_j) + \delta N_{sn}(q_j)$, Eq. (32) for $\beta = sn$. The combined and consistent solution of such equations and spectra up to second order in the deviations,

$$\delta N_{sn}(q_j) = N_{sn}(q_j) - N_{sn}^0(q_j)\,, \qquad j = 1,\ldots,L_{sn}\,, \qquad n = 1,\ldots,\infty\,, \tag{32}$$

leads to a $\delta E = E - E_{GS}$ energy spectrum of the following general form,

$$\begin{aligned}\delta E = &\sum_{n=1}^{\infty}\sum_{j=1}^{L_\beta}\varepsilon_{sn}(q_j)\delta N_{sn}(q_j) + 2\mu_B\,|h|\,(S+S^z) \\ &+ \frac{1}{L}\sum_{n=1}^{\infty}\sum_{n'=1}^{\infty}\sum_{j=1}^{L_{sn}}\sum_{j'=1}^{L_{sn'}}\frac{1}{2}\,f_{sn\,sn'}(q_j,q_{j'})\,\delta N_{sn}(q_j)\delta N_{sn'}(q_{j'})\,.\end{aligned} \tag{33}$$

The sn pseudoparticle energy dispersions $\varepsilon_{sn}(q_j)$ in this equation are given by,

$$\begin{aligned}&\varepsilon_{sn}(q_j) = \varepsilon_{sn}^0(q_j) + 2\mu_B\,|h|\,, \qquad j = 1,\ldots,L_{sn}\,, \\ &\varepsilon_{sn}^0(q_j) = -\frac{2t}{\pi}\int_{-\pi}^{\pi}dk\,\sin k\,\arctan\Big(\frac{\sin k - \Lambda_0^{sn}(q_j)}{nu}\Big) \\ &\qquad + \frac{t}{\pi^2}\int_{-\pi}^{\pi}dk\int_{-B/u}^{B/u}dr\,\sin k\,\frac{2\pi\,\bar{\Phi}_{s1,sn}\left(r,\frac{\Lambda_0^{sn}(q_j)}{u}\right)}{1+\left(\frac{\sin k}{u}-r\right)^2}\,, \qquad j = 1,\ldots,L_{sn}\,.\end{aligned} \tag{34}$$

The rapidity functions $\Lambda_0^{sn}(q_j)$ appearing here are the solution of Eq. (29) for the sn-band ground-state distribution function distributions, Eq. (26), and the parameter B reads,

$$B \equiv \Lambda_0^{s1}(k_{F\downarrow})\,; \qquad \lim_{m\to 0} B = \infty\,; \qquad \lim_{m\to 1} B = 0\,. \tag{35}$$

The rapidity dressed phase shift $2\pi\,\bar{\Phi}_{s1\,sn}(r,r')$ in Eq. (34) is uniquely defined by the integral equation,

$$\begin{aligned}2\pi\,\bar{\Phi}_{s1,sn}(r,r') = &\,\delta_{n,1}\,2\arctan\Big(\frac{r-r'}{2}\Big) + (1-\delta_{n,1})\Big(2\arctan\Big(\frac{r-r'}{n-1}\Big) + 2\arctan\Big(\frac{r-r'}{n+1}\Big)\Big) \\ &+ \int_{-B/u}^{B/u}dr''\,G(r,r'')\,2\pi\,\bar{\Phi}_{s1,s1}\left(r'',r'\right)\,,\end{aligned} \tag{36}$$

whose kernel is given by,

$$G(r,r') = -\frac{1}{2\pi}\left(\frac{1}{1+((r-r')/2)^2}\right)\,. \tag{37}$$

The f function in the second-order terms of the energy functional, Eq. (33), reads [45],

$$f_{sn\,sn'}(q_j,q_{j'}) = v_{sn}(q_j)\,2\pi\,\Phi_{sn\,sn'}(q_j,q_{j'}) + v_{sn'}(q_{j'})\,2\pi\,\Phi_{sn'\,sn}(q_{j'},q_j) + \frac{1}{2\pi}\sum_{\iota=\pm 1} v_{s1}\,2\pi\,\Phi_{s1\,sn}(\iota q_{Fs1},q_j)\,2\pi\,\Phi_{s1\,sn'}(\iota q_{Fs1},q_{j'})\,. \tag{38}$$

Within the TL one may use a continuum q representation for the sn-band discrete momentum values q_j such that $q_{j+1}-q_j = 2\pi/L$. Then the deviation values $\delta N_{sn}(q_j) = -1$ and $\delta N_{sn}(q_j) = +1$, Eq. (32), become $\delta N_{sn}(q) = -(2\pi/L)\,\delta(q-q_j)$ and $\delta N_{sn}(q) = +(2\pi/L)\,\delta(q-q_j)$, respectively. (Here $\delta(x)$ denotes the usual Dirac delta-function distribution.) According to Eqs. (9) and (10), under a transition to an excited energy eigenstate the sn band discrete momentum values $q_j = (2\pi/L)\,I_j^{sn}$ may undergo a collective shift, $(2\pi/L)\,\Phi_{sn}^0 = \pm\pi/L$. For q at the $s1$ and $\iota = \pm 1$ Fermi points, $\iota\,q_{Fs1} = \iota\,k_{F\downarrow}$, such an effect is captured within the continuum representation by additional deviations, $\pm(\pi/L)\,\delta(q-\iota\,k_{F\downarrow})$. For transitions to an excited energy eigenstate for which $\delta L_{sn} \neq 0$, the removal or addition of BA sn band discrete momentum values occurs in the vicinity of the band edges $q_{sn}^- = -q_{sn}^+$, Eq. (18). Those are zero-momentum and zero-energy processes.

Within the continuum q representation, the β band group velocities appearing in Eq. (38) are given by,

$$v_{sn}(q) = \frac{\partial\varepsilon_{sn}(q)}{\partial q}\,, \qquad n = 1,\ldots,\infty\,; \qquad v_{s1} \equiv v_{s1}(q_{Fs1})\,. \tag{39}$$

Since the ground states are not populated by sn pseudoparticles of $n>1$ branches, only the $s1$ pseudoparticles have Fermi points associated with the $s1$-band Fermi velocity $v_{s1} = v_{s1}(q_{Fs1})$.

The momentum dressed phase shift $2\pi\,\Phi_{sn\,sn}(q_j,q_{j'})$ in the f function expression, Eq. (38), are of the form,

$$2\pi\,\Phi_{sn\,sn'}(q_j,q_{j'}) = 2\pi\,\bar{\Phi}_{sn\,sn'}(r,r')\,; \quad r = \Lambda_0^{sn}(q_j)/u\,; \quad r' = \Lambda_0^{sn'}(q_{j'})/u\,, \tag{40}$$

where the general rapidity dressed phase shift $2\pi\,\bar{\Phi}_{sn\,sn'}(r,r')$ is for $n>1$ the solution of the integral equation,

$$2\pi\,\bar{\Phi}_{sn,sn'}(r,r') = \Theta_{n\,n'}(r-r') - \frac{1}{2\pi}\int_{-B/u}^{B/u} dr''2\pi\,\bar{\Phi}_{sn,sn'}(r'',r')\Theta_{n\,1}^{[1]}(r-r'')\,. \tag{41}$$

Here $\Theta_{n\,n'}(x)$ is the function given in Eq. (8) and $\Theta_{n\,n'}^{[1]}(x)$ is its derivative,

$$\Theta_{n\,n'}^{[1]}(x) = \frac{d\Theta_{n\,n'}(x)}{dx} = \delta_{n,n'}\Big\{\frac{1}{n[1+(\frac{x}{2n})^2]} + \sum_{l=1}^{n-1}\frac{2}{l[1+(\frac{x}{2l})^2]}\Big\} + (1-\delta_{n,n'})\Big\{\frac{2}{|n-n'|[1+(\frac{x}{|n-n'|})^2]} + \frac{2}{(n+n')[1+(\frac{x}{n+n'})^2]} + \sum_{l=1}^{\frac{n+n'-|n-n'|}{2}-1}\frac{4}{(|n-n'|+2l)[1+(\frac{x}{|n-n'|+2l})^2]}\Big\}\,. \tag{42}$$

The $s1$ pseudoparticle dispersion $\varepsilon^0_{s1}(q_j)$, Eq. (34) for $sn = s1$, defines the spin density curve as follows,

$$h(m) = -\frac{\varepsilon^0_{s1}(k_{F\downarrow})}{2\mu_B}|_{m=1-2k_{F\downarrow}/\pi} \in [0, h_c]\,. \tag{43}$$

Here h_c is the critical field for fully polarized ferromagnetism achieved when $m \to 1$ and $k_{F\downarrow} \to 0$. The corresponding energy scale $2\mu_B h_c$ reads [45],

$$2\mu_B h_c = -\varepsilon^0_{s1}(0)|_{m=1} = \frac{2t}{\pi}\int_{-\pi}^{\pi} dk\, \sin k \arctan\left(\frac{\sin k}{u}\right) = \sqrt{(4t)^2 + U^2} - 4t\,. \tag{44}$$

That as $m \to 1$ the spin energy scale $2\mu_B|h| = 2\mu_B h_c$, Eq. (44), and the charge Mott–Hubbard gap $2\mu_0$, Eq. (23), have exactly the same value is because at $m = 1$ the model on-site repulsion has no effects since all electrons have the same spin projection. The equality of these spin and charge energy scales is then associated with a recombination of the charge and spin degrees of freedom, which is only reached at $m = 1$. As reported below in Section 4, this charge-spin recombination leads to a qualitatively different form for the spin dynamical correlation functions for $h < h_c$ and at $h = h_c$, respectively.

As confirmed below in Section 4, important energy scales that control the u dependence of the (k, ω) plane spectrum on which these functions spectral weight is distributed are the ground-state $s1$ band energy bandwidth,

$$W_{s1} = \varepsilon_s(k_{F\uparrow}) - \varepsilon_s(0) = W^p_{s1} + W^h_{s1}\,, \tag{45}$$

the energy bandwidth $W^p_{s1} = \varepsilon_s(k_{F\downarrow}) - \varepsilon_s(0) = W_{s1} - 2\mu_B\,|h|$ of the occupied ground-state Fermi sea, and the energy bandwidth $W^h_{s1} = \varepsilon_s(k_{F\uparrow}) - \varepsilon_s(k_{F\downarrow}) = 2\mu_B\,|h|$ of the corresponding unoccupied $s1$ band. In Fig. 1(a) the $s1$ band energy bandwidth W_{s1}, Eq. (45), is plotted as a function of $1/u$ for several spin density values. It is a decreasing function of the ratio $u = U/4t$. The occupied Fermi sea energy bandwidths W^p_{s1} has the same type of u dependence behavior, as confirmed from analysis of Fig. 1(b) where the ratio W^p_{s1}/W_{s1} is also plotted as a function of $1/u$ for the same m values as in Fig. 1(a). That ratio is plotted as a function of the spin density m for $u = 1$ in Fig. 1(c).

Our present study does not refer to the PS of the $n_e = 1$ and $m = 0$ absolute ground state whose physics is qualitatively different from that of the present $h > 0$ spin quantum liquid. For such an absolute ground state the $s1$ band is full and the holes that emerge in that band under the transitions to the excited energy eigenstates are usually identified with spin-1/2 spinons [38,39,49]. Indeed at $h = 0$ the sn pseudoparticles of $n > 1$ branches created onto the absolute ground state have a sn dispersion with both vanishing momentum and energy bandwidth such that $\varepsilon_{sn}(q_j) = 0$ in Eq. (34). Hence the model $h = 0$ spin $SU(2)$ symmetry allows that the effects of their creation may be incorporated onto phase shifts of a spin-1/2 spinon only representation [49].

On the other hand, for $h > 0$ the energy dispersions $\varepsilon_{sn}(q_j)$, Eq. (34), of sn pseudoparticles of $n > 1$ branches have both a finite momentum and energy bandwidth. Hence they become elementary objects that exist in their own right. This renders the $h = 0$ spin-1/2 spinon only representation unsuitable for the $h > 0$ quantum problem considered here. Elsewhere it will be shown that the $s1$ band holes of the present $n_e = 1$ and $m > 0$ ground states and their excited energy eigenstates have scattering properties different from those of spin-1/2 objects, such as the $h = 0$ spin-1/2 spinons.

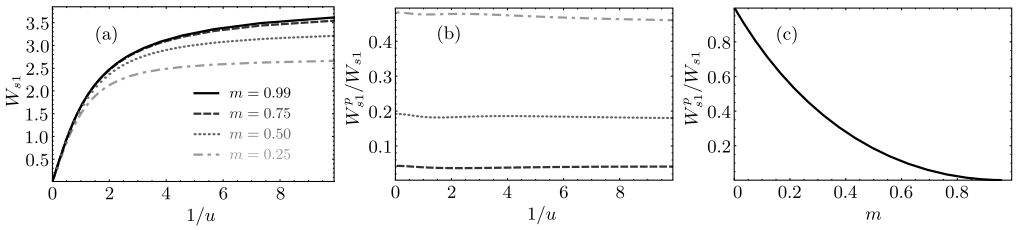

Fig. 1. (a) The $s1$ band energy bandwidth $W_{s1} = W^p_{s1} + W^h_{s1}$, Eq. (45), and (b) the ratio W^p_{s1}/W_{s1} plotted as a function of $1/u$ for several spin density m values, and (c) W^p_{s1}/W_{s1} plotted as a function of m for $u = 1$.

The functional energy spectrum, Eq. (33), rather describes the Mott–Hubbard insulator phase of the half-filled 1D Hubbard model at finite field h as a spin quantum liquid of sn pseudoparticles that have residual interactions associated with the f functions, Eq. (38). The $s1$ pseudoparticles play an important role in that quantum liquid, as the ground states are not populated by sn pseudoparticles of $n > 1$ branches. Consistently, the specific rapidity dressed phase shift $2\pi\,\bar{\Phi}_{s1\,s1}(r, r')$ plays a major role in the PDT expressions. Indeed only the $s1$ pseudoparticles have Fermi points, which are associated with the momentum values $\pm q_{Fs1} = \pm k_{F\downarrow}$. This applies as well to the corresponding $s1$ pseudofermions generated below from the $s1$ pseudoparticles by slightly shifting their discrete momentum values. The exponents that appear in the dynamical correlation functions expressions involve the following $l = 0, 1$ parameters that are fully controlled by the phase shifts acquired by $s1$ pseudofermions at the Fermi points under creation or annihilation of other $s1$ pseudofermions at or very near such points,

$$\xi^l_{s1,s1} = \xi^l_{s1,s1}(B/u) = 1 + \Phi_{s1,s1}\left(k_{F\downarrow}, k_{F\downarrow}\right) + (-1)^l \Phi_{s1,s1}\left(k_{F\downarrow}, -k_{F\downarrow}\right), \quad l = 0, 1. \tag{46}$$

(Due to the Pauli-like occupancies of the $s1$ band discrete momentum values being zero or one, the two Fermi momentum values in $\Phi_{s1,s1}\left(k_{F\downarrow}, k_{F\downarrow}\right)$ must differ by $2\pi/L$ with $2\pi/L \to 0$ in the present TL.)

The $l = 0, 1$ parameters in Eq. (46) are such that,

$$\xi^0_{s1,s1} = \frac{1}{\xi^1_{s1,s1}}, \tag{47}$$

where for $u > 0$ the parameter $\xi^1_{s1,s1}$ is an increasing function of m. For general m values it is u dependent whereas in the $m \to 0$ and $m \to 1$ limits it reaches universal u-independent values. Specifically, for $u > 0$ it reads $\xi^1_{s1,s1} = 1/\sqrt{2}$ in the $m \to 0$ limit and reaches its maximum value, $\xi^1_{s1,s1} = 1$, in the $m \to 1$ limit. In the $m \to 0$ limit this follows from the rapidity dressed phase shift $2\pi\,\bar{\Phi}_{s1,s1}(r, r')$ being given by,

$$\begin{aligned} 2\pi\,\bar{\Phi}_{s1,s1}(r, r') &= i \ln \frac{\Gamma\left(\frac{1}{2} + i\frac{(r-r')}{4}\right)\Gamma\left(1 - i\frac{(r-r')}{4}\right)}{\Gamma\left(\frac{1}{2} - i\frac{(r-r')}{4}\right)\Gamma\left(1 + i\frac{(r-r')}{4}\right)}; \quad r \neq \pm\infty \\ &= \frac{\iota\pi}{\sqrt{2}}; \qquad r = \iota B = \iota\infty, \qquad \iota = \pm 1, \qquad r' \neq r \\ &= \frac{\iota\pi}{\sqrt{2}}\left(3 - 2\sqrt{2}\right); \qquad r = r' = \iota B = \iota\infty, \qquad \iota = \pm 1, \end{aligned} \tag{48}$$

where $\Gamma(x)$ is the usual gamma function. Furthermore, in the $m \rightarrow 1$ limit its expression becomes,

$$2\pi\ \bar{\Phi}_{s1,s1}(r,r') = 2\arctan\Big(\frac{r-r'}{2}\Big)\,. \tag{49}$$

Within the present TL the problem concerning a *sn* pseudoparticle internal degrees of freedom in terms of electronic spins and that associated with its translational degrees of freedom center of mass motion separate. For $u > 0$ the *sn* pseudoparticle internal degrees of freedom involve the spins $1/2$ of the rotated electrons that occupy singly occupied sites, which we call here *rotated spins* $1/2$. These rotated electrons are generated from the electrons by a unitary transformation such that rotated-electron singly occupancy is a good quantum number for $u > 0$ [27,50]. There is an infinite number of such transformations, the specific rotated electrons associated with the BA quantum numbers corresponding to a unitary transformation uniquely defined by the BA.

Out of the many choices of $u \rightarrow \infty$ degenerate energy eigenstates belonging to the $N_c = L$ subspace, that transformation involves those obtained from the $u > 0$ Bethe states and corresponding non-LWSs, Eq. (24), as $|\infty, l_r, S, S^z\rangle = \lim_{u\rightarrow\infty} |u, l_r, S, S^z\rangle$. We call V *tower* the set of $N_c = L$ subspace energy eigenstates $|u, l_r, S, S^z\rangle$ with exactly the same independent-u quantum numbers l_r, S, S^z and different u values in the range $u > 0$. The amplitudes,

$$f_{u,l_r,S}(x_1\sigma_1,\ldots,x_L\sigma_L) = \langle x_1\sigma_1,\ldots,x_L\sigma_L|u,l_r,S,-S\rangle\,, \tag{50}$$

of Bethe states $|u, l_r, S, -S\rangle$ belonging to the same V tower smoothly and continuously behave as a function of u. Such amplitudes are uniquely defined in Eqs. (2.5)–(2.10) of Ref. [24] in terms of BA solution quantities. In the amplitudes, Eq. (50), $|x_1\sigma_1,\ldots,x_L\sigma_L\rangle$ denotes a local state in which the L electrons with spin projection $\sigma_1,\ldots,\sigma_L$ are located at sites of spatial coordinates $x,\ldots,x_L$, respectively. For a LWS their numbers are $N_\uparrow = L/2 + S$ and $N_\downarrow = L/2 - S$.

A useful property is that the amplitude $\langle x_1\sigma_1',\ldots,x_L\sigma_L'|u,l_r,S,S^z\rangle$ of a non-LWS $|u, l_r, S, S^z\rangle$ for which a number $n_s = 1,\ldots,2S$ of spins out of the L spins have been flipped relative to those of the corresponding LWS $|u, l_r, S, -S\rangle$ obeys the equality $\langle x_1\sigma_1',\ldots,x_L\sigma_L'|u,l_r,S,S^z\rangle = \langle x_1\sigma_1,\ldots,x_L\sigma_L|u,l_r,S,-S\rangle$. Hence $\langle x_1\sigma_1',\ldots,x_L\sigma_L'|u,l_r,S,S^z\rangle$ does not depend on the flipped spins and is given by $\langle x_1\sigma_1',\ldots,x_L\sigma_L'|u,l_r,S,S^z\rangle = f_{u,l_r,S}(x_1\sigma_1,\ldots,x_L\sigma_L)$.

For the $u \rightarrow \infty$ energy eigenstates $|\infty, l_r, S, S^z\rangle$ electron single occupancy is a good quantum number. It is not for the finite-u energy eigenstates $|u, l_r, S, S^z\rangle$ belonging to the same V tower because upon decreasing u there emerges a finite electron doubly occupancy expectation value, which vanishes for $u \rightarrow \infty$ [51]. Since for any $u > 0$ value the set of energy eigenstates $|u, l_r, S, S^z\rangle$ that belong to the same V tower are generated by exactly the same occupancy configurations of the u-independent quantum numbers l_r, S, and S^z, the $N_c = L$ subspace is the same for the whole $u > 0$ range. Hence for any $u > 0$ there is a uniquely defined unitary operator $\hat{V} = \hat{V}(u)$ such that $|u, l_r, S, S^z\rangle = \hat{V}^\dagger|\infty, l_r, S, S^z\rangle$. This operator $\hat{V}$ is the electron – rotated-electron unitary operator such that,

$$\tilde{c}^\dagger_{j,\sigma} = \hat{V}^\dagger\, c^\dagger_{j,\sigma}\, \hat{V}\,; \qquad \tilde{c}_{j,\sigma} = \hat{V}^\dagger\, c_{j,\sigma}\, \hat{V}\,; \qquad \tilde{n}_{j,\sigma} = \tilde{c}^\dagger_{j,\sigma}\, \tilde{c}_{j,\sigma}\,, \tag{51}$$

are the operators that create and annihilate, respectively, the rotated electrons as defined here. Moreover, $|\infty, l_r, S, S^z\rangle = \hat{G}^\dagger_{l_r,S,S^z}\,|0\rangle$ where $|0\rangle$ is the electron vacuum and $\hat{G}^\dagger_{l_r,S,S^z}$ a uniquely defined operator. It then follows that $|u, l_r, S, S^z\rangle = \tilde{G}^\dagger_{l_r,S,S^z}\,|0\rangle$ where the generator $\tilde{G}^\dagger_{l_r,S,S^z} = \hat{V}^\dagger\,\hat{G}^\dagger_{l_r,S,S^z}\,\hat{V}$ has the same expression in terms of the rotated-electron creation and annihilation operators as $\hat{G}^\dagger_{l_r,S,S^z}$ in terms of electron creation and annihilation operators, respectively.

For the 1D Hubbard model in the $N_c = L$ subspace such an electron – rotated-electron unitary operator $\hat{V}$ is uniquely defined by the set of the following matrix elements between the energy eigenstates that span such a subspace,

$$\langle u, l_{\rm r}, S, S^z|\hat{V}|u, l'_{\rm r}, S', S'^z\rangle = \delta_{S,S'}\delta_{S^z,S'^z}\sum_{x=1}^{L}\cdots\sum_{x_L=1}^{L} f^*_{u,l_{\rm r},S}(x_1\sigma_1,\ldots,x_L\sigma_L)\, f_{\infty,l'_{\rm r},S}(x_1\sigma_1,\ldots,x_L\sigma_L)\,. \quad (52)$$

Here $f_{u,l_{\rm r},S}(x_1\sigma_1,\ldots,x_L\sigma_L)$ and $f_{\infty,l'_{\rm r},S}(x_1\sigma_1,\ldots,x_L\sigma_L)$ are the amplitudes defined by Eqs. (2.5)–(2.10) of Ref. [24] for $u > 0$ and Eq. (2.23) of Ref. [25] for $u \to \infty$, respectively.

The electron – rotated-electron unitary operator $\hat{V}$ commutes with the three generators of the global $SU(2)$ symmetry algebra and the charge density operator. The rotated electrons have the same spins $1/2$ and charge as the electrons, the application of $\hat{V}$ only changing their spatial distribution. For $u > 0$ and $m < 1$ there is at all energy scales a non-perturbative charge-spin separation such that the L rotated-electron charges are associated with the L c pseudoparticles whose momentum band is full and the L rotated-electron spins $1/2$ are the rotated spins $1/2$ whose independent occupancy configurations determine the exotic properties of the 1D Mott Hubbard insulator.

The rotated spins $1/2$ occupancy configurations associated with the sn pseudoparticle internal degrees of freedom are implicitly accounted for by the BA solution. The microscopic details of such spin-singlet configurations are not needed for the studies of this paper. Here we only provide some general information on that interesting issue. The imaginary part of the $l = 1,\ldots,n$ rapidities $\Lambda^{sn,l}(q_j) = \Lambda^{sn}(q_j) + i\,(n+1-2l)\,u$, Eq. (31), with the same real part $\Lambda^{sn}(q_j)$ that emerge for $n > 1$ is for a q_j value occupied by a sn pseudoparticle associated with a set $l = 1,\ldots,n$ of singlet pairs of rotated spins $1/2$ and the binding of these pairs within the sn pseudoparticle. Each of such $l = 1,\ldots,n$ rapidities refers to one of the $l = 1,\ldots,n$ singlet pairs bound within the sn pseudoparticle. For $n = 1$ the rapidity imaginary part vanishes. Indeed, the $s1$ pseudoparticle internal degrees of freedom refer to a single singlet pair of rotated spins $1/2$.

For the quantum problem considered here one has that $2S_\eta = 0$ and $N_{\eta n} = 0$ for $n = 1,\ldots,\infty$ in Eq. (17). Hence the first sum rule given in that equation can be written as $L = 2S + \sum_{n=1}^{\infty} 2n\,N_{sn}$. Each of the original lattice $j = 1,\ldots,L$ sites is occupied by one rotated spin $1/2$. A number $\sum_{n=1}^{\infty} 2n\,N_{sn}$ of such rotated spins $1/2$ participate in $M_{s\,{\rm sp}} = \sum_{n=1}^{\infty} n\,N_{sn}$ spin-singlet pairs, Eq. (17) for $\alpha = s$. Those are contained in the set of the state sn pseudoparticles whose number is $N_{s\,ps} = \sum_{n=1}^{\infty} N_{sn}$. The latter number obeys the second sum rule in Eq. (15) for $\alpha = s$, which for the $N_c = L$ subspace reads $N_{s\,{\rm ps}} = \sum_{n=1}^{\infty} N_{sn} = (L - N^h_{s1})/2$. Similarly, the number $M_{s\,{\rm sp}}$ of spin-singlet pairs obeys the second sum rule in Eq. (17) for $\alpha = s$.

The remaining $2S$ rotated spins out of the system $L = 2S + \sum_{n=1}^{\infty} 2n\,N_{sn}$ rotated spins $1/2$ remain unpaired. They are those that participate in the $2S+1$ spin multiplet configurations, which are generated by an application of a number $n_s = 1,\ldots,2S$ of times of the off-diagonal spin operator $\hat{S}^+$ onto a LWS, as given in Eq. (24). Application of such an operator leaves the spin-singlet configurations of the $\sum_{n=1}^{\infty} n\,N_{sn}$ spin-singlet pairs contained in sn pseudoparticles unchanged. It merely flips the unpaired rotated spins $1/2$. For $u > 0$ the number $M^{un}_{\pm 1/2}$ of unpaired rotated spins of projection $\pm 1/2$ are good quantum numbers, which read,

$$M^{un}_{\pm 1/2} = (S \mp S^z)\,; \qquad M^{un} = (M^{un}_{-1/2} + M^{un}_{+1/2}) = 2S\,. \quad (53)$$

For the spin LWSs one has that $M^{un}_{+1/2} = M^{un} = 2S$ and $M^{un}_{-1/2} = 0$.

The *sn* pseudoparticle translational degrees of freedom associated with its center of mass motion are important for the PDT introduced below in Section 3, which implicitly accounts for its internal degrees of freedom through the BA quantities that contribute to the dynamical properties. The *sn* band momentum q_j in the argument of the rapidities real part $\Lambda^{sn}(q_j)$ is associated with such *sn* pseudoparticle translational degrees of freedom. That ground states are not populated by *sn* pseudoparticles containing $n > 1$ singlet pairs plays an important role in the PDT. Within it the dynamical correlation functions spectral weights are described by exotic quantum overlaps expressed in terms of $s1$ pseudofermion operators generated from $s1$ pseudoparticle operators by suitable shifts of the momentum values q_j. On the other hand, the quantum overlaps stemming from *sn* pseudoparticles of $n > 1$ branches are trivial to compute. The same applies to the overlaps associated with the unpaired rotated spins flipping processes.

For $u > 0$ the $s1$ pseudoparticles live in the TL on a squeezed $s1$ effective lattice [26,23,52]. Its number of sites equals that of $s1$ band discrete momentum values, Eq. (30) for $sn = s1$,

$$L_{s1} = N_{s1} + N^h_{s1}\,; \qquad N^h_{s1} = 2S + \sum_{n=2}^{\infty} 2(n-1)N_{sn}\,. \tag{54}$$

The N^h_{s1} unoccupied $s1$ effective lattice sites refer to the $2S = M^{un}$ sites occupied in the original lattice by the unpaired rotated spins $1/2$ and the sets of $2(n-1)$ sites of that lattice out of the $2n$ sites occupied by each *sn* pseudoparticle of $n > 1$ branches.

The line shape near the longitudinal and transverse dynamical structure factors, Eq. (1), spectra lower thresholds is below in Section 4 found to be determined by transitions to excited energy eigenstates that are not populated by *sn* pseudoparticles of $n > 1$ branches. The unpaired rotated spins $1/2$ of these states are used within the $s1$ pseudoparticle motion as unoccupied sites with which they interchange position. Within the BA solution such processes are accounted for by the $s1$ band occupancy configurations. Indeed the $M^{un} = 2S$ unpaired rotated spins $1/2$ have zero momentum. The energy of a unpaired rotated spin of spin projection $\pm 1/2$ relative to the ground state energy level is straightforwardly calculated by combining the LWSs momentum eigenvalues with such states and their non-LWSs transformation laws under the off-diagonal spin $SU(2)$ symmetry algebra generators, respectively, and is given by,

$$\varepsilon_{\pm 1/2} = 2\mu_s = 2\mu_B\,|h|\,; \qquad \varepsilon_{s,\mp 1/2} = 0\,, \qquad \text{sgn}\{m\} = \mp\,, \tag{55}$$

for $h \neq 0$ and vanishes at $h = 0$. The energy scale $2\mu_B\,|h|$ is that required for a spin flip. Spin flips generated by the off-diagonal spin operator $\hat{S}^+$ in Eq. (24) are the only processes whose energy is associated with the unpaired rotated spins $1/2$. They generate the transitions between the $2S+1$ multiplet configurations. An interesting related reference energy scale is that of a $S = 1$; $S^z = 0$ multiplet configuration involving two unpaired rotated spins of opposite spin projection. It is merely additive in the energies, Eq. (55), and reads,

$$\varepsilon_{1/2} + \varepsilon_{-1/2} = 2\mu_s = 2\mu_B\,|h|\,. \tag{56}$$

In general in this paper we use units of lattice spacing a one, so that the lattice length L equals the number of lattice sites N_a. In the TL the $s1$ effective lattice has $j = 1, \ldots, L_{s1}$ sites and length L. Hence it is a 1D lattice with spacing,

$$a_{s1} = \frac{N_a}{L_{s1}}\,a\,, \tag{57}$$

such that $L = L_{s1}\,a_{s1}$.

For the present $N_c = L$ subspace the general sum rules in Eqs. (15) and (17) lead to,

$$N_{s\,\mathrm{ps}} = \sum_{n=1}^{\infty} N_{sn} = \frac{1}{2}(L - N^h_{s1})\,; \qquad \sum_{n=1}^{\infty} 2n\, N_{sn} = L - 2S\,, \tag{58}$$

where $N_{s\,\mathrm{ps}}$ is the total number of sn pseudoparticles of all $n = 1, \ldots, \infty$ branches. Since $N^h_{s1} = L - 2N_{s\,\mathrm{ps}}$, the $s1$ effective lattice number of lattice sites L_{s1}, Eq. (54), remains unchanged provided that values of N_{s1} and $N_{s\,\mathrm{ps}}$ also do.

The $s1$ pseudoparticle translational degrees of freedom center of mass motion may be described by operators $f^{\dagger}_{j,s1}$ (and $f_{j,s1}$) that create (and annihilate) one $s1$ pseudoparticle at the $s1$ effective lattice site $x_j = a_{s1}\, j$ where $j = 1, \ldots, L_{s1}$. That each $s1$ band momentum value q_j where $j = 1, \ldots, L_{s1}$ has only Pauli-like occupancies zero and one is consistent with the local $s1$ pseudofermion operators obeying a Fermi algebra,

$$\{f^{\dagger}_{j,s1}, f_{j',s1}\} = \delta_{j,j'}\,. \tag{59}$$

Furthermore, one may introduce $s1$ pseudoparticle operators labeled by the $s1$ band momentum values,

$$f^{\dagger}_{q_j,s1} = \frac{1}{\sqrt{L}} \sum_{j'=1}^{L_{s1}} e^{iq_j\, j'} f^{\dagger}_{j',s1}; \qquad f_{q_j,s1} = \frac{1}{\sqrt{L}} \sum_{j'=1}^{L_{s1}} e^{-iq_j\, j'} f_{j',s1}, \quad j = 1, \ldots, L_{s1}. \tag{60}$$

That the pseudoparticle operators provide a faithful representation of the quantum problem and its BA solution and obey a fermionic algebra can be confirmed in terms of their statistical interactions [53]. This is a problem that we address here very briefly. The local operator $f^{\dagger}_{j,s1}$ may be written as $f^{\dagger}_{j,s1} = e^{i\phi_{j,s1}}\, g^{\dagger}_{j,s1}$ where $\phi_{j,s1} = \sum_{j'\neq j} f^{\dagger}_{j',s1}$ and $g^{\dagger}_{j,s1}$ obeys a hard-core bosonic algebra. This algebra is justified by the corresponding statistical interaction vanishing for the model in subspaces spanned by energy eigenstates with fixed L_{s1} value, Eq. (54). The $s1$ effective lattice has been constructed inherently to on it that algebra being of hard-core type. Therefore, through a Jordan–Wigner transformation, $f^{\dagger}_{j,s1} = e^{i\phi_{j,s1}}\, g^{\dagger}_{j,s1}$ [54], the operators $f^{\dagger}_{j,s1}$ obey indeed a fermionic algebra, Eq. (59). Besides acting within subspaces spanned by energy eigenstates with fixed L_{s1} values, the $s1$ pseudofermion operators labeled by momentum q_j, Eq. (60), also appear in the expressions of the shake-up effects generators that transform such subspaces quantum number values into each other.

2.3. The pseudofermion representation

From straightforward yet lengthly manipulations of the BA equations, Eq. (29), one finds that for PS excited energy eigenstates of $n_e = 1$ and $m > 0$ ground states the sn-band rapidity functionals $\Lambda^{sn}(q_j)$ can be written in terms of the corresponding ground-state rapidity function $\Lambda^{sn}_0(q_j)$ as follows,

$$\Lambda^{sn}(q_j) = \Lambda^{sn}_0\Big(\bar{q}(q_j)\Big)\,, \qquad j = 1, \ldots, L_{s1}\,. \tag{61}$$

Here $\bar{q}_j = \bar{q}(q_j)$ where $j = 1, \ldots, L_{sn}$ are the following discrete *canonical momentum* values,

$$\bar{q}_j = \bar{q}(q_j) = q_j + \frac{2\pi}{L}\Phi_{sn}(q_j) = \frac{2\pi}{L}\left(I^{sn}_j + \Phi_{sn}(q_j)\right)\,, \qquad j = 1, \ldots, L_{sn}\,. \tag{62}$$

The functional $\Phi_{sn}(q_j)$ in this equation reads,

$$\Phi_{sn}(q_j) = \sum_{n'=1}^{\infty} \sum_{j'=1}^{L_{sn'}} \Phi_{sn\,sn'}(q_j, q_{j'})\, \delta N_{sn'}(q_{j'})\,, \tag{63}$$

where the deviation $\delta N_{sn'}(q_{j'})$ and the dressed phase shift $2\pi\, \Phi_{sn\,sn'}(q_j, q_{j'})$ are given in Eqs. (32) and (40), respectively. The discrete canonical momentum values $\bar{q}_j = \bar{q}(q_j)$ have spacing $\bar{q}_{j+1} - \bar{q}_j = 2\pi/L +$ h.o. Here h.o. stands for terms of second order in $1/L$.

We call a *sn pseudofermion* each of the N_{sn} occupied *sn*-band discrete canonical momentum values $\bar{q}_j$ [28–30]. We call $s1$ *pseudofermion holes* the remaining N^h_{sn} unoccupied *sn*-band discrete canonical momentum values $\bar{q}_j$ of a PS energy eigenstate. There is a pseudofermion representation for each $n_e = 1$ and $m > 0$ ground state and its PS.

One generates from the $s1$ pseudoparticle creation and annihilation operators $f^{\dagger}_{q_j,s1}$ and $f_{q_j,s1}$, respectively, Eq. (60), the following corresponding $s1$ pseudofermion operators,

$$\bar{f}^{\dagger}_{\bar{q}_j,s1} = f^{\dagger}_{q_j+(2\pi/L)\,\Phi(q_j),s1} = \left(\hat{S}^{\Phi}\right)^{\dagger} f^{\dagger}_{q_j,s1}\, \hat{S}^{\Phi}\,; \qquad \bar{f}_{\bar{q}_j,s1} = (\bar{f}^{\dagger}_{\bar{q}_j,s1})^{\dagger}\,. \tag{64}$$

Here $\hat{S}^{\Phi}$ denotes the $s1$ pseudoparticle – $s1$ pseudofermion unitary operator,

$$\hat{S}^{\Phi} = e^{\sum_{j=1}^{L_{s1}} f^{\dagger}_{q_j+(2\pi/L)\,\Phi(q_j),s1} f_{q_j,s1}}\,; \qquad \left(\hat{S}^{\Phi}\right)^{\dagger} = e^{\sum_{j=1}^{L_{s1}} f^{\dagger}_{q_j-(2\pi/L)\,\Phi(q_j),s1} f_{q_j,s1}}\,. \tag{65}$$

In this equation and in the following we use the notation,

$$\Phi(q_j) \equiv \Phi_{s1}(q_j) = \sum_{n'=1}^{\infty} \sum_{j'=1}^{L_{sn'}} \Phi_{1n\,sn'}(q_j, q_{j'})\, \delta N_{sn'}(q_{j'})\,, \tag{66}$$

for the functional, Eq. (63), of the $sn = s1$ branch.

The *sn* pseudofermions have the same internal structure as the corresponding *sn* pseudoparticles. Indeed they differ in their discrete momentum values, which rather refer to the translational degrees of freedom. For the initial ground state one has that $\bar{q}_j = q_j$. Hence for that state the *sn* pseudofermions and *sn* pseudoparticles are identical objects. Several pseudofermion quantities are expressed in terms of such an initial-state unshifted *sn* pseudofermion canonical momentum values q_j. An example is the function $2\pi\, \Phi_{sn\,sn'}(q_j, q_{j'})$, Eq. (40), (and $-2\pi\, \Phi_{sn\,s1}(q_j, q_{j'})$) in the functional expression, Eq. (63). It is the phase shift acquired by a *sn* pseudofermion or a *sn* pseudofermion hole of canonical momentum occupied or unoccupied in the final state, respectively, upon scattering off a sn' pseudofermion (and $s1$ pseudofermion hole) created at the initial ground-state momentum $q_{j'}$ under a transition from the latter state to a PS excited energy eigenstate. (For $n > 1$ the phase shift $2\pi\, \Phi_{sn\,sn'}(q_j, q_{j'})$ or $-2\pi\, \Phi_{sn\,s1}(q_j, q_{j'})$ is acquired by a *sn* pseudofermion of canonical momentum $\bar{q}_j = q_j + (2\pi/L)\, \Phi_{sn}(q_j)$ associated with the initial-state canonical momentum q_j, which has also been created under such a transition.) As confirmed below, the functional $\Phi(q_j)$, Eq. (66), controls the spectral weights of the spin dynamical correlation functions.

Within the $s1$ pseudofermion motion in the $s1$ effective lattice the $M^{un} = 2S$ unpaired rotated spins $1/2$ play the role of unoccupied sites. Such unpaired rotated spins $1/2$ are zero-momentum objects that under the transitions from a ground state to its PS excited energy eigenstates do not acquire phase shifts. Furthermore the unpaired rotated spins flips that occur under some of such

transitions are scattering-less processes that do not lead to pseudofermion phase shifts. Hence the $M^{un} = 2S$ unpaired rotated spins $1/2$ are neither scatterers nor scattering centers.

Upon expressing the PS energy functional, Eq. (33), in terms of the discrete canonical momentum values $\bar{q}_j = \bar{q}(q_j)$, Eq. (62), it reads up to $\mathcal{O}(1/L)$ order,

$$\begin{aligned}\delta E &= \sum_{n=1}^{\infty}\sum_{j=1}^{L_{sn}} \varepsilon_{sn}(\bar{q}_j)\,\delta\mathcal{N}_{sn}(\bar{q}_j) + 2\mu_B\,|h|\,(S+S^z)\,, \\ &= \sum_{n=1}^{\infty}\sum_{j=1}^{L_{sn}} \varepsilon_{sn}(\bar{q}_j)\,\delta\mathcal{N}_{sn}(\bar{q}_j) + \varepsilon_{-1/2}\,M^{un}_{-1/2}\,. \end{aligned} \tag{67}$$

Here the sn pseudofermion energy dispersions $\varepsilon_{sn}(\bar{q}_j)$ have exactly the same form as those given in Eq. (34) with the momentum q_j replaced by the corresponding canonical momentum, $\bar{q}_j = \bar{q}(q_j)$. Moreover, $\varepsilon_{-1/2}\,M^{un}_{-1/2}$ where $\varepsilon_{-1/2} = 2\mu_B\,|h|$ corresponds for $m > 0$ to the energy associated with spin flipping a number $M^{un}_{-1/2}$ of unpaired rotated spins $1/2$.

If in Eq. (67) one expands the sn band canonical momentum $\bar{q}_j = q_j + (2\pi/L)\,\Phi_{sn}(q_j)$ around q_j and considers all energy contributions up to $\mathcal{O}(1/L)$ order, one arrives after some algebra to the energy functional, Eq. (33), which includes terms of second order in the deviations $\delta N_{sn}(q_j)$. Their absence from the corresponding energy spectrum, Eq. (67), results from the functional $\Phi_{sn}(q_j)$, Eq. (63), being incorporated in the sn band canonical momentum, Eq. (62).

It follows that in contrast to the equivalent energy functional, Eq. (33), that in Eq. (67) has no energy interaction terms of second-order in the deviations $\delta\mathcal{N}_{sn}(\bar{q}_j)$. This property simplifies the expression of the spin dynamical correlation functions in terms of $s1$ pseudofermion spectral functions. Specifically, their spectral weights can be expressed as Slater determinants of $s1$ pseudofermion operators. In the case of the PDT suitable for the metallic phase of the 1D Hubbard model [28,29], that property also allows the dynamical correlation functions being expressed as a convolution of c and $s1$ pseudofermion spectral functions. Such convolutions are absent though from the modified PDT introduced in the following.

That within the $s1$ pseudofermion representation the functional $\Phi(q_j) \equiv \Phi_{s1}(q_j)$, Eq. (66), is incorporated in the canonical momentum, Eq. (62), has also consequences on the form of the above mentioned Slater determinants of the $s1$ pseudofermion operators, Eq. (64), which can be written as,

$$\bar{f}^{\dagger}_{\bar{q}_j,s1} = \frac{1}{\sqrt{L}}\sum_{j'=1}^{L_{s1}} e^{i\bar{q}_j\,j'}\,\bar{f}^{\dagger}_{j',s1}; \qquad \bar{f}_{\bar{q}_j,s1} = \frac{1}{\sqrt{L}}\sum_{j'=1}^{L_{s1}} e^{-i\bar{q}_j\,j'}\,\bar{f}_{j',s1}, \quad j = 1,\ldots,L_{s1}. \tag{68}$$

As in the case of the corresponding $s1$ pseudoparticle operators, Eq. (60), the operator $\bar{f}^{\dagger}_{j',s1}$ (and $\bar{f}_{j',s1}$) creates (and annihilates) one $s1$ pseudofermion at the $s1$ effective lattice site $x_{j'} = a_{s1}\,j'$ where $j' = 1,\ldots,L_{s1}$. Indeed, the $s1$ pseudofermions also live in the squeezed $s1$ effective lattice. And as in Eq. (59) for the local $s1$ pseudoparticle operators, the corresponding local $s1$ pseudofermion operators obey the Fermi algebra,

$$\{\bar{f}^{\dagger}_{j,s1},\,\bar{f}_{j',s1}\} = \delta_{j,j'}\,. \tag{69}$$

Consider two $s1$ pseudofermions of canonical momentum $\bar{q}_j$ and $\bar{q}_{j'}$, respectively. Here $\bar{q}_j$ and $\bar{q}_{j'} = q_{j'}$ refer to a PS excited-energy-eigenstate and the corresponding initial ground-state

$s1$ band, respectively. From the use of Eqs. (62) for $sn = s1$, (68), and (69) one then finds the anticommutators,

$$\{\bar{f}^{\dagger}_{\bar{q}_j,s1}, \bar{f}_{\bar{q}_{j'},s1}\} = \{\bar{f}^{\dagger}_{\bar{q}_j,s1}, \bar{f}_{q_{j'},s1}\} = \frac{1}{L}\, e^{-i(\bar{q}_j - q_{j'})/2}\, e^{i\,2\pi\,\Phi^T(q_j)/2}\, \frac{\sin\left(2\pi\,\Phi^T(q_j)/2\right)}{\sin((\bar{q}_j - q_{j'})/2)}\,,$$
$$\Phi^T(q_j) = \Phi^0_{s1} + \Phi(q_j)\,, \tag{70}$$

and $\{\bar{f}^{\dagger}_{\bar{q}_j,s1}, \bar{f}^{\dagger}_{\bar{q}_{j'},s1}\} = \{\bar{f}_{\bar{q}_j,s1}, \bar{f}_{\bar{q}_{j'},s1}\} = 0$. Here $\Phi^T(q_j)$ is the overall phase shift acquired by a $s1$ pseudofermion of momentum q_j under the transition from the ground state to the PS excited-energy-eigenstate, Φ^0_{s1}, Eq. (28), is the corresponding non-scattering part of that phase shift, and $\Phi(q_j)$, Eq. (66), is its scattering part.

For $2\pi\,\Phi^T(q_j) \to 0$ the anticommutator relation, Eq. (70), would be the usual one, $\{f^{\dagger}_{\bar{q}_j,s1}, f_{q_{j'},s1}\} = \delta_{\bar{q}_j,\bar{q}'_j}$. That such an anticommutator relation has not that simple form is the price to pay to render the $s1$ pseudofermions non-interacting objects associated with an energy spectrum of form, Eq. (67). Indeed this is achieved by incorporating the functional $\Phi(q_j)$, Eq. (66), in the $s1$ band canonical momentum, Eq. (62) for $sn = s1$. The unusual form, Eq. (70), of that anticommutator relation is behind the phase-shift functional $\Phi(q_j)$ controlling the spectral weight distributions of spin dynamical correlation functions, as confirmed below.

The unitarity of the $s1$ pseudoparticle – $s1$ pseudofermion transformation preserves the $s1$ pseudoparticle operator algebra provided that the canonical momentum values $\bar{q}_j$ and $\bar{q}_{j'}$ belong to the $s1$ band of the same energy eigenstate. The exotic form of the anticommutator, Eq. (70), follows from $\bar{q}_j$ and $\bar{q}_{j'} = q_{j'}$ corresponding in it rather to the excited-energy-eigenstate $s1$ band and the ground-state $s1$ band, respectively.

3. The Mott–Hubbard insulator pseudofermion dynamical theory

The Mott–Hubbard insulator PDT considered here profits from the sn pseudofermions having no energy interactions, as given in Eq. (67), and accounts for such elementary objects scattering events. Its aim is the evaluation of finite-ω spin dynamical correlation functions of general form,

$$B(k,\omega) = \sum_f |\langle f|\,\hat{O}(k)|GS\rangle|^2\,\delta\Big(\omega - (E_f - E_{GS})\Big)\,, \qquad \omega > 0\,. \tag{71}$$

Here $\hat{O}(k)$ is a corresponding spin operator whose application onto the ground state conserves the BA number $N_c = L$ of c pseudoparticles, $|GS\rangle$ is that ground state, and $|f\rangle$ denotes its PS excited energy eigenstates contained in the excitation $\hat{O}(k)|GS\rangle$.

In the present case of the spin dynamical correlation functions of the half-filled 1D Hubbard model, the elementary processes that generate such excited energy eigenstates from ground states with spin densities $0 < m < 1$ can be classified into three (A)–(B) classes:

(A) High-energy elementary $s1$ pseudofermion (and $sn \neq s1$ pseudofermion) and (if any) unpaired rotated spins flipping processes. The pseudofermion processes involve creation or annihilation (and creation) of one or a finite number of $s1$ pseudofermions (and $sn \neq s1$ pseudofermions) with canonical momentum values $\bar{q}_j \neq \pm\bar{q}_{Fs1}$ (and canonical momentum values $\bar{q}_j \in [q^-_{sn}, q^+_{sn}]$).

(B) Zero-energy and finite-momentum processes that change the number of $s1$ pseudofermions at the $\iota = +1$ right and $\iota = -1$ left $s1$ Fermi points.

(C) Low-energy and small-momentum elementary $s1$ pseudofermion – $s1$ pseudofermion-hole processes in the vicinity of their right ($\iota = +1$) and left ($\iota = +1$) Fermi points, relative to the excited-state $s1$ pseudofermion momentum occupancy configurations generated by the above elementary processes (A) and (B).

3.1. Pseudofermion representation of the matrix elements of the spin operators between the ground state and the excited energy eigenstates

Within the PDT, the matrix elements $\langle f|\,\hat{O}(k)|GS\rangle$ in Eq. (71) of the spin operators between the ground state and the excited energy eigenstates are expressed in the pseudofermion representation. The $S > 0$ ground state in these matrix elements has in such a representation the simple form,

$$|GS\rangle = \prod_{\bar{q}=-k_{F\downarrow}}^{k_{F\downarrow}} \prod_{\bar{q}'=-\pi}^{\pi} \bar{f}^{\dagger}_{\bar{q},\,s1}\,\bar{f}^{\dagger}_{\bar{q}',\,c}|0\rangle = \prod_{j=1}^{N_{\downarrow}} \prod_{j'=1}^{L} \bar{f}^{\dagger}_{\bar{q}_j,\,s1}\,\bar{f}^{\dagger}_{\bar{q}_{j'},\,c}|0\rangle$$
$$\bar{f}^{\dagger}_{\bar{q},\,\beta} = f^{\dagger}_{q,\beta}\,, \qquad \beta = c, s1\,, \tag{72}$$

where $|0\rangle$ stands for the electron and rotated-electron vacuum, the ground-state generator has been written in terms of $s1$ and c pseudofermion creation operators, and the corresponding $s1$ and c band momentum values $\bar{q} = q = \bar{q}_j = q_j$ and $\bar{q}' = q' = \bar{q}_{j'} = q_{j'}$, respectively, are those of the corresponding occupied ground-state Fermi seas. The $s1$ and c band discrete momentum values of any energy eigenstate are uniquely defined in Eqs. (10) and (11). (We recall that the pseudofermion representation has been inherently constructed to $\bar{q} = q$ for a PS initial ground state.)

To express the matrix elements $\langle f|\,\hat{O}(k)|GS\rangle$ appearing in Eq. (71) in the pseudofermion representation, one must introduce the local spin operators associated with the rotated spins $1/2$ whose singlet pairs refer to the internal degrees of freedom of the n-pair sn pseudofermions. On the other hand and as discussed below, within the pseudofermion representation the $M^{un} = 2S$, Eq. (53), unpaired rotated spins are used by the $s1$ pseudofermions as unoccupied sites of their $s1$ effective lattice. Hence all the system L rotated spins $1/2$ are accounted for by the pseudofermion representation.

The first step to express the matrix elements $\langle f|\,\hat{O}(k)|GS\rangle$ in the pseudofermion representation is to express the corresponding one- and two-electron operator $\hat{O}(k)$ in terms of creation and annihilation rotated-electron operators, Eq. (51). Indeed, the rotated spins $1/2$ are the spins of the rotated electrons generated from the electrons by the specific unitary operator $\hat{V}$ defined in Eq. (52). Some of the procedures followed to achieve that expression differ from those used within the metallic-phase PDT of Refs. [28,29]. Indeed, the latter refers to operators $\hat{O}(k)$ that change the c pseudoparticle occupancies, which except for possible overall $\pm\pi/L$ momentum shifts of all $N_c = L$ c pseudofermions remain unchanged for the quantum problem considered here.

The use of the Baker–Campbell–Hausdorff formula leads to the following expression of a general operator $\hat{O}$ in terms of the creation and annihilation rotated-electron operators, Eq. (51),

$$\hat{O} = \sum_{i=0}^{\infty} \hat{O}_i = \tilde{O} + [\tilde{O}, \tilde{S}\,] + \frac{1}{2}[[\tilde{O}, \tilde{S}\,], \tilde{S}\,] + \ldots\,,$$
$$\hat{O}_i = [\tilde{O}, \tilde{S}\,]_i = [[\tilde{O}, \tilde{S}\,]_{i-1}, \tilde{S}\,], \quad i = 1, \ldots, \infty\,; \qquad [\tilde{O}, \tilde{S}\,]_0 = \tilde{O} = \hat{V}^{\dagger}\,\hat{O}\,\hat{V}\,, \tag{73}$$

where the operators $\tilde{O}$ and $\tilde{S}$ have the same expression in terms of creation and annihilation rotated-electron operators as $\hat{O}$ and $\hat{S}$, respectively, in terms of creation and annihilation electron operators.

There are two qualitatively different situations that follow from symmetry. The first refers to operators $\hat{O}$ that commute with the electron – rotated-electron unitary operator $\hat{V}$, Eq. (52). It follows from Eq. (73) that $\hat{O} = \tilde{O} = \hat{V}^{\dagger}\,\hat{O}\,\hat{V}$, so that such operators have exactly the same expression in terms of creation/annihilation electron and rotated-electron operators, respectively. Trivial examples are $\hat{V} = e^{\hat{S}}$ and $\hat{S}$, which commute with theirself, and thus according to the general formulas, Eq. (73), are such that $\hat{V} = e^{\hat{S}} = \tilde{V} = e^{\tilde{S}}$ and $\hat{S} = \tilde{S}$, respectively. Other examples of such operators are the six generators of the model spin and η-spin $SU(2)$ symmetry algebras and the momentum operator whose eigenvalues are given in Eq. (19).

On the other hand, for most operators it holds that $[\hat{O}, \hat{S}] \neq 0$. Their expressions have in terms of creation and annihilation rotated-electron operators an infinite number of terms, $\hat{O} = \sum_{i=0}^{\infty} \hat{O}_i$, as given in Eq. (73). This is the case of the model Hamiltonian and most one- and two-electron operators $\hat{O}(k)$ in dynamical correlation functions Lehmann representations, Eq. (71). Except in the $u \rightarrow \infty$ limit, the same applies to the three $l = z, \pm$ local spin operators $\hat{S}^l_j$, which when expressed in terms of rotated-electron operators have thus an infinite number of terms,

$$\hat{S}^l_j = \sum_{i=0}^{\infty} \hat{S}^l_{j,i} = \tilde{S}^l_j + [\tilde{S}^l_j, \tilde{S}] + \frac{1}{2}[[\tilde{S}^l_j, \tilde{S}], \tilde{S}] + \ldots , \qquad l = z, \pm . \tag{74}$$

Interestingly,

$$\tilde{S}^l_j = \hat{V}^{\dagger}\,\hat{S}^l_j\,\hat{V} , \quad l = z, \pm ; \qquad \tilde{S}^{\pm}_j = \tilde{S}^x_j \pm i\,\tilde{S}^y_j , \tag{75}$$

are here the $l = z, \pm$ local operators associated with the rotated spins $1/2$.

The creation and annihilation rotated-electron operators, Eq. (51), can be uniquely expressed in terms of such three $l = z, \pm$ rotated-spin-$1/2$ operators, three corresponding rotated-η-spin-$1/2$ operators, and c pseudoparticle operators, and vice versa. Here we are interested in the 1D Hubbard model in the subspace for which $N_c = L$. For that quantum problem, the number of rotated-electron doubly occupied sites vanishes for $u > 0$, so that the η-spin degrees of freedom are frozen and one may omit the rotated-η-spin-$1/2$ operators from all operational expressions. The corresponding more general operational expressions valid for the 1D Hubbard model in its full Hilbert space of the rotated-spin $1/2$, rotated-η-spin $1/2$, and c pseudoparticle operators in terms of rotated-electron operators and of the latter operators in terms of the former are given in Appendix A. Those provided in the following are particular cases of the general expressions in that Appendix.

The three $l = z, \pm$ local rotated spin operators $\tilde{S}^l_j$, which in Appendix A are denoted by $\tilde{S}^l_{j,s}$, and corresponding three $l = z, \pm$ generators $\hat{S}^l = \tilde{S}^l$ of the global spin $SU(2)$ symmetry algebra, which commute with the electron – rotated-electron unitary operator $\hat{V}$, Eq. (52), can be written in terms of the rotated-electron operators, Eq. (51), as follows,

$$\begin{aligned} &\tilde{S}^-_j = (\tilde{S}^+_j)^{\dagger} = \tilde{c}^{\dagger}_{j,\uparrow}\,\tilde{c}_{j,\downarrow}; \qquad \tilde{S}^z_j = (\tilde{n}_{j,\downarrow} - 1/2); \\ &\tilde{S}^l = \sum_{j=1}^{L} \tilde{S}^l_j = \sum_{j=1}^{L} \tilde{c}^{\dagger}_{j,\uparrow}\,\tilde{c}_{j,\downarrow}, \quad l = z, \pm , \end{aligned} \tag{76}$$

where the operator $\tilde{n}_{j,\downarrow}$ is given in Eq. (51) for $\sigma = \downarrow$.

Moreover, the c pseudoparticle operators labeled by the discrete momentum values $q_{j'} = (2\pi/L)\, I^c_{j'}$, Eqs. (9) and (10) for $\beta = c$, are given by,

$$f^{\dagger}_{q_{j'},c} = (f_{q_{j'},c})^{\dagger} = \frac{1}{\sqrt{L}} \sum_{j=1}^{L} e^{+iq_{j'}j}\, f^{\dagger}_{j,c}\,, \qquad j' = 1,\ldots,L\,, \tag{77}$$

where for the present case of the 1D Hubbard model in the $N_c = L$ subspace the general expression of the operator $f^{\dagger}_{j,c} = (f_{j,c})^{\dagger}$ in terms of creation and annihilation rotated-electron operators, Eq. (A.1) of Appendix A, simplifies to,

$$f^{\dagger}_{j,c} = (f_{j,c})^{\dagger} = \tilde{c}^{\dagger}_{j,\uparrow}\,(1-\tilde{n}_{j,\downarrow})\,; \qquad n_{j,c} = f^{\dagger}_{j,c}\, f_{j,c}\,, \qquad j = 1,\ldots,L\,. \tag{78}$$

The operators $f^{\dagger}_{j,c}$ and $f_{j,c}$ create and annihilate, respectively, one c pseudoparticle at the $j = 1,\ldots,L$ site of the c *effective lattice*, which is identical to the model original lattice.

Furthermore, the expression in terms of rotated-electron operators given in Eq. (A.2) of Appendix A for c pseudofermion operators, Eq. (64) for $\beta = c$, becomes for the model in the $N_c = L$ subspace,

$$\bar{f}^{\dagger}_{\bar{q}_j,c} = \frac{1}{\sqrt{L}} \sum_{j'=1}^{L} e^{+i\bar{q}_j j'}\, \tilde{c}^{\dagger}_{j',\uparrow}\,(1-\tilde{n}_{j',\downarrow})\,; \qquad \bar{f}_{\bar{q}_j,c} = (\bar{f}^{\dagger}_{\bar{q}_j,c})^{\dagger}\,, \qquad j = 1,\ldots,L\,. \tag{79}$$

In the $u \rightarrow \infty$ limit, the ground-state momentum rapidity function $k^c_0(q_j)$ simplifies to $k^c_0(q_j) = q_j$. Hence, according to Eq. (61), for its PS excited energy eigenstates such a function reads, $k^c(q_j) = \bar{q}_j$. The $u \rightarrow \infty$ spinless fermions of Refs. [22,23] have been constructed inherently to carry the momentum rapidity $k_j = k^c(q_j) = \bar{q}_j$. This reveals that such spinless fermions are the c pseudofermions as defined here in the $u \rightarrow \infty$ limit. Indeed, $\bar{f}^{\dagger}_{\bar{q}_j,c} = \hat{V}^{\dagger}\, b^{\dagger}_{k_j}\, \hat{V}$ and $\bar{f}_{\bar{q}_j,c} = \hat{V}^{\dagger}\, b_{k_j}\, \hat{V}$ where $b^{\dagger}_{k_j}$ and b_{k_j} stand for the $u \rightarrow \infty$ spinless fermions creation and annihilation operators that appear in the anti-commutators given in the first equation of Section IV of Ref. [23]. Such a relation between $u \rightarrow \infty$ spinless fermions and $u > 0$ c pseudofermions holds provided that $\hat{V}$ is the electron – rotated-electron unitary operator defined in terms of its matrix elements in Eq. (52).

Inversion of the relations, Eqs. (76) and (78), leads to the following simplified form of the general expressions given in Eq. (A.6) of Appendix A,

$$\begin{aligned} &\tilde{c}^{\dagger}_{j,\uparrow} = f^{\dagger}_{j,c}\left(\frac{1}{2} - \tilde{S}^{z}_{j}\right)\,; \qquad \tilde{c}_{j,\uparrow} = (\tilde{c}^{\dagger}_{j,\uparrow})^{\dagger}\,, \\ &\tilde{c}^{\dagger}_{j,\downarrow} = f^{\dagger}_{j,c}\,\tilde{S}^{+}_{j}\,; \qquad \tilde{c}_{j,\downarrow} = (\tilde{c}^{\dagger}_{j,\downarrow})^{\dagger}\,, \end{aligned} \tag{80}$$

where $(\tilde{S}^{+}_{j})^{\dagger} = \tilde{S}^{-}_{j}$. The rotated-electron degrees of freedom separation, Eq. (80), is such that the rotated-spin 1/2 operators, Eq. (76), and the c pseudoparticle operators, Eq. (78), emerge from the rotated-electron operators by an exact local transformation that does not introduce constraints.

The unitarity of the electron – rotated-electron transformation implies that the rotated-electron operators $\tilde{c}^{\dagger}_{j,\sigma}$ and $\tilde{c}_{j,\sigma}$, Eq. (51), have the same anticommutation relations as the corresponding electron operators $c^{\dagger}_{j,\sigma}$ and $c_{j,\sigma}$, respectively. From the combination of that result with the use of Eq. (76), one confirms that the $SU(2)$ algebra obeyed by the local rotated-spin operators $\tilde{s}^{l}_{j}$ is the usual one,

$$[\tilde{S}^{+}_{j,s}, \tilde{S}^{-}_{j',s}] = \delta_{j,j'} 2\tilde{S}^{z}_{j,s}\,; \quad [\tilde{S}^{\pm}_{j}, \tilde{S}^{z}_{j',s}] = \mp\delta_{j,j'}\tilde{S}^{\pm}_{j,s}\,; \quad [\tilde{S}^{l}_{j}, \tilde{S}^{l}_{j'}] = 0, \quad l = z,\pm. \tag{81}$$

Furthermore, straightforward manipulations based on Eqs. (76) and (78) lead to the operator algebra $\{f^{\dagger}_{j,c}\,,\,f_{j',c}\}=\delta_{j,j'}$ and $\{f^{\dagger}_{j,c}\,,\,f^{\dagger}_{j',c}\}=\{f_{j,c}\,,\,f_{j',c}\}=0$ for the c pseudoparticle operators, Eq. (78), and,

$$[f^{\dagger}_{j,c}\,,\,\tilde{S}^{l}_{j'}]=[f_{j,c}\,,\,\tilde{S}^{l}_{j'}]=0\,,\qquad l=z,\pm\,, \tag{82}$$

for the c pseudoparticle operators and the local spin operators, Eq. (76).

The 1D Hubbard model is a non-perturbative quantum problem in terms of electron processes. This is behind the computation of its dynamical correlation functions, Eq. (71), which involve a given one- or two-electron operator $\hat{O}(k)$, being a very complex many-electron problem. On the other hand, a property that plays a central role in the PDT follows from expressing the operator $\hat{O}(k)$ in the terms of the rotated-electron operators, Eq. (51), generated by application of the unitary operator $\hat{V}$ defined in Eq. (52) as $\hat{O}(k)=\sum_{i=0}^{\infty}\hat{O}_i(k)$, Eq. (73). It is that the latter expression renders the computation of the dynamical correlation functions, Eq. (71), a perturbative problem in terms of the processes involving the rotated spins $1/2$ that emerge from the rotated electrons and the *sn* pseudofermions within which the corresponding rotated-spin singlet pairs are contained. Indeed, the inconvenience that in terms of rotated-electron operators the one- or two-electron operator $\hat{O}(k)=\sum_{i=0}^{\infty}\hat{O}_i(k)$, Eq. (73), has an infinite number of terms is the price that must be paid to render the computation of such dynamical functions a perturbative problem.

The next step of our program consists in rewriting the rotated-electron expression $\hat{O}(k)=\sum_{i=0}^{\infty}\hat{O}_i(k)$ within a related uniquely defined pseudofermion representation as,

$$\hat{O}(k)=\sum_{i'=0}^{\infty}\hat{G}_{i'}(k)\,\hat{O}^{\odot}_{GS}\,. \tag{83}$$

The new index $i'=0,1,\ldots,\infty$ refers here to *sn* pseudofermions processes and $\hat{O}^{\odot}_{GS}$ is a generator that transforms the initial ground state $|GS\rangle$ into a state with the same electron and rotated-electron numbers $N_{\uparrow}$ and $N_{\downarrow}$ and compact symmetrical $s1$ band momentum occupancies as the intermediate final ground state, which we call $|GS_f\rangle$. The only difference between the states $\hat{O}^{\odot}_{GS}|GS\rangle$ and $|GS_f\rangle$ is the $s1$ band discrete momentum values of the former state being those of the initial ground state, $\bar{q}'=q'$. (For one- or two-electron operators that conserve the numbers $N_{\uparrow}$ and $N_{\downarrow}$, one has that $\hat{O}(k)=\sum_{i'=0}^{\infty}\hat{G}_{i'}(k)$ in Eq. (83).)

Each term of index $i'=0,1,\ldots,\infty$ in Eq. (83) may have contributions from several terms of different index $i=0,1,\ldots,\infty$ in $\hat{O}(k)=\sum_{i=0}^{\infty}\hat{O}_i(k)$, Eq. (73). Fortunately, one can compute the operational form in terms of pseudofermion operators of the leading $i'=0,1,\ldots,\infty$ orders of $\hat{O}(k)=\sum_{i'=0}^{\infty}\hat{G}_{i'}(k)\,\hat{O}^{\odot}_{GS}$ from the transformation laws of the ground state $|GS\rangle$, Eq. (72), upon acting onto it the related operators $\hat{O}_i(k)$ in the expression $\hat{O}(k)=\sum_{i=0}^{\infty}\hat{O}_i(k)$.

Note that both the expressions $\hat{O}(k)=\sum_{i=0}^{\infty}\hat{O}_i(k)$ and $\hat{O}(k)=\sum_{i'=0}^{\infty}\hat{G}_{i'}(k)\,\hat{O}^{\odot}_{GS}$ are not small-parameter expansions. Consistently, the perturbative character of the *sn* pseudofermions processes refers to the spectral weight contributing to the dynamical correlation functions being dramatically suppressed upon increasing the number of corresponding elementary processes of classes (A) and (B). Those are generated by application onto the ground state, Eq. (72), of operators in $\sum_{i'=0}^{\infty}\hat{G}_{i'}(k)\,\hat{O}^{\odot}_{GS}$ with an increasingly large value of the index $i'=0,1,\ldots,\infty$.

The perturbative character of the 1D Hubbard model upon expressing the one- or two-electron operators $\hat{O}(k)$ in dynamical correlation functions, Eq. (71), in terms of rotated-spins $1/2$ operators and corresponding *sn* pseudofermion operators follows from the exact energy eigenstates being generated by occupancy configurations of these elementary objects. The non-perturbative

character of the problem in terms of electrons results from their relation to the rotated-spins 1/2 and corresponding *sn* pseudofermions having as well a non-perturbative nature, qualitatively different from that of the electrons to the quasiparticles of a Fermi liquid.

For simplicity, in the following we denote the $i' = 0$ operator $\hat{G}_0(k)$ associated with any one- or two-electron operator $\hat{O}(k)$ by $\hat{G}(k)$. Such a $i' = 0$ leading-order operator term in the one- or two-electron operator expression,

$$\hat{O}(k) = (\hat{G}(k) + \sum_{i'=1}^{\infty} \hat{G}_{i'}(k))\, \hat{O}_{GS}^{\odot}\,, \tag{84}$$

plays a key role in our study.

As a particularly simple yet very convenient example of the expression of the matrix elements $\langle f|\, \hat{O}(k)|GS\rangle$ in Eq. (71) in the pseudofermion representation, we consider in the following the spin dynamical correlation functions studied in this paper, Eq. (1). As often below in Sec. 4, we chose as corresponding operators $\hat{O}(k)$ the three $l = z, \pm$ spin operators $\hat{S}^l_k$ associated with the local spin operators $\hat{S}^l_j$. The corresponding spin dynamical correlation functions are $S^{zz}(k,\omega)$, $S^{+-}(k,\omega)$, and $S^{-+}(k,\omega)$, which are such that the spin dynamical structure factors $S^{xx}(k,\omega) = S^{yy}(k,\omega)$ in Eq. (1) read $S^{xx}(k,\omega) = S^{yy}(k,\omega) = \frac{1}{4}\left(S^{+-}(k,\omega) + S^{-+}(k,\omega)\right)$. For the model in the $N_c = L$ subspace, the *c* pseudofermion operators in the rotated-electron expressions, Eq. (80), do not play any active role.

Importantly, all the singular spectral features in the spin dynamical structure factors $S^{zz}(k,\omega)$, $S^{+-}(k,\omega)$, and $S^{-+}(k,\omega)$ studied below in Sec. 4 are produced by application onto the ground state of the corresponding leading-order operators $\hat{G}(k)\, \hat{O}_{GS}^{\odot}$. Since application of these operators onto that state does not generate $n > 1$ composite *sn* pseudofermions, in the subspaces spanned by the excited energy eigenstates generated by these operators the number $M^{un}_{+1/2} = 2S$, Eq. (53), of up-spin unpaired rotated spins equals that of $N^h_{s1} = 2S$ unoccupied sites of the squeezed $s1$ effective lattice and thus of $s1$-band $N^h_{s1} = 2S$ $s1$ pseudofermion-holes. Indeed, upon moving in the $s1$ effective lattice, the $s1$ pseudofermions use the $N^h_{s1} = 2S$ up-spin unpaired rotated spins as unoccupied sites. This is why the unpaired rotated spins are implicitly accounted for in the $s1$ pseudofermion representation through the $s1$ pseudofermion-holes.

Upon acting onto subspaces spanned by energy eigenstates populated by *sn* pseudofermions with $n > 1$ singlet pairs, the $s1$ pseudofermions use as well the $M^{un}_{+1/2} = 2S$ original-lattice sites occupied by unpaired rotated spins as $s1$ effective lattice unoccupied sites. Similarly to the $s1$ pseudoparticles, in that case the $s1$ pseudofermions use also as $s1$ effective lattice unoccupied sites the $2(n-1)$ sites out of the $2n$ original-lattice sites occupied by the $2n$ rotated spins 1/2 in the n singlet pairs bound within each $n > 1$ *sn* pseudofermion. This justifies the form of the general N^h_{s1} expression, Eq. (54).

Concerning the relation between the rotated-spin 1/2 representation $\hat{S}^l_k = \sum_{i=0}^{\infty} \hat{S}^l_{k,i}$ and the pseudofermion representation, we recall that the internal degrees of freedom of each $s1$ pseudofermion that populates a $S > 0$ ground-state Fermi sea, Eq. (72), refer to a singlet pair of two rotated spins 1/2. Moreover, all ground-state $\downarrow$ rotated spins are paired with $\uparrow$ rotated spins, which gives $N_{s1} = N_{\downarrow}$ $s1$ pseudofermion singlet pairs. The $M^{un}_{+1/2} = N_{\uparrow} - N_{\downarrow}$ ground-state $\uparrow$ rotated spins left over remain unpaired.

Hence a $\uparrow$–$\downarrow$ spin-flip process onto a $S > 0$ ground state transforms two $\uparrow$ unpaired rotated spins into one spin-singlet pair, which leads to deviations $\delta M^{un}_{+1/2} = -2$ and $\delta M_{s\,\mathrm{sp}} = 1$. Such a process thus "annihilates" two $\uparrow$ unpaired rotated spins. As discussed below, to leading order the deviation $\delta M_{s\,\mathrm{sp}} = 1$ refers to creation of one $s1$ pseudofermion, *i.e.* $\delta N_{s1} = 1$.

Conversely, a $\downarrow$–$\uparrow$ spin-flip process onto a $S > 0$ ground state leads to deviations $\delta M_{s\,\mathrm{sp}} = -1$ and $\delta M^{un}_{+1/2} = 2$, since one $s1$ pseudofermion rotated-spin singlet pair is broken under it. This thus gives rise to the annihilation of one $s1$ pseudofermion and creation of two $\uparrow$ unpaired rotated spins. A deviation $\delta M^{un}_{+1/2} = 2$ in the number of $\uparrow$ unpaired rotated spins leads to a deviation $\delta N^h_{s1} = \delta M^{un}_{+1/2} = 2$ in the number of the $s1$ band holes. In the usual condensed-matter bands, annihilation of one particle gives rise to creation of one hole. In contrast, here annihilation of one $s1$ pseudofermion upon a $\downarrow$–$\uparrow$ spin-flip process leads to creation of two $s1$ band holes. Indeed, the annihilation of the $s1$ pseudofermion results from a pair breaking process of the two rotated spins $1/2$ within it, which trasform into two $\uparrow$ unpaired rotated spins that play the role of unoccupied sites of the squeezed $s1$ effective lattice, so that $\delta N^h_{s1} = \delta M^{un}_{+1/2} = 2$.

These transformation processes are behind the squeezed $s1$ effective lattice and corresponding $s1$ momentum band being exotic, since their number of sites and discrete momentum values, respectively, which both are given by $L_{s1} = N_1 + N^h_1$, has different values for different subspaces. Hence within the $s1$ pseudofermion operator algebra, one distinguishes the $s1$-band holes created and annihilated under processes within which one $s1$ pseudofermion is annihilated and created, respectively, from the $s1$-band holes created and annihilated upon changing the number $L_{s1} = N_1 + N^h_1$ of squeezed $s1$ effective lattice sites, which equals that of $s1$-band discrete momentum values. (For $S > 0$ states such exotic L_{s1} variations only lead to N^h_1 variations.) Specifically, the former processes are described by application of the operators $\bar{f}_{\bar{q},s1}$ and $\bar{f}^{\dagger}_{\bar{q},s1}$, respectively, onto the initial state. On the other hand, the latter N^h_1 variations that do not conserve $L_{s1} = N_1 + N^h_1$ result from vanishing energy and vanishing momentum processes within which discrete momentum values are added to and removed from one of the $s1$ band limiting momentum values $q^{\pm}_{s1}$, Eq. (18) for $\alpha n = s1$. Whether such an addition or removal occurs at the left limiting momentum q^{-}_{s1} or at right limiting momentum q^{+}_{s1} is uniquely defined, since the process must leave invariant the $s1$ band symmetrical relation $q^{+}_{s1} = -q^{-}_{s1}$ for the final state.

In the case of the leading-order processes generated by application of the operators $\hat{S}^{+}_{k}$ and $\hat{S}^{-}_{k}$ onto a $S > 0$ ground state considered below, one discrete momentum is removed from and added to, respectively, the $s1$ band limiting momentum values. Such vanishing energy and vanishing momentum processes are not generated by the $s1$ pseudofermion operators in the expressions given below for the three $l = z, \pm$ spin operators $\hat{S}^{l}_{k}$. Nonetheless, they are implicitly accounted for by the pseudofermion representation through the $s1$ band discrete momentum values of the final states, which are uniquely defined.

In the following we use the transformation laws of the ground state, Eq. (72), upon acting onto it with the $i = 0, 1, \ldots, \infty$ operators on the right-hand side of the equations, $\hat{S}^{l}_{k} = \sum_{i=0}^{\infty} \hat{S}^{l}_{k,i}$, for the three $l = z, \pm$ spin operators to derive the expression of the corresponding leading-order operators $\hat{G}(k)\,\hat{O}^{\odot}_{GS}$, Eq. (84), in terms of $s1$ pseudofermion operators. Our goal is to approximate the expression of these rotated-spin operators in terms of pseudofermion operators by the corresponding leading-order term, $\hat{S}^{l}_{k} \approx \hat{G}(k)\,\hat{O}^{\odot}_{GS}$.

First, in the case of the operator $\hat{S}^{z}_{k} = \sum_{i=0}^{\infty} \hat{S}^{z}_{k,i}$ such ground-state transformation laws leave invariant both the number $M^{un}_{+1/2} = 2S$, Eq. (53), of $\uparrow$ unpaired rotated spins and $M_{s\,\mathrm{sp}} = \sum_{n=1}^{\infty} n\,N_{sn}$, Eq. (17) for $\alpha = s$, of spin-singlet pairs. Hence the leading-order operator $\hat{G}(k)\,\hat{O}^{\odot}_{GS} = \hat{G}(k)$ in the expression $\hat{O}(k) = \sum_{i'=0}^{\infty} \hat{G}_{i'}(k)$ generates one $s1$ pseudofermion – $s1$ pseudofermion-hole processes. The $i' > 0$ operator terms generate additional $s1$ pseudofermion – $s1$ pseudofermion-hole processes and transform $s1$ pseudofermions into $n > 1$ sn pseudofermions. Within such transformation processes, the creation of each new $n > 1$ sn pseudo-

fermion involves the annihilation of a number n of $s1$ pseudofermions, so that $M^{un}_{+1/2} = 2S$ and $M_{s\,\mathrm{sp}} = \sum_{n=1}^{\infty} n\, N_{sn}$ are conserved. Both the additional $s1$ pseudofermion – $s1$ pseudofermion-hole processes and the transformation of $s1$ pseudofermions into $n > 1$ sn pseudofermions preserve such numbers values and give rise to very little spectral weight. For the present operator one has that $\hat{O}^{\odot}_{GS} = 1$, so that to leading order,

$$\hat{S}^z_k \approx \hat{G}(k) = \sum_{q=-k_{F\downarrow}}^{k_{F\downarrow}} \theta(k_{F\uparrow} - |k+q|)\,\theta(|k+q| - k_{F\downarrow})\, \bar{f}^{\dagger}_{\bar{q}(k+q),s1}\, \bar{f}_{\bar{q}(q),s1}\,, \tag{85}$$

where $\bar{q}(q) = q + \frac{2\pi}{L}\Phi_{s1}(q)$ here and in the following operator expressions.

Second, the transformation laws of the ground state, Eq. (72), upon acting onto it with the $i = 0, 1, \ldots, \infty$ operators on the right-hand side of the equation, $\hat{S}^+_k = \sum_{i=0}^{\infty} \hat{S}^+_{k,i}$, lead to deviations $\delta M^{un}_{+1/2} = -2$ and $\delta M_{s\,\mathrm{sp}} = 1$ in the number values of $\uparrow$ unpaired rotated spins and spin-singlet pairs, respectively. In this case the leading-order operator $\hat{G}(k)\,\hat{O}^{\odot}_{GS}$ generates deviations $\delta N_{s1} = 1$ and $\delta N^h_{s1} = -2$ and corresponding one $s1$ pseudofermion – $s1$ pseudofermion-hole processes. All $i' > 0$ operator terms also generate deviations $\delta M^{un}_{+1/2} = -2$ and $\delta M_{s\,\mathrm{sp}} = 1$ along with additional $s1$ pseudofermion – $s1$ pseudofermion-hole processes and the transformation of $s1$ pseudofermions into $n > 1$ sn pseudofermions. The latter processes originate again very little spectral weight. One then finds the following leading-order expression,

$$\hat{S}^+_k \approx \hat{G}(k)\,\hat{O}^{\odot}_{GS}\,; \qquad \hat{O}^{\odot}_{GS} = \bar{f}^{\dagger}_{\pm k_{F\downarrow},s1}\,,$$
$$\hat{G}(k) = \sum_{q=-k_{F\downarrow}}^{k_{F\downarrow}} \theta(k_{F\uparrow} - |\pi - k - q|)\,\theta(|\pi - k - q| - k_{F\downarrow})\, \bar{f}^{\dagger}_{\bar{q}(k-\pi+q),s1}\, \bar{f}_{\bar{q}(q),s1}\,. \tag{86}$$

Third, in the case of the $i = 0, 1, \ldots, \infty$ operators on the right-hand side of $\hat{S}^-_k = \sum_{i=0}^{\infty} \hat{S}^-_{k,i}$, the corresponding ground-state transformation laws give rise to deviations $\delta M^{un}_{+1/2} = 2$ and $\delta M_{s\,\mathrm{sp}} = -1$ in the number values of $\uparrow$ unpaired rotated spins and spin-singlet pairs, respectively. One then finds that the leading-order operator $\hat{G}(k)\,\hat{O}^{\odot}_{GS}$ generates two $s1$ pseudofermion-holes processes such that $\delta N^h_{s1} = 2$ and $\delta N_{s1} = -1$. All $i' > 0$ operator terms generate also deviations $\delta M^{un}_{+1/2} = 2$ and $\delta M_{s\,\mathrm{sp}} = -1$ together with additional $s1$ pseudofermion – $s1$ pseudofermion-hole processes and the transformation of $s1$ pseudofermions into $n > 1$ sn pseudofermions. As for the previous two spin operators, the latter processes produce very little spectral weight. The leading-order expression found for this operator reads,

$$\hat{S}^-_k \approx \hat{G}(k)\,\hat{O}^{\odot}_{GS}\,; \qquad \hat{O}^{\odot}_{GS} = \bar{f}_{\mp k_{F\downarrow},s1}\,,$$
$$\hat{G}(k) = \sum_{q=-k_{F\downarrow}}^{k_{F\downarrow}} \theta(k_{F\uparrow} - |\pi - k - q|)\,\theta(|\pi - k - q| - k_{F\downarrow})$$
$$\times\, \bar{f}^{\dagger}_{\bar{q}^-_{F\downarrow},s1}\, \bar{f}^{\dagger}_{\bar{q}^+_{F\downarrow},s1}\, \bar{f}_{\bar{q}(\pi-k-q),s1}\, \bar{f}_{\bar{q}(q),s1}\,. \tag{87}$$

In the above expressions, the $s1$ pseudofermion momentum values $\pm k_{F\downarrow}$ appearing in the operators $\hat{O}^{\odot}_{GS}$ belong to the initial ground state $s1$ band whereas the $s1$ pseudofermion momentum values $\bar{q}(q) = q + \frac{2\pi}{L}\Phi_{s1}(q)$ in the operators $\hat{G}(k)$ expressions belong to the excited energy eigenstates $s1$ band. As further discussed in Sec. 4, in the case of the $\hat{S}^+_k$ and $\hat{S}^-_k$ expressions, Eqs. (86) and (87), respectively, there occurs under the transitions from the ground

state to the excited energy eigenstates generated by these operators an overall $s1$-band discrete momentum shift, $q_j \rightarrow q_j + (2\pi/L)\,\Phi^0_\beta$, for which $\Phi^0_{s1} = \mp 1/2$ in Eq. (28). This leads to a shift of the whole $s1$ band occupied Fermi sea that gives rise to an overall momentum $\mp k_{F\downarrow}$ given by $\mp(2\pi/L)\,\Phi^0_{s1}\,N_\downarrow = \pi N_\downarrow/L$. Such an overall momentum $\mp k_{F\downarrow}$ exactly cancels that of the operators $\hat{O}^{\odot}_{GS} = \bar{f}^{\dagger}_{\pm k_{F\downarrow},s1}$ and $\hat{O}^{\odot}_{GS} = \bar{f}_{\mp k_{F\downarrow},s1}$ in such $\hat{S}^{+}_{k}$ and $\hat{S}^{-}_{k}$ expressions, respectively.

Concerning the general dynamical correlation functions, Eq. (71), which in the pseudofermion representation read,

$$B(k,\omega) = \sum_{i'=0}^{\infty}\sum_{f} |\langle f|\,\hat{G}_{i'}(k)\,\hat{O}^{\odot}_{GS}|GS\rangle|^2\,\delta\Big(\omega - (E_f - E_{GS})\Big)\,, \qquad \omega > 0\,, \tag{88}$$

following the above properties one approximates them by their leading-order term,

$$B(k,\omega) \approx B^{\odot}(k,\omega) = \sum_{f} |\langle f|\,\hat{G}(k)\,\hat{O}^{\odot}_{GS}|GS\rangle|^2\,\delta\Big(\omega - (E_f - E_{GS})\Big)\,, \qquad \omega > 0\,, \tag{89}$$

where for the three spin dynamical correlation functions studied in Sec. 4 the corresponding operators $\hat{G}(k)\,\hat{O}^{\odot}_{GS}$ are given in Eqs. (85)–(87). Since the properties studied in the following are valid for operators that preserve the number value $N_c = L$ other than those in Sec. 4, we consider a general situation within which the form of the operators $\hat{O}(k)$ and $\hat{G}(k)\,\hat{O}^{\odot}_{GS}$ is not specified.

For such general operators and as in the case of those considered above, both the generator onto the electron vacuum of the initial ground state in Eq. (72) and the operator $\hat{O}^{\odot}_{GS}$ in $\hat{O}^{\odot}_{GS}|GS\rangle$ are written in terms of $s1$ pseudofermion creation operators, Eqs. (64) and (68), whose discrete canonical momentum values equal the corresponding momentum values q_j, Eqs. (9) and (10), of that initial ground state. (The only role of the c pseudofermion sea of that ground state also present in Eq. (72) is providing an overall momentum contribution π upon processes that change the number value $N_{s\,\mathrm{ps}} = \sum_{n=1}^{\infty} N_{sn}$ in Eq. (15) by an odd integer number.) On the other hand, both the operator $\hat{G}(k)$ and the generators onto the electron vacuum of the excited energy eigenstates $|f\rangle$ are written in terms of $s1$ pseudofermion operators and sn pseudofermion operators of $n > 1$ branches whose discrete canonical momentum values $\bar{q}_j$, Eq. (62), are those of these excited energy eigenstates. These two types of $s1$ band discrete canonical momentum values that correspond to the initial ground state and excited energy eigenstates subspaces, respectively, account for the Anderson orthogonality catastrophe [55] occurring in the $s1$ band under the transitions to the excited energy eigenstates $|f\rangle$.

Such an Anderson orthogonality catastrophe is behind the exotic character of the quantum overlaps that control the spin dynamical correlation functions of the Mott–Hubbard insulator. Concerning that orthogonality catastrophe and the corresponding shake-up effects, there is a major difference relative to the metallic-phase PDT of Refs. [28–30]. Indeed for it the Anderson orthogonality catastrophe occurs both in the c and $s1$ bands under the transitions to the excited energy eigenstates $|f\rangle$. On the other hand, for the half-filled 1D Hubbard model at finite field h in the PSs considered here only the $s1$ band has Fermi points.

Besides the ground states not being populated by sn pseudofermions of $n > 1$ branches, for $S > 0$ the leading-order operator $\hat{G}(k)$ does not give rise to the transformation of $s1$ pseudofermions onto such $n > 1$ sn pseudofermions. Moreover, for $S > 0$ the spectral weight generated by such transformation processes, which results from application of $i' > 0$ higher order operators $\hat{G}_{i'}(k)\,\hat{O}^{\odot}_{GS}$ onto the ground state, is very small. For simplicity, in the following we ignore such small-weight contributions, which as discussed below can also be accounted for by the PDT.

There is always an exact excited energy eigenstate $|f_G\rangle$ of $|GS_f\rangle$ such that,

$$|f_G\rangle = \hat{G}(k)|GS_f\rangle\,. \tag{90}$$

The excitation $\hat{G}(k)\,\hat{O}^{\odot}_{GS}|GS\rangle$ has then finite overlap with such a specific energy eigenstate, which gives,

$$\begin{aligned}\langle f_G|\,\hat{G}(k)\,\hat{O}^{\odot}_{GS}|GS\rangle &= \langle GS^{\rm ex}_f|\,\hat{O}^{\odot}_{GS}|GS\rangle \\ &= \langle 0|\bar{f}_{\bar{q}_{N^{\odot}_{s1}},s1}\cdots\bar{f}_{\bar{q}_2,s1}\,\bar{f}_{\bar{q}_1,s1}\bar{f}^{\dagger}_{q'_1,s1}\,\bar{f}^{\dagger}_{q'_2,s1}\cdots\bar{f}^{\dagger}_{q'_{N^{\odot}_{s1}},s1}|0\rangle \\ &= \langle 0|\bar{f}_{q'_{N^{\odot}_{s1}},s1}\cdots\bar{f}_{q'_2,s1}\,\bar{f}_{q'_1,s1}\bar{f}^{\dagger}_{\bar{q}_1,s1}\,\bar{f}^{\dagger}_{\bar{q}_2,s1}\cdots\bar{f}^{\dagger}_{\bar{q}_{N^{\odot}_{s1}},s1}|0\rangle^{*}\,,\end{aligned} \tag{91}$$

where $|GS^{\rm ex}_f\rangle$ is a state with the same $s1$ pseudofermion occupancy as $|GS_f\rangle$ but whose $s1$ band discrete momentum values are those of its excited energy eigenstate $|f_G\rangle = \hat{G}(k)|GS_f\rangle$ and $N^{\odot}_{s1}$ is the number of $s1$ pseudofermions of the states $\hat{O}^{\odot}_{GS}|GS\rangle$ and $|GS_f\rangle$

The discrete canonical momentum values $q'_1, q'_2, \ldots, q'_{N^{\odot}_{s1}}$ in Eq. (91) equal the corresponding initial ground state discrete momentum values whereas $\bar{q}_1, \bar{q}_2, \ldots, \bar{q}_{N^{\odot}_{s1}}$ are the discrete canonical momentum values of the excited energy eigenstate $|f_G\rangle$, Eq. (90). In contrast to a Fermi liquid, such two sets of discrete momenta have different values, so that their relative canonical momentum shifts give rise to the Anderson orthogonality catastrophe. It consists in excited energy eigenstates of general form,

$$|f_{GC}\rangle = \hat{G}_C(m_{+1}, m_{-1})\,\hat{G}(k)|GS_f\rangle\,, \tag{92}$$

which result from application onto the state $|f_G\rangle$, Eq. (90), of the generator $\hat{G}_C(m_{+1}, m_{-1})$ of the low-energy and small-momentum processes (C), also having overlap with the excitation $\hat{G}(k)\,\hat{O}^{\odot}_{GS}|GS\rangle$. Hence,

$$\begin{aligned}&\langle f_G|\hat{G}_C(m_{+1}, m_{-1})^{\dagger}\hat{G}(k)\,\hat{O}^{\odot}_{GS}|GS\rangle \\ &= \langle GS^{\rm ex}_f|\hat{G}_C(m_{+1}, m_{-1})^{\dagger}\,\hat{O}^{\odot}_{GS}|GS\rangle \\ &= \langle 0|\bar{f}_{\bar{q}_{N^{\odot}_{s1}},s1}\cdots\bar{f}_{\bar{q}_2,s1}\,\bar{f}_{\bar{q}_1,s1}\,\hat{G}_C(m_{+1}, m_{-1})^{\dagger}\,\bar{f}^{\dagger}_{q'_1,s1}\,\bar{f}^{\dagger}_{q'_2,s1}\cdots\bar{f}^{\dagger}_{q'_{N^{\odot}_{s1}},s1}|0\rangle \\ &= \langle 0|\bar{f}_{q'_{N^{\odot}_{s1}},s1}\cdots\bar{f}_{q'_2,s1}\,\bar{f}_{q'_1,s1}\,\hat{G}_C(m_{+1}, m_{-1})\,\bar{f}^{\dagger}_{\bar{q}_1,s1}\,\bar{f}^{\dagger}_{\bar{q}_2,s1}\cdots\bar{f}^{\dagger}_{\bar{q}_{N^{\odot}_{s1}},s1}|0\rangle^{*}\,.\end{aligned} \tag{93}$$

The number of elementary $s1$ pseudofermion – $s1$ pseudofermion-hole processes (C) of momentum $\pm 2\pi/L$ in the vicinity of the $s1;\iota = \pm 1$ Fermi points of $|GS_f\rangle$ is denoted here and in the following by $m_{\iota} = 1, 2, 3, \ldots$. Such processes conserve the number $N^{\odot}_{s1}$ of $s1$ pseudofermions, so that the matrix elements, Eq. (93), have the same form as that in Eq. (91) but with the excited-state occupied discrete canonical momentum values $\bar{q}_1, \bar{q}_2, \ldots, \bar{q}_{N^{\odot}_{s1}}$ in the vicinity of the $s1$ band Fermi points being slightly different from those in that equation.

In the case of the general dynamical correlation function expression in the pseudofermion representation, Eq. (88), there are also exact excited energy eigenstates $|f_G(i')\rangle$ of $|GS_f\rangle$ such that,

$$|f_G(i')\rangle = \hat{G}_{i'}(k)|GS_f\rangle\,, \qquad i' = 0, 1, \ldots, \infty\,. \tag{94}$$

These exact excited energy eigenstates may be populated by sn pseudofermions of $n > 1$ branches. Their small contribution to the general dynamical correlation functions is simpler to compute than that from the $s1$ pseudofermions. The reason is that the initial ground state is not

populated by *sn* pseudofermions of $n > 1$ branches. Since as above for the $i' = 0$ operator $\hat{G}(k)$, the *sn* pseudofermion operators in the expression of any $i' \geq 0$ operator $\hat{G}_{i'}(k)$ that appears both in the dynamical correlation function expression, Eq. (88), and in Eq. (94) have discrete canonical momentum values that belong to the excited energy eigenstate *sn* band, one finds that,

$$\langle f_G|\hat{G}_{i'}(k)\,\hat{O}^{\odot}_{GS}|GS\rangle = \langle GS_f|\hat{G}^{\dagger}_{i'}(k)\,\hat{G}_{i'}(k)\,\hat{O}^{\odot}_{GS}|GS\rangle = \langle GS^{\mathrm{ex(i')}}_{f}|\hat{O}^{\odot}_{GS}|GS\rangle\,, \tag{95}$$

where $|GS^{\mathrm{ex(i')}}_{f}\rangle$ is a state with the same $s1$ pseudofermion occupancy as $|GS_f\rangle$ but whose $s1$ band discrete momentum values are those of its excited energy eigenstate $|f_G(i')\rangle = \hat{G}_{i'}(k)|GS_f\rangle$.

Hence the quantum overlaps resulting from the excited energy eigenstates *sn* pseudofermion occupancies associated with $\hat{G}^{\dagger}_{i'}(k)\,\hat{G}_{i'}(k)$ in Eq. (95) are Fermi-liquid like due to the lack of such occupancies in the ground states $|GS_f\rangle$ and $|GS\rangle$. Indeed, the matrix elements $\langle GS^{\mathrm{ex(i')}}_{f}|\hat{O}^{\odot}_{GS}|GS\rangle$ that result from such overlaps only involve $s1$ pseudofermion operators and have the same general form as that in Eq. (91). However, $|\langle GS^{\mathrm{ex(i')}}_{f}|\hat{O}^{\odot}_{GS}|GS\rangle|$ strongly decreases upon increasing the index $i' = 0, 1, \ldots, \infty$, most of the spectral weight being associated with the $i' = 0$ matrix element $\langle GS^{\mathrm{ex(0)}}_{f}|\hat{O}^{\odot}_{GS}|GS\rangle = \langle GS^{\mathrm{ex}}_{f}|\hat{O}^{\odot}_{GS}|GS\rangle$, Eq. (91). This is why in the following we approximate the general dynamical correlation function expression, Eq. (88), by that given in Eq. (89).

3.2. The dynamical correlation functions and corresponding state summations

The energy and momentum spectra,

$$\delta E^{\odot} = E^{\odot} - E_{GS}\,; \qquad \delta P^{\odot} = P^{\odot} - P_{GS}\,, \tag{96}$$

of the excited energy eigenstates $|f_G\rangle$, Eq. (90), generated by the processes (A) and (B), which have finite quantum overlap with the excitation $\hat{G}(k)\,\hat{O}^{\odot}_{GS}|GS\rangle$, are important pieces of the present PDT dynamical correlation function expressions. Within the theory, the function $B^{\odot}(k,\omega)$, Eq. (89), can be written as follows,

$$B^{\odot}(k,\omega) = \sum_{f} \Theta\Big(\Omega - \delta\omega_f\Big)\,\Theta\Big(\delta\omega_f\Big)\,\Theta\left(|v_f| - v_{s1}\right)\,B_Q(\delta\omega_f, v_f)\,, \tag{97}$$

where the Θ distribution $\Theta(x)$ is different from $\theta(x)$ at $x = 0$, being given here and in the following by $\Theta(x) = 1$ for $x \geq 0$ and $\Theta(x) = 0$ for $x < 0$. A difference relative to the metallic-phase PDT is that the $s1$ band Fermi velocity v_{s1} in Eq. (97) is in that dynamical theory replaced by a velocity $v_{\bar{\beta}} = \min\{v_c, v_{s1}\}$. Here v_c is the c band Fermi velocity, which is absent for the $n_e = 1$ ground states and their PS excited energy eigenstates considered here.

The summation $\sum_f$ on the right-hand side of Eq. (97) runs over PS excited energy eigenstates $|f_{G_C}\rangle$, Eq. (92), which are generated by processes (A), (B), and (C) at fixed values of k and ω. Such states have excitation energy and momentum, Eq. (96), in the ranges $\delta E^{\odot}_{f} \in [\omega - \Omega, \omega]$ and $\delta P^{\odot}_{f} \in [k - \Omega/v_f, k]$ where,

$$\begin{aligned} &\delta\omega_f = (\omega - \delta E^{\odot}_{f}) = (\omega - E^{\odot}_{f} + E_{GS})\,; \qquad \delta k_f = k - \delta P^{\odot}_{f}\,, \\ &\delta E_f = \delta E^{\odot}_{f} + \delta\omega_f = \omega\,; \qquad P_f = \delta P^{\odot}_{f} + \delta k_f = k\,, \end{aligned} \tag{98}$$

and the velocity v_f in Eqs. (97) and (98) is defined as,

$$v_f = \delta\omega_f/\delta k_f\,. \tag{99}$$

The energy deviation $\delta E_f = \omega$ and momentum deviation $\delta P_f = k$ denote in Eq. (98) the excitation energy and momentum, respectively, of the excited energy eigenstates. Moreover, in Eq. (97) Ω is the energy range of the elementary processes (C). That energy scale is self-consistently determined as that for which the velocity v_f, Eq. (98), remains nearly unchanged.

The function $B_Q(\delta\omega_f, v_f)$ in Eq. (97) is the pseudofermion spectral function $B_Q(k', \omega')$ given below. Another important difference relative to the metallic-phase PDT of Refs. [28–30] is that for it the function $B_Q(\delta\omega_f, v_f)$ is replaced in Eq. (97) by a convolution of c and $s1$ pseudofermion spectral functions. In the present case such a function is only controlled by the Anderson orthogonality catastrophe associated with the $s1$ band shake-up effects in the $s1$ pseudofermion spectral function $B_Q(k', \omega')$. Those involve all $s1$ Fermi-sea pseudofermions and result from the $s1$ band discrete canonical momentum value shifts, $(2\pi/L)\,\Phi^T(q_j)$, under the transitions to the excited energy eigenstates. They are behind a large number of small-momentum and low-energy $s1$ pseudofermion – $s1$ pseudofermion-hole processes (C) in the linear part of the $s1$ pseudofermion energy dispersions leading to finite spectral-weight contributions. (In a Fermi liquid there are no such discrete momentum shifts, so that only a single quasiparticle–quasihole process contributes.)

Creation of $sn \neq s1$ pseudofermions are processes (A). They do not contribute to the Anderson orthogonality catastrophes, since the corresponding quantum overlaps are non-interacting like. Creation of $sn \neq s1$ pseudofermions is accounted for both by their contribution to the spectra $\delta E^{\odot}$ and $\delta P^{\odot}$, Eq. (96), and the phase shifts acquired by the $s1$ pseudofermions upon scattering off the created $sn \neq s1$ pseudofermions.

The present dynamical theory $s1$ pseudofermion spectral functions on the right-hand side of Eq. (97) have a general form similar to that of the metallic-phase PDT of Refs. [28–30]. Their expression involves sums that run over the processes (C) numbers $m_\iota = 1, 2, 3, \ldots$ and reads,

$$B_Q(k', \omega') = \frac{L}{2\pi} \sum_{m_{+1};m_{-1}} A^{(0,0)}\, a(m_{+1}, m_{-1}) \times \delta\Big(\omega' - \frac{2\pi}{L}\, v_{s1} \sum_{\iota=\pm1} (m_\iota + \Delta^\iota)\Big)\, \delta\Big(k' - \frac{2\pi}{L} \sum_{\iota=\pm1} \iota\,(m_\iota + \Delta^\iota)\Big)\,, \tag{100}$$

where the *lowest peak weight* $A^{(0,0)}$ is associated with a transition from the $n_e = 1$ and $m > 0$ ground state to a PS excited energy eigenstate generated by processes (A) and (B), the relative weights $a = a(m_{+1}, m_{-1})$ are generated by additional processes (C), and Δ^ι refers to the functional $2\Delta^\iota$ defined below.

The weights $A^{(0,0)}\, a(m_{+1}, m_{-1})$ in Eq. (100) are reached after the quantum overlaps stemming from creation of sn pseudofermions of $n > 1$ branches and/or unpaired rotated spin flip processes are trivially computed. They are associated with matrix elements of general form, Eq. (91), and thus only involve $s1$ pseudofermion operators and read,

$$|\langle 0|\bar{f}_{q'_{N^{\odot}_{s1}},\,s1} \ldots \bar{f}_{q'_2,\,s1}\, \bar{f}_{q'_1,\,s1}\, \bar{f}^{\dagger}_{\bar{q}_1,\,s1}\, \bar{f}^{\dagger}_{\bar{q}_2,\,s1} \ldots \bar{f}^{\dagger}_{\bar{q}_{N^{\odot}_{s1}},\,s1}|0\rangle|^2\,, \tag{101}$$

where $N^{\odot}_{s1}$ is the PS excited energy eigenstate number of $s1$ pseudofermions and $|0\rangle$ denotes the electron vacuum. The matrix element square, Eq. (101), can be expressed in terms of a corresponding Slater determinant of $s1$ pseudofermion operators that involves the $s1$ pseudofermion anticommutators, Eq. (70), as follows,

$$\left\|\begin{array}{llll}\{\bar{f}^{\dagger}_{\bar{q}_1,s1},\bar{f}_{q'_1,s1}\} & \{\bar{f}^{\dagger}_{\bar{q}_1,s1},\bar{f}_{q'_2,s1}\} & \cdots & \{\bar{f}^{\dagger}_{\bar{q}_1,s1},\bar{f}_{q'_{N^{\odot}_{s1}},s1}\} \\ \{\bar{f}^{\dagger}_{\bar{q}_2,s1},\bar{f}_{q'_1,s1}\} & \{\bar{f}^{\dagger}_{\bar{q}_2,s1},\bar{f}_{q'_2,s1}\} & \cdots & \{\bar{f}^{\dagger}_{\bar{q}_2,s1},\bar{f}_{q'_{N^{\odot}_{s1}},s1}\} \\ \cdots & \cdots & \cdots & \cdots \\ \{\bar{f}^{\dagger}_{\bar{q}_{N^{\odot}_{s1}},s1},\bar{f}_{q'_1,s1}\} & \{\bar{f}^{\dagger}_{\bar{q}_{N^{\odot}_{s1}},s1},\bar{f}_{q'_2,s1}\} & \cdots & \{\bar{f}^{\dagger}_{\bar{q}_{N^{\odot}_{s1}},s1},\bar{f}_{q'_{N^{\odot}_{s1}},s1}\}\end{array}\right\|^2 . \tag{102}$$

In the case of the lowest peak weight $A^{(0,0)}$ associated with a transition to an excited energy eigenstate generated by processes (A) and (B) the use of the $s1$ pseudofermion anticommutators, Eq. (70), in Eq. (102) leads after some suitable algebra to,

$$\begin{aligned}A^{(0,0)} = & \left(\frac{1}{L}\right)^{2N^{\odot}_{s1}} \prod_{j=1}^{L_{s1}} \sin^2\left(\frac{\pi}{2}\left(1-(1-2\Phi^T(q_j))N^{\odot}_{s1}(q_j)\right)\right) \prod_{j=1}^{L_{s1}-1}\left(\sin\left(\frac{\pi j}{L}\right)\right)^{2(L_{s1}-j)} \\ & \times \prod_{i=1}^{L_{s1}}\prod_{j=1}^{L_{s1}} \theta(j-i) \\ & \times \sin^2\left(\frac{\pi}{2}\left(1-\left(1-\frac{(2(j-i)+2\Phi^T(q_j)-2\Phi^T(q_i))}{L}\right)N^{\odot}_{s1}(q_j)N^{\odot}_{s1}(q_i)\right)\right) \\ & \times \prod_{i=1}^{L_{s1}}\prod_{j=1}^{L_{s1}} \frac{1}{\sin^2\left(\frac{\pi}{2}\left(1-\left(1-\frac{2(j-i)+2\Phi^T(q_j)}{L}\right)N^{\odot}_{s1}(q_i)N^{\odot}_{s1}(q_j)\right)\right)} .\end{aligned} \tag{103}$$

The numbers of $s1$ band discrete momentum values, L_{s1}, $s1$ pseudofermions, $N^{\odot}_{s1} = \sum_{j=1}^{L_{s1}} N^{\odot}_{s1}(q_j)$, and the corresponding $s1$ band momentum distribution function, $N^{\odot}_{s1}(q_j)$, are in this expression those of the excited energy eigenstate generated by the processes (A) and (B) and $\Phi^T(q_j)$ is the phase-shift functional in Eq. (70).

The general expression of the relative weights $a = a(m_{+1}, m_{-1})$ in Eq. (100), which are associated with the tower of excited energy eigenstates generated by the processes (C) and corresponding matrix elements, Eq. (93), reads [28],

$$a(m_{+1}, m_{-1}) = \left(\prod_{\iota=\pm 1} a_{\iota}(m_{\iota})\right)\left(1+\mathcal{O}\left(\ln L/L\right)\right), \tag{104}$$

where,

$$a_{\iota}(m_{\iota}) = \prod_{j=1}^{m_{\iota}} \frac{(2\Delta^{\iota}+j-1)}{j} = \frac{\Gamma(m_{\iota}+2\Delta^{\iota})}{\Gamma(m_{\iota}+1)\,\Gamma(2\Delta^{\iota})}, \qquad \iota = \pm 1 . \tag{105}$$

For $m_{\iota} = 1$, Eq. (105) leads to,

$$a_{\iota}(1) = 2\Delta^{\iota} = \left(\frac{\delta\bar{q}^{\iota}_{Fs1}}{(2\pi/L)}\right)^2, \qquad \iota = \pm 1 . \tag{106}$$

That for the metallic-phase PDT of Refs. [28–30] there are four $\beta = c, s1; \iota = \pm 1$ pseudofermion Fermi points whereas here there are only two $\iota = \pm 1$ $s1$ pseudofermion Fermi points implies that for the present Mott–Hubbard insulator PDT there are only two functionals $2\Delta^{\iota}$, Eq. (106). They play a major role in the half-filled 1D Hubbard model spin dynamical properties, being fully controlled by the excited-state canonical momentum $\iota = \pm 1$ Fermi-point deviations

$\delta\bar{q}^{\iota}_{Fs1}$ such that $\delta\bar{q}^{\iota}_{Fs1}/(2\pi/L) = \iota\,\delta N^{F}_{s1,\iota} + \Phi(\iota q_{Fs1})$. Here $\delta N^{F}_{s1,\iota} = \delta N^{0,F}_{s1,\iota} + \iota\,\Phi^{0}_{s1}$ and thus $\delta\bar{q}^{\iota}_{Fs1}/(2\pi/L) = \iota\,\delta N^{0,F}_{s1,\iota} + \Phi^{T}(\iota q_{Fs1})$ where the bare deviation $\delta N^{0,F}_{s1,\iota}$ accounts for the number of $s1$ pseudofermions created or annihilated at the right ($\iota = +1$) and left ($\iota = +1$) $s1$ band Fermi points.

The two functionals, Eq. (106), can be written as,

$$2\Delta^{\iota} = \left(\frac{\delta\bar{q}^{\iota}_{Fs1}}{(2\pi/L)}\right)^{2} = \left(\iota\delta N^{0,F}_{s1,\iota} + \Phi^{T}(\iota q_{Fs1})\right)^{2}$$
$$= \left(\frac{\iota}{2\xi^{1}_{s1,s1}}\,\delta N^{F}_{s1} + \xi^{1}_{s1,s1}\,\delta J^{F}_{s1} + \sum_{n=1}^{\infty}\sum_{j=1}^{L_{sn}}\Phi_{s1\,sn}(\iota q_{Fs1}, q_j)\delta N^{NF}_{sn}(q_j)\right)^{2}. \qquad (107)$$

In this expression $\xi^{1}_{s1,s1}$ is the two-pseudofermion phase-shift parameter, Eqs. (46) and (47), $\delta N^{F}_{s1} = \delta N^{F}_{s1,+1} + \delta N^{F}_{s1,-1}$, and $2J^{F}_{s1} = \delta N^{F}_{s1,+1} - \delta N^{F}_{s1,-1}$. The deviations $\delta N^{NF}_{sn}(q_{j'})$ refer to sn band momentum values q_j, which for the $s1$ branch are away from the $s1$ Fermi points. (The $s1$ pseudofermion creation or annihilation at and in the vicinity of such points is rather accounted for by the deviations δN^{F}_{s1} and δJ^{F}_{s1} in the second expression of Eq. (107).) The form of the $\iota = \pm 1$ functionals, Eq. (107), confirms that the $s1$ pseudofermion phase shifts acquired upon scattering off the sn pseudofermions of $n > 1$ branches created under transitions to the PS excited energy eigenstates contribute to the spin dynamical properties. In addition, creation of sn pseudofermions with $n > 1$ singlet pairs is accounted for in the dynamical correlation functions energy and momentum. On the other hand, the unpaired rotated spins flipping processes do not lead to phase shifts and thus do not contribute to the $\iota = \pm 1$ functionals, Eq. (107).

The occurrence of four Fermi points in the metallic-phase PDT implies that the expression of its four functionals that play the role of those in Eq. (107) involves, instead of a single two-Fermi-points phase-shift parameter $\xi^{1}_{s1,s1}$, the four entries $\xi^{1}_{c\,c}$, $\xi^{1}_{c\,s1}$, $\xi^{1}_{s1\,c}$, $\xi^{1}_{s1\,s1}$ of the 2×2 dressed-charge matrix Z^{1} [20,45]. For the c and $s1$ pseudofermion representation used within the PDT of Refs. [28–30] such entries are combinations of two-pseudofermion phase shifts whose two momentum values are at the Fermi points, as here in Eq. (46).

On the one hand, the lack of $s1$ pseudofermion interaction terms in the energy spectrum, Eq. (67), is associated with the weights $A^{(0,0)}\,a(m_{+1},\,m_{-1})$ in Eq. (100) being merely of the form, Eqs. (101) and (102). On the other hand, the lack of such interaction terms is reached by incorporating in the $s1$ band canonical momentum the functional $\Phi(q_j)$, Eq. (66). This leads to the unusual form of the anticommutator relation, Eq. (70), which is behind the phase-shift functional $\Phi^{T}(q_j) = \Phi^{0}_{s1} + \Phi(q_j)$ and related functional $2\Delta^{\iota} = (\iota\delta N^{0,F}_{s1,\iota} + \Phi^{T}(\iota q_{Fs1}))^{2}$ controlling the weights $A^{(0,0)}\,a(m_{+1},\,m_{-1})$, as confirmed by the form of the expressions given in Eqs. (103) and (104)–(106).

According to Eq. (106), the functional, Eq. (107), is the relative weight of the $s1,\iota$ pseudofermion spectral function $m_{\iota} = 1$ peaks. They correspond to relative weights, Eq. (104),

$$a(1,\,0) = 2\Delta^{+1}; \qquad a(0,\,1) = 2\Delta^{-1}. \qquad (108)$$

The δ-functions in the pseudofermion spectral function expression, Eq. (100), impose that $((L/4\pi\,v_{s1})(\omega' + \iota\,v_{s1}\,k') - \Delta^{\iota}) = m_{\iota}$. In the present TL, the k' and ω' values for which the quantity $((L/4\pi\,v_{s1})(\omega' + \iota\,v_{s1}\,k') - \Delta^{\iota})$ equals the integer numbers m_{ι} of elementary processes (C) near both the $\iota = \pm 1$ Fermi points refer to a dense distribution of (k', ω') points. Moreover, in the TL the factor $(L/4\pi\,v_{s1})$ in $((L/4\pi\,v_{s1})(\omega' + \iota\,v_{s1}\,k') - \Delta^{\iota}) = m_{\iota}$ ensures

that for any arbitrarily small k' and ω' values for which $0 < (\omega' + \iota\, v_{s1}\, k')/(4\pi\, v_{s1}) \ll 1$ the corresponding values of the $\iota = \pm 1$ integer numbers $m_\iota = ((L/4\pi\, v_{s1})(\omega' + \iota\, v_{s1}\, k') - \Delta^\iota)$ of elementary processes (C) are such that $m_\iota \gg 1$. Hence within the TL one can use a large-m_ι expansion for the relative weight expression in Eq. (105). To derive it one uses the asymptotic expansion $\Gamma(x) \approx e^{-x}\, x^x \sqrt{\frac{2\pi}{x}}(1 + 1/(12\, x) + \ldots)$ of the $\Gamma(x)$ function valid for $x \gg 1$ in the ratio $\Gamma(m_\iota + 2\Delta^\iota)/\Gamma(m_\iota + 1)$ appearing in Eq. (105). This gives to leading order [23], $\Gamma(m_\iota + 2\Delta^\iota)/\Gamma(m_\iota + 1) \approx (m_\iota + \Delta^\iota)^{-1+2\Delta^\iota}$. Its further use in the $\iota = \pm 1$ relative weight expression, Eq. (105), then leads to the following asymptotic behavior for that weight, which in the TL is used in the derivation of the corresponding exact spin dynamical correlation function expressions near their spectra thresholds,

$$a_\iota(m_\iota) \approx \frac{1}{\Gamma(2\Delta^\iota)}(m_\iota + \Delta^\iota)^{-1+2\Delta^\iota}\,, \qquad 2\Delta^\iota \neq 0\,, \qquad \iota = \pm 1\,. \tag{109}$$

A relation also useful for such a derivation involves the lowest peak weight $A^{(0,0)}$, Eq. (103), in the $s1$ pseudofermion spectral function $B_Q(k', \omega')$, Eq. (100), which can be written as,

$$A^{(0,0)} = F^{(0,0)} \left(\frac{1}{L\, S^0}\right)^{-1+2\Delta^{+1}+2\Delta^{-1}}\,. \tag{110}$$

Here $F^{(0,0)}$ and S^0 are in the TL independent of L and $2\Delta^{+1}$ and $2\Delta^{-1}$ are the two functionals, Eq. (107).

In the general case in which these two functionals are finite the $s1$ pseudofermion spectral function $B_Q(k', \omega')$, Eq. (100), can be written as [28,30],

$$\begin{aligned} B_Q(k', \omega') &= \frac{L}{4\pi\, v_{s1}}\, A^{(0,0)} \prod_{\iota=\pm 1} a_\iota \left(\frac{L}{4\pi\, v_{s1}}(\omega' + \iota\, v_{s1}\, k') - \Delta^\iota\right) \\ &\approx \frac{F^{(0,0)}}{4\pi\, S^0\, v_{s1}} \prod_{\iota=\pm 1} \frac{\Theta(\omega' + \iota\, v_{s1}\, k')}{\Gamma(2\Delta^\iota)} \left(\frac{\omega' + \iota\, v_{s1}\, k'}{4\pi\, S^0\, v_{s1}}\right)^{-1+2\Delta^\iota}\,. \end{aligned} \tag{111}$$

To reach the second expression given here, which in the TL is exact, Eqs. (109) and (110) were used.

On the other hand, when $2\Delta^\iota > 0$ and $2\Delta^{-\iota} = 0$ the $s1$ pseudofermion spectral function has a different form given by [30],

$$\begin{aligned} B_Q(k', \omega') &= \frac{A^{(0,0)}}{v_{s1}}\, a_\iota \left(\frac{L}{2\pi\, v_{s1}}\, \omega' - \Delta^\iota\right) \delta\Big(k' - \frac{\iota\, \omega'}{v_{s1}}\Big) \\ &\approx \frac{F^{(0,0)}}{v_{s1}\, \Gamma(2\Delta^\iota)}\, \Theta(\iota\, \omega') \left(\frac{\omega'}{2\pi\, S^0\, v_{s1}}\right)^{-1+2\Delta^\iota} \delta\Big(k' - \frac{\iota\, \omega'}{v_{s1}}\Big). \end{aligned} \tag{112}$$

Again the second expression provided in this equation is obtained from the use of Eqs. (109) and (110).

Finally, when $2\Delta^\iota = 2\Delta^{-\iota} = 0$ such a function reads,

$$B_Q(k', \omega') = \frac{2\pi}{L}\, A^{(0,0)}\, \delta(k')\, \delta(\omega') \approx 2\pi\, F^{(0,0)}\, S^0\, \delta(k')\, \delta(\omega')\,. \tag{113}$$

The numerical computation of the momentum and state summations in Eqs. (88) and (89) needed to access the corresponding finite-u spectral-weight distributions over the whole (k, ω)

plane is an extremely difficult technical task. Fortunately, the use of Eqs. (111)–(113) for the spectral function $B_Q(\delta\omega_f, v_f)$ in Eq. (89), enables partially performing the summations in the latter equation for the (k,ω)-plane vicinity of important singular spectral features.

The more important of such features is a *branch line*. A particle (and hole) branch line is generated by elementary processes (A) where one pseudofermion is created (and annihilated) at an initial-ground-state $s1$ band momentum value q_j outside the Fermi points $\pm k_{F\downarrow}$ plus elementary processes (B). In the cases of a particle and hole branch line, the set of such transitions scans the whole corresponding range $|q_j| \in [k_{F\downarrow}, k_{F\uparrow}]$ and $q_j \in [-k_{F\downarrow}, k_{F\downarrow}]$, respectively. On the other hand, all remaining $s1$ pseudofermions are created or annihilated at the $s1$ Fermi points $\pm q_{Fs1} = \pm k_{F\downarrow}$, Eq. (27). Such a feature may also involve unpaired rotated spins flipping processes. Moreover, the $sn \neq s1$ pseudofermions (if any) are created at their sn band limiting values, $\pm q_{sn}$, Eq. (25). This gives a (k,ω)-plane branch line defined by the following equations,

$$\omega(k) = \omega_0 + c_0\,\varepsilon_{s1}(q_j)\,; \qquad k = k_0 + c_0\,q_j\,, \qquad c_0 = \pm 1\,, \tag{114}$$

where $c_0 = +1$ and $c_0 = -1$ refers to a particle and hole branch line, respectively, $\varepsilon_{s1}(q_j)$ is the $s1$ band energy dispersion, Eq. (34), and,

$$\omega_0 = 2\mu_B\,|h|\,(M^{un}_{-1/2} + M_{s\,\mathrm{sp}} - N_{s1})\,; \qquad k_0 = \frac{\pi}{2}\,(1-(-1)^{\delta M_{s\,\mathrm{sp}}}) + 2k_{F\downarrow}\,2J^F_{s1}\,. \tag{115}$$

The only contribution from the full c band corresponds to the momentum $(\pi/2)\,(1-(-1)^{\delta M_{s\,\mathrm{sp}}})$, which reads 0 or π when the deviation $\delta M_{s\,\mathrm{sp}}$ is an even or odd integer, respectively.

For simplicity we consider the more general case for which the two $\iota = \pm 1$ parameters $2\Delta^{\iota}$, Eq. (107), are finite, so that the corresponding pseudofermion spectral function has the form given in Eq. (111). We then consider a (k,ω)-plane point located just above the branch line whose momentum k expression is of the form given in Eq. (114) and the energy ω is such that $(\omega - \omega(k))$ is small and positive. The spectral-weight distribution expression in the vicinity of that point is controlled by the elementary processes (C), which generate from the initial excited energy eigenstates corresponding to the branch line a set of tower states whose momentum and energy relative to the ground state are precisely k and ω.

By performing the summations in the general expression, Eq. (89), over *all* PS excited energy eigenstates generated from the ground state by the elementary processes (A) and (B), which correspond to branch-line points in the vicinity of the (k,ω)-plane point, and then accounting for the elementary processes (C) that combined with the former elementary processes (A) and (B) determine the line shape at that point, one finds from the use of manipulations similar to those reported in Appendix B of Ref. [28] for the metallic-phase PDT the following spectral-weight distribution expression for the line shape in the vicinity of the branch line,

$$\begin{aligned} &B(k,\omega) \propto (\omega - \omega(k))^{\xi(k)}\,; \qquad (\omega - \omega(k)) \geq 0\,, \\ &\xi(k) = -1 + \sum_{\iota=\pm 1} 2\Delta^{\iota}(q_j)|_{q_j = c_0\,(k-k_0)}\,. \end{aligned} \tag{116}$$

That in the vicinity of a branch line the above state summations can be partially performed follows in part from the lowest peak weights $A^{(0,0)}$, Eq. (103), for the corresponding set of states generated by elementary processes (A) and (B) having nearly the same magnitude.

In Eq. (116) the $2\Delta^{\iota}(q_j)$ momentum q_j dependence stems from a phase-shift contribution, $c_0\,2\pi\,\Phi_{\beta'\,\beta}(\iota q_{Fs1}, q_j)$, within the scattering phase shift $2\pi\,\Phi(\iota k_{F\downarrow})$, Eq. (66). The momentum q_j is that of the $s1$ pseudofermion created or annihilated under the transition. Its q_j value spans the whole above corresponding particle or hole branch-line range $|q_j| \in [k_{F\downarrow}, k_{F\uparrow}]$ or

$q_j \in [-k_{F\downarrow}, k_{F\downarrow}]$, respectively. In the case of the spin dynamical correlation functions studied in this paper the general expression, Eq. (116), is exact for branch lines that coincide with the lower thresholds of such functions spectra.

The corresponding high-energy dynamical correlation functions line shapes are beyond the reach of the techniques associated with the low-energy Tomonaga–Luttinger liquid [18–20,29]. In the limit of low-energy the PDT considered here describes the well-known behaviors predicted by such techniques. This refers specifically to the vicinity of (k,ω)-plane points $(k_0, 0)$ of which (k_0, ω_0), Eq. (115), is a generalization for $\omega_0 > 0$. Alike for the metallic-phase PDT [29], near them the spectral-function behavior is,

$$
\begin{aligned}
B(k,\omega) &\propto \left(\omega-\omega_0\right)^{\zeta}, \qquad (\omega-\omega_0)\geq 0\,,\\
\zeta &= -2+\sum_{\iota=\pm 1} 2\Delta^{\iota}\,, \qquad (\omega-\omega_0)\neq \pm v_{s1}\,(k-k_0)\,,\\
B(k,\omega) &\propto \left(\omega-\omega_0\mp v_{s1}\,(k-k_0)\right)^{\zeta^{\pm}}, \qquad (\omega-\omega_0\mp v_{s1}\,(k-k_0))\geq 0\,,\\
\zeta^{\pm} &= -1+2\Delta^{\pm}_{s1}\,, \qquad (\omega-\omega_0)\approx \pm v_{s1}\,(k-k_0)\,.
\end{aligned}
\tag{117}
$$

The expressions given here apply to the finite-weight region above the (k,ω) plane point.

4. The longitudinal and transverse dynamical structure factors in the vicinity of their spectra lower thresholds

In this section we use the Mott–Hubbard insulator PDT to study the line shape behavior of the spin dynamical structure factors $S^{zz}(k,\omega)$ and $S^{xx}(k,\omega)$, Eq. (1), in the vicinity of their spectra lower thresholds at finite fields $h > 0$. As discussed in Section 1, previous studies of these factors focused mainly onto magnetic fields $h = 0$ when $S^{zz}(k,\omega) = S^{xx}(k,\omega) = S^{yy}(k,\omega)$ [38,39]. For large u values the spin degrees of freedom of the half-filled 1D Hubbard model can be mapped onto a spin-1/2 *XXX* chain [56]. Previous studies on that model spin dynamical structure factors $S^{zz}(k,\omega)$ and $S^{xx}(k,\omega)$ refer to *finite systems* and rely on numerical diagonalizations [57], evaluation of matrix elements between BA states [56,58], and the form-factor method [8–13].

The singularities that dominate the line shape for small excitation energy values $(\omega-\omega^{\tau}(k))$ near the lower thresholds $\omega^{\tau}(k)$ of the longitudinal $(\tau = l)$ and transverse $(\tau = t)$ dynamical structure factors $S^{zz}(k,\omega)$ and $S^{xx}(k,\omega)$ spectra, respectively, are for $h > 0$ controlled by well-defined types of excited energy eigenstates. In the case of the related spin-1/2 *XXX* chain, such states have already been identified within the pioneering study of Ref. [56] and later investigations, such as those reported in Refs. [10,58]. Such states have a one to one correspondence with the excited energy eigenstates $|f_G\rangle = \hat{G}(k)|GS_f\rangle$, Eq. (90), of the half-filled 1D Hubbard model in the PSs considered in this paper for which $N_c = L$, whose generators $\hat{G}(k)$ are given in Eqs. (85)–(87). As confirmed below, the effects of u are mainly onto the spin dynamical correlation functions spectra energy bandwidths, the form of these spectra remaining for finite fields the same for the whole $u > 0$ range. Also the line-shape singularities occurring in the vicinity of their lower thresholds are found to have the same qualitative behavior for the whole $u > 0$ range.

Our study, based on the Mott–Hubbard insulator PDT approach introduced in Section 3, confirms that in the vicinity of such lower thresholds the singularities are determined by transitions from the $n_e = 1$ and $m > 0$ ground state to a class (ii) of excited energy eigenstates populated only by $s1$ pseudofermions and thus described by real BA rapidities. They are the excited energy eigenstates $|f_G\rangle = \hat{G}(k)|GS_f\rangle$, Eq. (90), whose generators, Eqs. (85)–(87), give rise to

specific leading-order elementary processes (A) and (B). (Here we have used the classification of Ref. [56] for the related spin-1/2 *XXX* chain, according to which class (ii) excitations are $|S^z| = S$ excited states.)

Consistently with the general form of the dynamical correlation functions in the pseudofermion representation, Eq. (88), higher-order class (ii) excitations described by real BA rapidities and generated by additional higher-order $s1$ pseudofermion elementary processes (A) also contribute to the dynamical structure factors. However, they lead to contributions in (k,ω)-plane regions other than the vicinity of the lower thresholds $\omega^{\tau}(k)$ of the longitudinal and transverse dynamical structure factors spectra and thus do not change the momentum dependent exponents obtained in this section. Moreover, class (ii) excitations described by complex BA rapidities and thus associated with excited energy eigenstates populated by sn pseudofermions of $n > 1$ branches are gapped for $h > 0$, their energy gap being for the spin density values considered in the studies of this section larger than the maximum lower threshold energy. Except for very small magnetic fields h these excitations have nearly vanishing spectral weight. For instance, at spin density $m = 0.5$ and large u one estimates from the results of Ref. [12] for a directly related model that their contributions correspond to a relative intensity not larger than 10^{-6}. This holds as well for smaller u values. All higher-order class (ii) excitations, including those described only by real BA rapidities and both by real and complex BA rapidities, respectively, refer within the pseudofermion representation to the $i' > 0$ energy eigenstates $|f_G(i')\rangle = \hat{G}_{i'}(k)|GS_f\rangle$, Eq. (94),

For simplicity, our study focuses mainly on the $u > 0$ and $m > 0.25$ region for which the contribution of class (ii) excited energy eigenstates populated by sn pseudofermions of $n > 1$ branches is negligible and their energy gap is larger than the maximum lower threshold energy. (This applies as well for $m > 0.15$.) Hence in this section we limit our analysis to $h > 0$ subspaces spanned by energy eigenstates described by real spin rapidities $\Lambda_{s1}(q_j)$. For $h > 0$ the transitions from the ground state to such excited energy eigenstates fully control the singularities of the longitudinal and transverse dynamical structure factors.

In the case of the transverse dynamical structure factor, $S^{xx}(k,\omega) = \frac{1}{4}(S^{+-}(k,\omega) + S^{-+}(k,\omega))$, we must consider the transitions to excited energy eigenstates that determine the line shape in the vicinity of the lower thresholds of both the dynamical structure factors $S^{+-}(k,\omega)$ and $S^{-+}(k,\omega)$, respectively. Indeed, the corresponding transverse dynamical structure factor spectrum $\omega^{t}(k)$, is here expressed as the superposition of the spectra $\omega^{+-}(k)$ and $\omega^{-+}(k)$.

The spectra $\omega^{\mp\pm}(k)$ that contain most of the dynamical structure factors $S^{-+}(k,\omega)$ and $S^{+-}(k,\omega)$ spectral weight refer to excited energy eigenstates $|f_G\rangle = \hat{G}(k)|GS_f\rangle$, Eq. (90), whose generators $\hat{G}(k)$ are given in Eqs. (86) and (87), respectively. Such states are generated from the $n_e = 1$ and $m > 0$ ground state by high-energy and finite-momentum elementary processes (A) and zero-energy and finite-momentum processes (B) that involve a $\delta N^{0,F}_{s1,\iota} = \pm 1$ deviation at a $\iota = \pm 1$ Fermi point and an overall $s1$ band momentum shift $\delta q_j = \mp(2\pi/L)\Phi^0_{s1} = \mp\iota\pi/L$ where $\Phi^0_{s1} = \iota/2$ is the shift parameter Φ^0_{sn} given in Eq. (28) for $n = 1$. As discussed in Sec. 3.1, the specific elementary processes (A) generated by the operators $\hat{G}(k)$ in Eqs. (86) and (87) that are associated with the spectra $\omega^{-+}(k)$ and $\omega^{+-}(k)$ are one $s1$ pseudofermion – $s1$ pseudofermion-hole elementary processes and two $s1$ pseudofermion-hole elementary processes, respectively.

For spin densities $m \in]0,1]$ the spectra generated by such processes (A) and (B) read,

$$\begin{aligned}
&\omega^{-+}(k) = \varepsilon_{s1}(q_2) - \varepsilon_{s1}(q_1)\,; \qquad k = \pi + q_2 - q_1 \in]0,\pi[\,;\\
&\omega^{+-}(k) = -\varepsilon_{s1}(q_1) - \varepsilon_{s1}(q_2)\,; \qquad k = \pi - q_1 - q_2 \in]0,\pi[\,,
\end{aligned} \tag{118}$$

where $\varepsilon_{s1}(q)$ is the energy dispersion, Eq. (34), $q_1 \in [-k_{F\downarrow}, k_{F\downarrow}]$, and $q_2 \in [-k_{F\uparrow}, -k_{F\downarrow}]$ for the $-+$ spectrum and $q_2 \in [-k_{F\downarrow}, k_{F\downarrow}]$ for the $+-$ spectrum.

On the other hand, for the longitudinal dynamical structure factor $S^{zz}(k,\omega)$, the exact line shape in the vicinity of its spectrum lower thresholds is within the Mott–Hubbard insulator PDT determined by transitions to excited energy eigenstates $|f_G\rangle = \hat{G}(k)|GS_f\rangle$, Eq. (90), whose generator $\hat{G}(k)$ is given in Eq. (85). These states are generated from the $n_e = 1$ and $m > 0$ ground state by high-energy one $s1$ pseudofermion – $s1$ pseudofermion-hole elementary processes (A) that conserve the number of down spins. The corresponding energy spectrum, $\omega^l(k) = \omega^l(-k)$, which contains most of the longitudinal dynamical structure factor spectral weight, is for spin densities $m \in]0, 1]$ of the form,

$$\omega^l(k) = -\varepsilon_{s1}(q_1) + \varepsilon_{s1}(q_2)\,; \qquad k = q_2 - q_1 \in]0, \pi[\,. \tag{119}$$

Here $q_1 \in [-k_{F\downarrow}, k_{F\downarrow}]$ and $q_2 \in [k_{F\downarrow}, k_{F\uparrow}]$. The PDT high-energy and finite-momentum elementary processes (A) associated with the dominant contributions to the longitudinal dynamical structure factor line shape are the one $s1$ pseudofermion – $s1$ pseudofermion-hole elementary processes associated with the spectrum, Eq. (119).

For $u > 0$ and both spin densities $m \to 0$ and $m > m_* \approx 0.15$, the lower threshold of $\omega^l(k)$ (and $\omega^t(k)$) coincides with a hole branch line for $k \in [0, 2k_{F\downarrow}]$ (and $k \in [\pi - 2k_{F\downarrow}, \pi]$) and with a particle branch line for $k \in [2k_{F\downarrow}, \pi]$ (and $k \in [0, \pi - 2k_{F\downarrow}]$). On the other hand, for $0 < m < m_* \approx 0.15$, the lower threshold of the spectrum $\omega^l(k)$ (and $\omega^t(k)$) does not coincide with the hole branch line for a small momentum width near $k = 0$ (and $k = \pi$). As mentioned above and for simplicity, we consider mostly spin densities $m \to 0$ and $m > 0.25$ for which $\omega^\tau(k)$ coincides with branch lines and the Mott–Hubbard insulator PDT gives the exact momentum and spin density dependence of the exponents that control the line shape in its vicinity.

The use of that dynamical theory reveals that the lower threshold singularities of $S^{xx}(k,\omega)$ are those of $S^{-+}(k,\omega)$ near the particle branch line and of $S^{+-}(k,\omega)$ near the hole branch line. Accounting for the $s1$ band energy dispersion vanishing at the Fermi points, $\varepsilon_{s1}(\pm k_{F\downarrow}) = 0$, the longitudinal $S^{zz}(k,\omega)$ and transverse $S^{xx}(k,\omega)$ hole branch lines spectra read,

$$\begin{aligned}
&\omega_h^\tau(k) = -\varepsilon_{s1}(q)\,, \qquad \tau = l, t\,, \\
&\quad k = k_{F\downarrow} - q \in]0, 2k_{F\downarrow}[\,, \qquad \tau = l\,, \\
&\quad k = \pi - k_{F\downarrow} - q \in]\pi - 2k_{F\downarrow}, \pi[\,, \qquad \tau = t\,,
\end{aligned} \tag{120}$$

where $q \in [-k_{F\downarrow}, k_{F\downarrow}]$. The corresponding particle branch lines spectra are given by,

$$\begin{aligned}
&\omega_p^\tau(k) = \varepsilon_{s1}(q)\,, \qquad \tau = l, t\,, \\
&\quad k = k_{F\downarrow} + q \in]2k_{F\downarrow}, \pi[\,, \qquad \tau = l\,, \\
&\quad k = \pi - k_{F\downarrow} + q \in]0, \pi - 2k_{F\downarrow}[\,, \qquad \tau = t\,,
\end{aligned} \tag{121}$$

with $q \in [k_{F\downarrow}, k_{F\uparrow}]$ and $q \in [-k_{F\uparrow}, -k_{F\downarrow}]$ for the l and t particle branch lines, respectively.

From the use of Eq. (116) one finds that the spectral-weight distribution expression for the line shape in the vicinity of the longitudinal and transverse dynamical structure factors spectrum lower threshold is of the general form,

$$S^{aa}(k,\omega) = C^\tau\,(\omega - \omega^\tau(k))^{\xi^\tau(k)}\,, \qquad k \in]0, \pi[\,, \tag{122}$$

where the momentum dependent exponents are given by,

$$\xi^{\tau}(k) = -1 + \sum_{\iota=\pm 1}\left(\iota\frac{\delta N^{F}_{s1}}{2\xi^{1}_{s1,s1}} + \xi^{1}_{s1,s1}\,\delta J^{F}_{s1} + c_0\,\Phi_{s1,s1}(k^{\iota}_{F\downarrow}, q)\right)^{2}. \quad (123)$$

Here $\alpha = z$ for $\tau = l$, $\alpha = x$ for $\tau = t$, and C^{τ} is a k and ω independent constant. Moreover, $q = k_{F\downarrow} - k$ and $q = -k_{F\downarrow} + k$ for the $S^{zz}(k,\omega)$ hole and particle branch lines, respectively, whereas $q = \pi - k_{F\downarrow} - k$ for the hole branch line and $q = -\pi + k_{F\downarrow} + k$ for the particle branch line of $S^{xx}(k,\omega)$.

The behavior, Eq. (122), is valid for small positive values $(\omega - \omega^{\tau}(k))$ in the vicinity of the lower thresholds $\omega^{\tau}(k) > 0$. In that equation $2\Delta^{\iota}_{\tau}(q)$ are the $\iota = \pm 1$ functionals, Eq. (107), whose specific expression $2\Delta^{\iota}_{\tau}(q) = (\iota\delta N^{F}_{s1}/(2\xi^{1}) + \xi^{1}\,\delta J^{F}_{s1} + c_0\,\Phi(\iota\,k_{F\downarrow}, q))^2$ appearing in Eq. (123) is that suitable for the line shape near the branch lines of the $\tau = l, t$ dynamical structure factors. Here $\iota = \pm 1$ refers to the two $s1$ band Fermi points, the momentum q is that of the $s1$ pseudofermion created ($c_0 = 1$) or annihilated ($c_0 = -1$) under the transitions to the excited energy eigenstates, and the q value was above expressed in terms of the corresponding k value, which is given in Eqs. (120) and (121). Moreover, the $s1$ band Fermi points number deviations read $\delta N^{F}_{s1} = -c_0$ and $\delta J^{F}_{s1} = \frac{1}{2}$ for the $c_0 = 1$ particle and $c_0 = -1$ hole l branch lines and $\delta N^{F}_{s1} = 0$ and $\delta J^{F}_{s1} = \frac{1}{2}$ for the t branch lines.

It follows that for the longitudinal and transverse dynamical structure factors the $\iota = \pm 1$ functionals, Eq. (107), in the exponent expression, Eq. (123), suitable for the line shape near their spectrum lower threshold are given by,

$$2\Delta^{\iota}_{l}(q) = \left(\frac{(\xi^{1}_{s1,s1})^2 - \iota\,c_0}{2\xi^{1}_{s1,s1}} + c_0\,\Phi_{s1,s1}(\iota k_{F\downarrow}, q)\right)^{2};$$
$$2\Delta^{\iota}_{t}(q) = \left(\frac{\xi^{1}_{s1,s1}}{2} + c_0\,\Phi_{s1,s1}(\iota k_{F\downarrow}, q)\right)^{2}, \quad (124)$$

respectively. Here $q \in [-k_{F\downarrow}, k_{F\downarrow}]$ for $c_0 = -1$ and $\tau = l, t$, $q \in [k_{F\downarrow}, k_{F\uparrow}]$ for $c_0 = 1$ and $\tau = l$, and $q \in [-k_{F\uparrow}, -k_{F\downarrow}]$ for $c_0 = 1$ and $\tau = t$.

Higher-order processes (A) and (B) beyond those considered here associated with excited energy eigenstates described both only by real rapidities and real and complex rapidities, respectively, that contribute to the dynamical correlation functions overall spectral weight lead to contributions in (k,ω)-plane regions other than those in the vicinity of the (k,ω)-plane lower thresholds. Since for the spin densities $m > m_* \approx 0.15$ the dynamical structure factors branch lines, Eqs. (120) and (121), have no (k,ω)-plane spectral weight below them, for that spin density range their corresponding line shape expressions, Eq. (122), and momentum dependent exponents, Eq. (123), are exact.

The longitudinal spin spectrum $\omega^{l}(k)$, Eq. (119), and the transverse spin spectrum $\omega^{t}(k)$ that results from combination of the spectra $\omega^{-+}(k)$ and $\omega^{+-}(k)$, Eq. (118), are plotted in Figs. 2 and 3, respectively, for several values of the spin density m and on-site repulsion u. The main effect of the on-site repulsion is on these spectra energy bandwidths. Indeed and as illustrated in these figures, at fixed spin density m their form remains nearly the same for the whole $u > 0$ range. Such on-site repulsion effects are controlled by the u dependence of the $s1$ energy dispersion bandwidths plotted in Fig. 1(a) and (b) as a function of $1/u$ for several spin density values.

The corresponding exponents $\xi^{l}(k)$ and $\xi^{t}(k)$, Eq. (123), that control the singularities in the vicinity of the lower threshold of the longitudinal spin spectrum $\omega^{l}(k)$ of Fig. 2 and transverse spin spectrum $\omega^{t}(k)$ of Fig. 3 are plotted in Figs. 4 and 5, respectively, as a function of the momentum $k \in]0,\pi[$ for several values of u and spin density m. The exponent $\xi^{l}(k)$, Eq. (123)

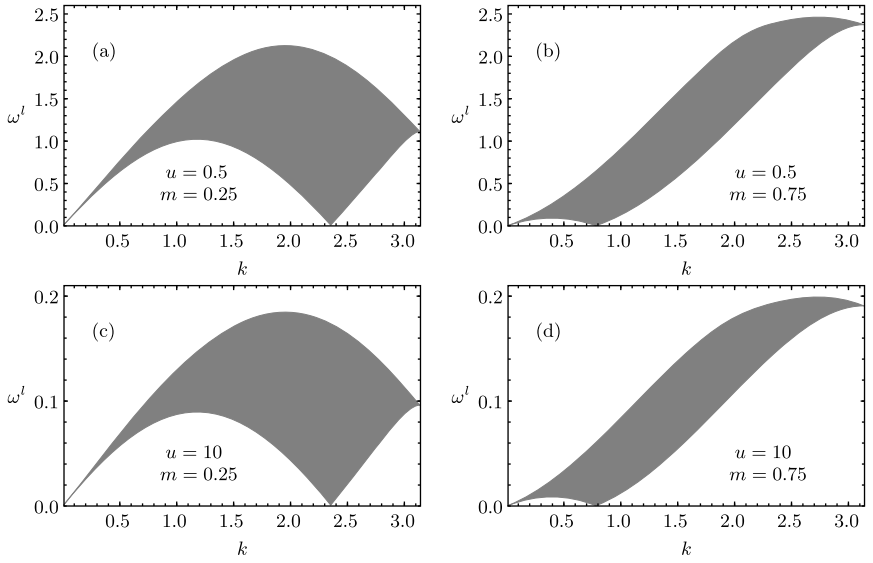

Fig. 2. The longitudinal spin spectrum $\omega^l(k)$ for (a) $m = 0.25$ and $u = 0.5$, (b) $m = 0.75$ and $u = 0.5$, (c) $m = 0.25$ and $u = 10.0$, and (d) $m = 0.75$ and $u = 10.0$. The main effect of the on-site repulsion is on the spectrum energy bandwidth. At fixed spin density m its form remains nearly the same for the whole $u > 0$ range.

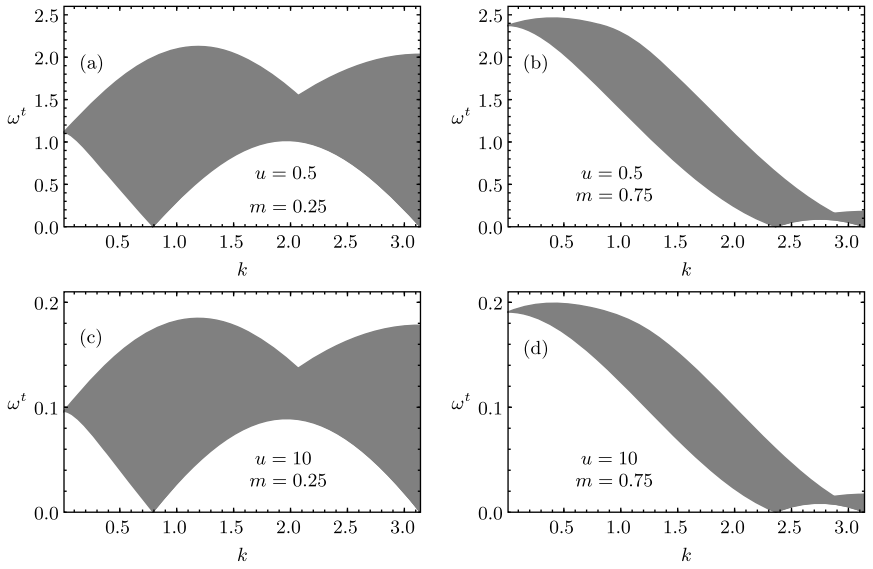

Fig. 3. The transverse spin spectrum $\omega^t(k)$ for (a) $m = 0.25$ and $u = 0.5$, (b) $m = 0.75$ and $u = 0.5$, (c) $m = 0.25$ and $u = 10.0$, and (d) $m = 0.75$ and $u = 10.0$. As in the case of the longitudinal spin spectrum plotted in Fig. 2, the main effect of the on-site repulsion is on the spectrum energy bandwidth.

for $\tau = l$, is negative for $k > 0$ at any u and m values, whereas the exponent $\xi^t(k)$ given in that equation for $\tau = t$ is negative for an u and m-dependent range $k \in [k_t, \pi]$ where the momentum k_t is for $u > 0$ an increasing function of m. Furthermore, analysis of Fig. 4 reveals that the

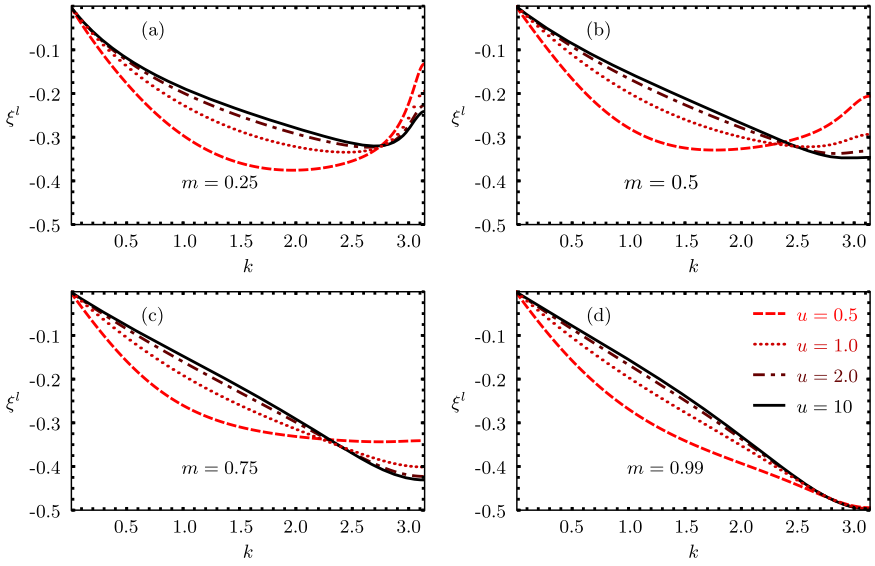

Fig. 4. The exponent $\xi^l(k)$, Eq. (123), that controls the singularities in the vicinity of the lower thresholds of the longitudinal spin spectrum $\omega^l(k)$ plotted in Fig. 2 as a function of $k \in]0, \pi[$ for several values of u and spin densities (a) $m = 0.25$, (b) $m = 0.50$, (c) $m = 0.75$, and (d) $m = 0.99$.

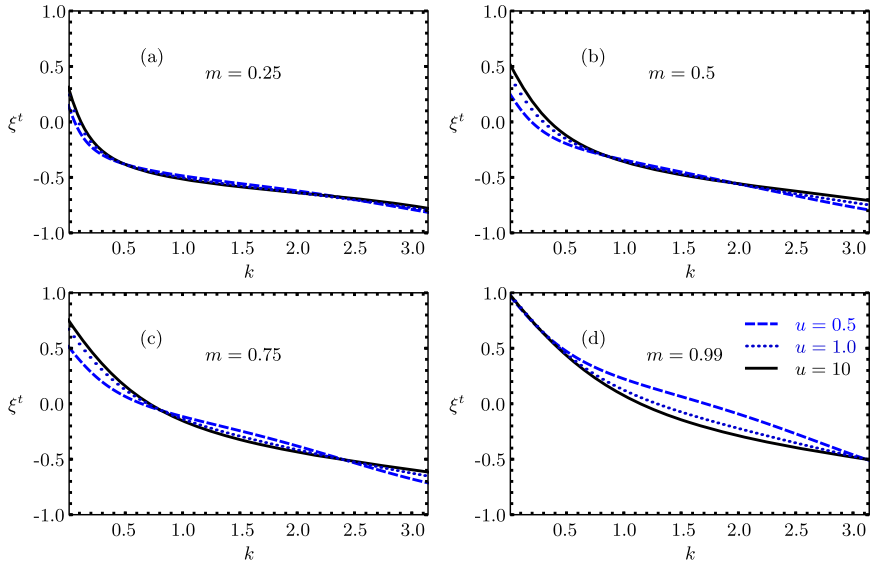

Fig. 5. The exponent $\xi^t(k)$, Eq. (123), that controls the singularities in the vicinity of the lower thresholds of the transverse spin spectrum $\omega^t(k)$ plotted in Fig. 3 as a function of $k \in]0, \pi[$ for several values of u and spin densities (a) $m = 0.25$, (b) $m = 0.50$, (c) $m = 0.75$, and (d) $m = 0.99$.

negative exponent $\xi^l(k)$ is an increasing and decreasing function of u for the momentum ranges $k \in [0, k_l]$ and $k \in [k_l, \pi]$, respectively. Here k_l is a spin density dependent momentum at which the exponent $\xi^l(k)$ has similar value for the whole $u > 0$ range.

For the ranges of the momentum k for which the exponent $\xi^{\tau}(k)$ is negative, there are lower threshold singularity cusps in $S^{aa}(k,\omega)$, Eq. (122). Hence analysis of Figs. 4 and 5 provides valuable information on the k ranges for which there are singularities in the lower thresholds of the dynamical structure factors $S^{zz}(k,\omega)$ and $S^{xx}(k,\omega) = S^{yy}(k,\omega)$.

In the $m \rightarrow 0$ limit, the spectra $\omega^{l}(k)$ and $\omega^{+-}(k)$, Eq. (118), reduce to their lower thresholds. At finite m, the thresholds of these two spectra correspond to different (k,ω)-plane lines. On the other hand, as $m \rightarrow 0$ they become the same (k,ω)-plane line. For finite m values the lower threshold of the spectrum $\omega^{+-}(k)$, Eq. (118), coincides with that of $\omega^{-+}(k)$ for $k \in [\pi - 2k_{F\downarrow}, \pi]$, whereas for $k \in [0, \pi - 2k_{F\downarrow}]$ it does not exist. In the $m \rightarrow 0$ limit the lower threshold of the spectrum $\omega^{+-}(k)$ extends to the whole $k \in [0,\pi]$ range and coincides with those of $\omega^{l}(k)$ and $\omega^{-+}(k)$. However, in contrast to the latter spectra, $\omega^{+-}(k)$ does not reduce in that limit to its lower threshold. The spectrum of the class (ii) two $s1$ pseudofermion-hole excited energy eigenstates populated by $s1$ pseudofermions and a single $s2$ pseudofermion and thus described by real and complex rapidities is gapped for $m > 0$, but in the $m \rightarrow 0$ limit becomes gapless and degenerate with that of $\omega^{-+}(k)$.

At $h = 0$ the spectrum $\omega^{+-}(k)$ is also that of the $S^{z} = 0$ and $S = 1$ two $s1$ pseudofermion-hole excitations of class (i), which due to a selection rule [56] do not contribute to the spin dynamical structure factors at $h > 0$. Hence upon smoothly turning off h there is for the whole $u > 0$ range a large weight transfer from $|S^{z}| = S$ class (ii) excitations for $h \rightarrow 0$ to degenerate $S^{z} = 0$ and $S = 1$ class (i) two $s1$ pseudofermion-hole excited energy eigenstates at $h = 0$. While the spectra change smoothly upon turning off h, from the point of view of the type of excitations behind the corresponding spin spectral weight distribution the $h \rightarrow 0$ limit is singular.

For $u > 0$ and the $m \rightarrow 0$ limit one finds from the use of Eq. (122),

$$S^{zz}(k,\omega) = S^{xx}(k,\omega) = C\,(\omega - \omega(k))^{-1/2}\,, \tag{125}$$

for $k \in]0,\pi[$ where the lower thresholds $\omega^{l}(k) = \omega^{t}(k) = \omega(k)$ coincide with that of the $u > 0$ and $m = 0$ two – $s1$ pseudofermion-hole spectrum. Consistently, $\xi^{\tau}(k) = -1/2$ is also the value of the known exponent that controls the line shape in the vicinity of the lower threshold of the latter spectrum [38,39].

In the opposite limit, $m \rightarrow 1$, the lower thresholds $\omega^{\tau}(k)$ coincide with the particle branch line for all k values. Furthermore, $S^{zz}(k,\omega) \rightarrow 0$ as $h \rightarrow h_c$ in the TL, the two-component $S^{xx}(k,\omega)$ and $S^{zz}(k,\omega)$ dynamical structure factor being dominated by $S^{xx}(k,\omega)$. Here h_c is the critical field associated with the spin energy scale $2\mu_B h_c$, Eq. (44), at which fully polarized ferromagnetism is achieved. Due to the charge-spin recombination occurring at $h = h_c$ when the spin energy scale $2\mu_B|h| = 2\mu_B h_c$, Eq. (44), and the charge Mott–Hubbard gap $2\mu_0$, Eq. (23), reach exactly the same value, $\sqrt{(4t)^2 + U^2} - 4t$, the PDT expression given in Eq. (122) for the spin dynamical structure factor is not valid, being replaced by a δ-function like distribution,

$$S^{xx}(k,\omega) = \frac{\pi}{2}\delta\left(\omega - \varepsilon_{s1}(\pi - k)\right)\,, \qquad k \in]0,\pi[\,, \tag{126}$$

for $\alpha\alpha = xx$ and by $S^{zz}(k,\omega) = 0$ for $\alpha\alpha = zz$ where the energy dispersion $\varepsilon_{s1}(q)$ reads,

$$\begin{aligned}
\varepsilon_{s1}(q) &= -\frac{2t}{\pi}\int_{-\pi}^{\pi} dk \sin k \arctan\left(\frac{\sin k - \Lambda^{0}_{s1}(q)}{u}\right) + \sqrt{(4t)^2 + U^2} - U\,, \\
q &= -\frac{1}{\pi}\int_{-\pi}^{\pi} dk \arctan\left(\frac{\sin k - \Lambda^{0}_{s1}(q)}{u}\right)\,,
\end{aligned} \tag{127}$$

and the second expression given here defines the ground-state rapidity function $\Lambda^0_{s1}(q)$ in terms of its inverse function.

Finally, the line shapes, Eq. (122), and corresponding exponents $\xi^\tau(k)$, Eq. (123), do not apply at and near the $\omega = 0$ lower threshold soft modes such as $(k^\tau_0, 0)$ where $k^l_0 = 2k_{F\downarrow}$ and $k^t_0 = \pi - 2k_{F\downarrow}$ in the (k,ω)-plane. In this low-energy case the spin part of the half-filled 1D Hubbard model spectrum can be described by a Gaussian field theory with central charge $c = 1$ [20]. The present more general Mott–Hubbard insulator PDT reaches in the low-energy limit the same results as that Gaussian field theory. (Also the metallic-phase PDT describes the known low-energy expressions [29].) Indeed, near the points $(k^\tau_0, 0)$ the PDT expressions given in Eq. (117) apply, the two $\iota = \pm 1$ functionals, Eq. (107), becoming the $\iota = \pm 1$ operator dimensions of that theory,

$$2\Delta^\iota_l = (\xi^1_{s1,s1})^2\,; \qquad 2\Delta^\iota_t = \left(\frac{\iota}{2\xi^1_{s1,s1}} - \xi^1_{s1,s1}\right)^2 . \tag{128}$$

For the case of the longitudinal and transverse spin dynamical structure factors considered in this section the general expressions provided in Eq. (117) lead for the finite-weight region above the $(k^\tau_0, 0)$ plane points for which the low excitation energy ω is not in the vicinity of the low-energy thresholds $\omega \approx \pm v_{s1}\,(k - k^\tau_0)$, to the following line shape,

$$S^{aa}(k,\omega) = C^\tau_0\,|\omega|^{\zeta^\tau_0}\,, \qquad \omega \neq \pm v_{s1}\,(k - k^\tau_0)\,, \tag{129}$$

where C^τ_0 is a constant and the exponent reads $\zeta^l_0 = -2 + \sum_{\iota=\pm 1} 2\Delta^\iota_l$, which gives,

$$\zeta^l_0 = -2\,(1 - (\xi^1_{s1,s1})^2)\,; \qquad \zeta^t_0 = -2\left(1 - \frac{1}{4(\xi^1_{s1,s1})^2} - (\xi^1_{s1,s1})^2\right). \tag{130}$$

On the other hand, according to the general expressions given in Eq. (117) for low excitation energy ω near the low-energy thresholds, $\omega \approx \pm v_{s1}\,(k - k^\tau_0)$, the spin dynamical correlation functions line shape is rather of the form,

$$S^{aa}(k,\omega) = C^\tau_{-1}\,(\omega + v_{s1}\,(k - k^\tau_0))^{\zeta^\tau_{-1}}\,, \qquad k < k^\tau_0\,, \qquad \tau = l,t\,, \tag{131}$$

for $\omega \approx -v_{s1}\,(k - k^\tau_0)$ and,

$$S^{aa}(k,\omega) = C^\tau_{+1}\,(\omega - v_{s1}\,(k - k^\tau_0))^{\zeta^\tau_{+1}}\,, \qquad k > k^\tau_0\,, \qquad \tau = l,t\,, \tag{132}$$

for $\omega \approx +v_{s1}\,(k - k^\tau_0)$ where $C^\tau_{\pm 1}$ are constants and the exponents are given by $\zeta^\tau_{\pm 1} = -1 + 2\Delta^{\pm 1}_l$ and thus read,

$$\zeta^l_{\pm 1} = -1 + (\xi^1_{s1,s1})^2\,; \qquad \zeta^t_{\pm 1} = -1 \mp 1 + \frac{1}{4(\xi^1_{s1,s1})^2} + (\xi^1_{s1,s1})^2\,. \tag{133}$$

5. Concluding remarks

The PDT reported in Refs. [28–30] for the metallic-phase of the 1D Hubbard model does not apply to the spin dynamical correlation functions of the half-filled 1D Hubbard model. In this paper we have introduced a modified PDT that applies to the latter problem. This has allowed to study the line shape of singularities in the vicinity of the lower thresholds of the model longitudinal and transverse dynamical spin structure factors, Eq. (1).

Specifically, the exact momentum dependence of the exponents, Eq. (123), that control such line shapes in the TL was derived. The corresponding exact line-shape of the structure form factors $S^{zz}(k,\omega)$ and $S^{xx}(k,\omega)$ is reported in Eq. (122). Importantly, for the k ranges for which the $\tau = l,t$ exponents $\xi^{\tau}(k)$ given in Eq. (123) (which are plotted in Figs. 4 and 5) are negative, there are lower threshold singularity cusps in the corresponding $\tau = l,t$ spin dynamical structure factors. Our results on these form factors of the Mott–Hubbard insulator phase of the 1D Hubbard model at finite magnetic fields $h > 0$ refer to the TL. To our knowledge, no previous investigations accessed the corresponding exact spin density and momentum dependence of the exponents that control the singularities of the longitudinal and transverse spin structure form factors in the vicinity of their lower thresholds.

Mott–Hubbard insulators are in 1D a paradigm for the importance of strong correlations and are known to exhibit a wide variety of unusual physical phenomena. Experimental realizations within condensed matter include inelastic neutron scattering in chain cuprates and a number of organic compounds [41,59]. In the limit of very strong on-site repulsion U the spin degrees of freedom of such condensed-matter systems are commonly modeled by the spin-1/2 XXX chain [41]. However, for general Mott–Hubbard insulating materials there is no reason for the on-site repulsion to be much stronger than the electron hopping amplitude t. This situation is realized in the Bechgaard salts [59]. A question that arises then is how electron itinerancy affects the spin dynamics. As discussed in Section 4, the analysis of the u dependences of the dynamical spin structure factor spectra and corresponding exponents that control the line shape near such spectra lower thresholds plotted in Figs. 2–5 provides important information on that issue.

An interesting experimental possibility is the potential observation of the spin dynamical structure factors peaks we predict in inelastic neutron scattering experiments on actual spin-chain compounds. The structure form factors $S^{zz}(k,\omega)$ and $S^{xx}(k,\omega)$ may be investigated separately in $h > 0$ experiments on such compounds by using a carefully oriented crystal. If the crystal is misoriented, or if a micro crystalline sample is used, the $S^{zz}(k,\omega)$ and $S^{xx}(k,\omega)$ spectral features should appear superimposed. Such superimposition changes the excitations lower thresholds and leads to the broadening of the singularities, Eq. (122). However, this does not occur at $h = 0$, since $S^{zz}(k,\omega) = S^{xx}(k,\omega)$. These two different situations are clearly seen in the magnetic scattering intensity measured at zero- and finite-field inelastic neutron scattering experiments of Ref. [41] on a spin-chain compound, respectively, (See Figs. 2 (a)–(c) of that reference.) We suggest that more demanding $h > 0$ experiments with a carefully oriented crystal be carried out on spin-chain compounds. This should yield separately $S^{zz}(k,\omega)$ and $S^{xx}(k,\omega)$ whose magnetic scattering intensities are expected to display the cusp singularities found theoretically in this paper.

On the other hand, the recent progress in implementing the present repulsive Hubbard model with ultra-cold atoms on optical lattices has led to the observation of the Mott–Hubbard insulating state studied in this paper [60]. Another interesting program would be the observation of the spin spectral weight distributions over the (k,ω) plane associated with the dynamical correlation functions studied in this paper in systems of ultra-cold atoms on optical lattices.

Acknowledgements

We thank D.K. Campbell, A. Moreno, and P.D. Sacramento for illuminating discussions and the support by the Beijing CSRC and the FEDER through the COMPETE Program and the Portuguese FCT in the framework of the Strategic Projects PEST-C/FIS/UI0607/2013, PEst-OE/FIS/UI0091/2014, and UID/CTM/04540/2013.

Appendix A. Three fractionalized particles emerging from the rotated-electron separation for the 1D Hubbard model in its full Hilbert space

Here general operational expressions valid for the 1D Hubbard model in its full Hilbert space of the rotated-spin 1/2, rotated-η-spin 1/2, and c pseudoparticle operators in terms of rotated-electron operators and of the latter operators in terms of the former are provided.

The rotated-electron operators, Eq. (51), can also be defined for the 1D Hubbard model in its full Hilbert space. The corresponding extension of the electron–rotated-electron unitary operator $\hat{V}$ definition in Eq. (52) accounts for the occupancy configurations associated with the η-spin degrees of freedom [61]. The c pseudoparticle operators that emerge from such generalized rotated-electron operators are then given by,

$$f^{\dagger}_{j,c} = (f_{j,c})^{\dagger} = \tilde{c}^{\dagger}_{j,\uparrow}(1-\tilde{n}_{j,\downarrow}) + (-1)^{j}\tilde{c}_{j,\uparrow}\tilde{n}_{j,\downarrow}; \quad n_{j,c} = f^{\dagger}_{j,c}\, f_{j,c},\ j = 1,\ldots,L, \quad \text{(A.1)}$$

where $\tilde{n}_{j,\sigma}$ is given in Eq. (51).

The creation operator $f^{\dagger}_{j,c}$ and annihilation operator $f_{j,c}$ create and annihilate, respectively, one c pseudoparticle at the $j = 1,\ldots,L$ site of the c effective lattice, which is identical to the model original lattice. The corresponding momentum-dependent c pseudoparticle operators $f^{\dagger}_{q_j,c} = (f_{q_j,c})^{\dagger}$ are then given by Eq. (77) but with the operator $f^{\dagger}_{j',c}$ being that in Eq. (A.1). Furthermore, on combining Eqs. (A.1) and (77), the c pseudofermion operators, Eq. (64) for $\beta = c$, can be formally expressed in terms of rotated-electron operators as,

$$\bar{f}^{\dagger}_{\tilde{q}_j,c} = \frac{1}{\sqrt{L}}\sum_{j'=1}^{L} e^{+i\tilde{q}_j j'}\left(\tilde{c}^{\dagger}_{j',\uparrow}(1-\tilde{n}_{j',\downarrow}) + (-1)^{j'}\tilde{c}_{j',\uparrow}\tilde{n}_{j',\downarrow}\right); \qquad \bar{f}_{\tilde{q}_j,c} = (\bar{f}^{\dagger}_{\tilde{q}_j,c})^{\dagger}. \quad \text{(A.2)}$$

The three electron-rotated local operators $\tilde{S}^{l}_{j,\eta}$ and three electron-rotated local operators $\tilde{S}^{l}_{j,s}$ and corresponding six generators $\tilde{S}^{l}_{\alpha}$ of the global η-spin and spin $SU(2)$ symmetry algebras may be written as,

$$\tilde{S}^{l}_{j,\eta} = (1-n_{j,c})\tilde{q}^{l}_{j}; \qquad \tilde{S}^{l}_{j,s} = n_{j,c}\tilde{q}^{l}_{j}; \qquad \tilde{S}^{l}_{\alpha} = \sum_{j=1}^{L}\tilde{s}^{l}_{j,\alpha}, \quad \alpha = \eta, s,\ l = z,\pm, \quad \text{(A.3)}$$

respectively. Here $n_{j,c}$ is the c pseudoparticle local density operator, Eq. (A.1). The *ηs quasi-spin* operators,

$$\tilde{q}^{l}_{j} = \tilde{S}^{l}_{j,s} + \tilde{S}^{l}_{j,\eta}, \qquad l = \pm, z, \quad \text{(A.4)}$$

such that $\tilde{q}^{\pm}_{j} = \tilde{q}^{x}_{j} \pm i\,\tilde{q}^{y}_{j}$ and $\tilde{q}^{z}_{j}$, where x, y, z denote the Cartesian coordinates, have the following expressions in terms of rotated-electron creation and annihilation operators,

$$\tilde{q}^{-}_{j} = (\tilde{q}^{+}_{j})^{\dagger} = (\tilde{c}^{\dagger}_{j,\uparrow} + (-1)^{j}\,\tilde{c}_{j,\uparrow})\,\tilde{c}_{j,\downarrow}; \qquad \tilde{q}^{z}_{j} = (\tilde{n}_{j,\downarrow} - 1/2). \quad \text{(A.5)}$$

Inversion of the relations, Eqs. (A.1) and (A.5), along with the use of Eq. (A.4) leads to,

$$\tilde{c}^{\dagger}_{j,\uparrow} = f^{\dagger}_{j,c}\left(\frac{1}{2} - \tilde{S}^{z}_{j,s} - \tilde{S}^{z}_{j,\eta}\right) + (-1)^{j}\, f_{j,c}\left(\frac{1}{2} + \tilde{S}^{z}_{j,s} + \tilde{S}^{z}_{j,\eta}\right); \qquad \tilde{c}_{j,\uparrow} = (\tilde{c}^{\dagger}_{j,\uparrow})^{\dagger},$$
$$\tilde{c}^{\dagger}_{j,\downarrow} = (f^{\dagger}_{j,c} + (-1)^{j}\, f_{j,c})(\tilde{S}^{+}_{j,s} + \tilde{S}^{+}_{j,\eta}), \qquad \tilde{c}_{j,\downarrow} = (\tilde{c}^{\dagger}_{j,\downarrow})^{\dagger}, \quad \text{(A.6)}$$

where $(\tilde{S}^{+}_{j,s} + \tilde{S}^{+}_{j,\eta})^{\dagger} = (\tilde{S}^{-}_{j,s} + \tilde{S}^{-}_{j,\eta})$.

The electron-rotated local operators $\tilde{S}^{l}_{j,s}$ and $\tilde{S}^{l}_{j,\eta}$, Eq. (A.3), are associated with the rotated-spins 1/2 and rotated-η-spins 1/2, respectively. The rotated-electron degrees of freedom separation, Eq. (A.6), is such that the c pseudoparticle operators, Eq. (A.1), rotated-spin 1/2 and rotated-η-spin 1/2 operators, Eq. (A.3), and the related ηs quasi-spin operators, Eqs. (A.5) and (A.4), emerge from the rotated-electron operators by an exact local transformation that does not introduce constraints.

References

[1] M. Karowski, P. Weisz, Nucl. Phys. B 139 (1978) 455;
B. Berg, M. Karowski, P. Weisz, Phys. Rev. D 19 (1979) 2477.
[2] F.A. Smirnov, Form Factors in Completely Integrable Models of Quantum Field Theory, Advanced Series in Mathematical Physics, vol. 14, World Scientific, Singapore, 1992.
[3] J.L. Cardy, G. Mussardo, Nucl. Phys. B 340 (1990) 387;
A. Fring, G. Mussardo, P. Simonetti, Nucl. Phys. B 393 (1993) 413.
[4] V.P. Yurov, Al.B. Zamolodchikov, Int. J. Mod. Phys. A 6 (1991) 3419;
S. Lukyanov, Commun. Math. Phys. 167 (1995) 183;
S. Lukyanov, A.B. Zamolodchikov, Nucl. Phys. B 493 (1997) 2541;
S. Lukyanov, Mod. Phys. Lett. A 12 (1990) 2543.
[5] F.H.L. Essler, A.M. Tsvelik, G. Delfino, Phys. Rev. B 56 (1997) 11001;
F.H.L. Essler, A.M. Tsvelik, Phys. Rev. B 57 (1998) 10592.
[6] B.L. Altshuler, R.M. Konik, A.M. Tsvelik, Nucl. Phys. B 739 (2006) 311.
[7] F.H.L. Essler, R.M. Konik, J. Stat. Mech. (2009) 09018.
[8] M. Jimbo, T. Miwa, Algebraic Analysis of Solvable Lattice Models, American Mathematical Society, Providence, 1994.
[9] A.H. Bougourzi, M. Couture, M. Kacir, Phys. Rev. B 54 (2006) 12669;
A. Abada, A.H. Bougourzi, B. Si-Lakhal, Nucl. Phys. B 497 (1997) 733;
M. Karbach, G. Müller, A.H. Bougourzi, A. Fledderjohann, K.H. Mütter, Phys. Rev. B 55 (1997) 12510.
[10] D. Biegel, M. Karbach, G. Müller, Europhys. Lett. 59 (2002) 882.
[11] N. Kitanine, J.M. Maillet, V. Tetras, Nucl. Phys. B 554 (1999) 647.
[12] J.-S. Caux, J.M. Maillet, Phys. Rev. Lett. 95 (2005) 077201.
[13] J.-S. Caux, H. Konno, M. Sorrell, R. Weston, Phys. Rev. Lett. 106 (2011) 217203.
[14] E.H. Lieb, F.Y. Wu, Phys. Rev. Lett. 20 (1968) 1445.
[15] E.H. Lieb, F.Y. Wu, Physica A 321 (2003) 1.
[16] M. Takahashi, Prog. Theor. Phys. 47 (1972) 69.
[17] M.J. Martins, P.B. Ramos, Nucl. Phys. B 522 (1998) 413.
[18] J. Voit, Rep. Prog. Phys. 57 (1994) 977.
[19] H.J. Schulz, Phys. Rev. Lett. 64 (1990) 2831.
[20] H. Frahm, V.E. Korepin, Phys. Rev. B 42 (1990) 10553.
[21] K.-V. Pham, M. Gabay, P. Lederer, Phys. Rev. B 61 (16) (2000) 397.
[22] K. Penc, K. Hallberg, F. Mila, H. Shiba, Phys. Rev. Lett. 77 (1996) 1390.
[23] K. Penc, K. Hallberg, F. Mila, H. Shiba, Phys. Rev. B 55 (15) (1997) 475.
[24] F. Woynarovich, J. Phys. C, Solid State Phys. 15 (1982) 85.
[25] F. Woynarovich, J. Phys. C, Solid State Phys. 15 (1982) 97.
[26] M. Ogata, H. Shiba, Phys. Rev. B 41 (1990) 2326.
[27] J.M.P. Carmelo, J.M. Román, K. Penc, Nucl. Phys. B 683 (2004) 387.
[28] J.M.P. Carmelo, K. Penc, D. Bozi, Nucl. Phys. B 725 (2005) 421;
J.M.P. Carmelo, K. Penc, D. Bozi, Nucl. Phys. B 737 (2006) 351, Erratum.
[29] J.M.P. Carmelo, L.M. Martelo, K. Penc, Nucl. Phys. B 737 (2006) 237.
[30] J.M.P. Carmelo, D. Bozi, K. Penc, J. Phys. Condens. Matter 20 (2008) 415103.
[31] M. Sing, U. Schwingenschlögl, R. Claessen, P. Blaha, J.M.P. Carmelo, L.M. Martelo, P.D. Sacramento, M. Dressel, C.S. Jacobsen, Phys. Rev. B 68 (2003) 125111.
[32] J.M.P. Carmelo, K. Penc, L.M. Martelo, P.D. Sacramento, J.M.B. Lopes dos Santos, R. Claessen, M. Sing, U. Schwingenschlögl, Europhys. Lett. 67 (2004) 233.
[33] J.M.P. Carmelo, K. Penc, P.D. Sacramento, M. Sing, R. Claessen, J. Phys. Condens. Matter 18 (2006) 5191.

[34] A. Imambekov, T.L. Schmidt, L.I. Glazman, Rev. Mod. Phys. 84 (2012) 1253.
[35] F.H.L. Essler, Phys. Rev. B 81 (2010) 205120.
[36] L. Seabra, F.H.L. Essler, F. Pollmann, I. Schneider, T. Veness, Phys. Rev. B 90 (2014) 245127.
[37] R.G. Pereira, K. Penc, S.R. White, P.D. Sacramento, J.M.P. Carmelo, Phys. Rev. B 85 (2012) 165132.
[38] F.H.L. Essler, V.E. Korepin, Phys. Rev. B 59 (1999) 1734.
[39] M.J. Bhaseen, F.H.L. Essler, A. Grage, Phys. Rev. B 71 (2005) 020405(R).
[40] D. Controzzi, F.H.L. Essler, Phys. Rev. B 66 (2002) 165112.
[41] M.B. Stone, D.H. Reich, C. Broholm, K. Lefmann, C. Rischel, C.P. Landee, M.M. Turnbull, Phys. Rev. Lett. 91 (2003) 037205.
[42] M.A. Cazalilla, R. Citro, T. Giamarchi, E. Orignac, M. Rigol, Rev. Mod. Phys. 83 (2011) 1405.
[43] D. Braak, N. Andrei, Nucl. Phys. B 542 (1999) 551.
[44] F.H.L. Essler, V.E. Korepin, K. Schoutens, Phys. Rev. Lett. 67 (1991) 3848.
[45] J.M.P. Carmelo, P. Horsch, Phys. Rev. Lett. 68 (1992) 871;
J.M.P. Carmelo, P. Horsch, P.A. Bares, A.A. Ovchinnikov, Phys. Rev. B 44 (1991) 9967;
J.M.P. Carmelo, P. Horsch, A.A. Ovchinnikov, Phys. Rev. B 45 (1992) 7899;
J.M.P. Carmelo, P. Horsch, A.A. Ovchinnikov, Phys. Rev. B 46 (1992) 14728.
[46] J.M.P. Carmelo, A.H. Castro Neto, Phys. Rev. Lett. 70 (1993) 1904;
J.M.P. Carmelo, A.H. Castro Neto, Phys. Rev. Lett. 74 (1995) 3089, Erratum;
J.M.P. Carmelo, A.H. Castro Neto, D.K. Campbell, Phys. Rev. Lett. 73 (1994) 926;
J.M.P. Carmelo, A.H. Castro Neto, D.K. Campbell, Phys. Rev. Lett. 74 (1995) 3089, Erratum;
J.M.P. Carmelo, A.H. Castro Neto, D.K. Campbell, Phys. Rev. B 50 (1994) 3667;
J.M.P. Carmelo, A.H. Castro Neto, D.K. Campbell, Phys. Rev. B 50 (1994) 3683;
J.M.P. Carmelo, N.M.R. Peres, D.K. Campbell, A.W. Sandvik, Z. Phys. B 103 (1997) 217.
[47] A.A. Ovchinnikov, Sov. Phys. JETP 30 (1970) 1160.
[48] E.H. Lieb, Phys. Rev. Lett. 62 (1989) 1201.
[49] F.H.L. Essler, H. Frahm, F. Göhmann, A. Klümper, V.E. Korepin, The One-Dimensional Hubbard Model, Cambridge University Press, Cambridge, UK, 2005, Section 7.2.
[50] J.M.P. Carmelo, S. Östlund, M.J. Sampaio, Ann. Phys. 325 (2010) 1550.
[51] J.M.P. Carmelo, P.D. Sacramento, Phys. Rev. B 68 (2003) 085104.
[52] H.V. Kruis, I.P. McCulloch, Z. Nussinov, J. Zaanen, Phys. Rev. B 70 (2004) 075109.
[53] F.D.M. Haldane, Phys. Rev. Lett. 67 (1991) 937.
[54] Y.R. Wang, Phys. Rev. B 46 (1992) 151.
[55] P.W. Anderson, Phys. Rev. Lett. 18 (1967) 1049.
[56] G. Müller, H. Thomas, H. Beck, J.C. Bonner, Phys. Rev. B 24 (1981) 1429.
[57] K. Lefmann, C. Rischel, Phys. Rev. B 54 (1996) 6340.
[58] M. Karbach, G. Müller, Phys. Rev. B 62 (2000) 14871;
M. Karbach, D. Biegel, G. Müller, Phys. Rev. B 66 (2002) 054405.
[59] M. Raczkowski, F.F. Assaad, L. Pollet, Phys. Rev. B 91 (2015) 045137.
[60] R. Sensarma, D. Pekker, M.D. Lukin, E. Demler, Phys. Rev. Lett. 103 (2009) 035303.
[61] J.M.P. Carmelo, P.D. Sacramento, 2015, submitted for publication.